IN THE UNITED STATES PATENT AND TRADEMARK OFFICE

Applicants:	Kevin Jeffrey Barnham, et al.	**Examiner:**	D. Margaret M. Seaman
Serial No.:	10/521,902	**Art Unit:**	1625
Filed:	August 10, 2005	**Docket:**	18583
For:	8-HYDROXY QUINOLINE DERIVATIVES		

Confirmation No.: 7111

Commissioner for Patents
P. O. Box 1450
Alexandria, VA 22313-1450

DECLARATION OF DR. ROBERT CHERNY

I, Robert Cherny, hereby declare and state as follows:

1. I am currently a consultant to Prana Biotechnology Ltd. ("Prana"), the assignee of the above-identified application. I hold the position of Head of Research – Prana and am seconded from the Mental Health Research Institute (MHRI).

2. I hold a Bachelor of Science (B.S.) Degree in Biochemistry & Immunology from Monash University, which I received in 1980 and a Doctorate Degree in Biochemistry from Prince Henry's Hospital Medical Research Institute, Monash University in 1990. Besides being a consultant of Prana, I am also a Senior Research Fellow and have been Co-Head of Oxidation Biology (Neuropathology Laboratory) at the MHRI of Victoria since 1995. A copy of my *Curriculum Vitae* is attached hereto as **Exhibit 1**.

3. I have conducted extensive research in the area of neurodegenerative diseases, including Alzheimer's disease, and in particular, protein chemistry, metallochemistry free-radical

biology and oxidative stress in the context of neurodegenerative disorders. The laboratory of MHRI has been the site of critical discoveries in the area of neurodegenerative diseases, especially with respect to the biology of Alzheimer's disease, including the expression and biology of the Alzheimer's amyloid precursor protein ("APP"), and its toxic cleavage product – "Abeta" protein. During my tenure at MHRI, I had the pleasure to collaborate with both Prof. Ashley Bush- a world renowned expert regarding the interaction of metals and Abeta, and with Prof. Colin Masters- the discoverer of Abeta and an acknowledged world authority on the role of that protein in Alzheimer's disease. From these experiences, I believe that I qualify as an expert in this area.

4. In preparing this Declaration, I have reviewed the underlying patent application and am familiar with its contents. The application describes 8-hydroxyquinoline derivatives of the formula

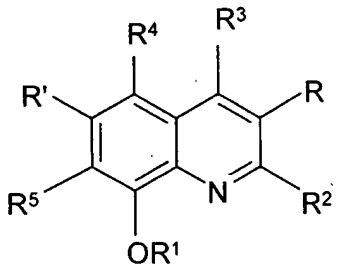

I

wherein the variables R, R', R^1, R^2, R^3, R^4 and R^5 are as defined in the underlying application. The underlying application indicates that these compounds are useful for the treatment, amelioration and/or prophylaxis of neurological conditions, e.g., Alzheimer's disease.

Two of the compounds within the scope of Formula I have the formula

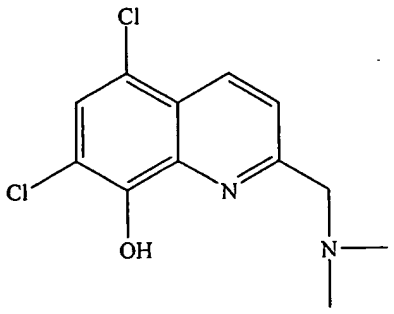

PBT 1033

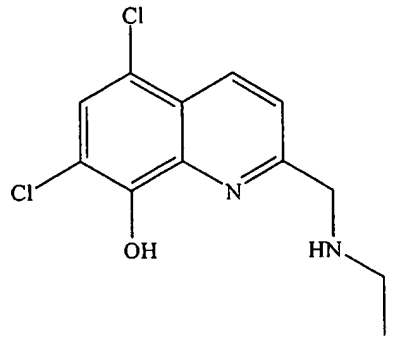

PBT 1051

and will be designated herein as 1033 and 1051, respectively.

5. I have also reviewed U.S. Patent No. 3,682,927 to Carissimi et al. ("Carissimi et al.") and Paragraph 6 of an Office Action dated April 18, 2008, which discusses this patent.

6. Carissimi et al. discuss various compounds as being useful as antiseptics and fungicides. The Office Action refers to a compound having the structure

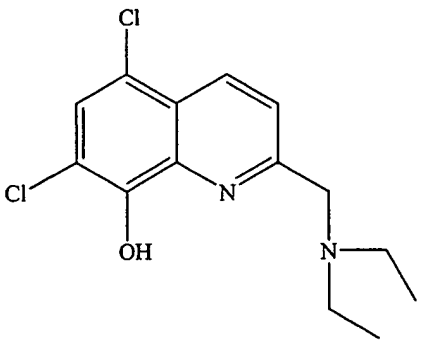

which I refer to as the "CC compound".

7. I have been advised by counsel for Prana that the Office Action in Paragraph 6 alleges that the 1033 and 1051 are structurally similar and obvious relative to the CC compound, and that the Office Action is requesting data to show unexpected properties of 1033 and 1051 relative to the CC compound.

8. I have been asked by counsel for Prana to compare the properties of this CC compound with compounds of the present invention, as described hereinbelow.

9. For an understanding of the data herein below, which I used to compare the properties of the compounds, a digression is in order.

10. One of the hallmarks of Alzheimer's disease ("AD") is the buildup of the above mentioned protein -Abeta in the brain, forming dense insoluble aggregates called 'plaques'. Abeta is produced and secreted by neurons. In addition to forming plaques in AD, secreted Abeta is considered to be toxic to neurons and found to impede normal nerve transmission, which can result in cognitive impairment and other symptoms associated with AD.

11. AD therapies currently in development include those that are aimed at reducing the levels of Abeta in the brain. The strategy of these therapies is to either inhibit enzymes that cleave

Abeta from its precursor protein APP, or by degrading and/or removing the Abeta through the use of technologies such as monoclonal antibody therapy.

12. Another approach to reducing the levels of Abeta in the brain can be the use of a compound having ionophoric properties. An ionophoric property is the ability to transport metal ions across the membrane and into a cell, including a neuronal cell. Once inside the cell, metal ions such as copper, zinc and iron are available to potentially affect cellular metabolism.

13. In relation to the treatment of AD, a substantial body of literature evidences that APP, of which Abeta is a cleavage product, has its expression and cleavage altered by copper metal ions. The role of copper in particular has been intensively investigated, as exemplified by the article by Cater M.A *et al* in the Biochemical Journal attached hereto as **Exhibit 2**. In this article, the authors demonstrate that by increasing the level of copper in cells which express APP, the cleavage of APP can be altered and the production of Abeta diminished. By virtue of its *ionophoric* character, clioquinol ("CQ") was chosen as the agent for delivery of copper to the cultured cells to demonstrate this effect.

14. Another important way in which the ionophoric property of a compound may influence the levels of Abeta in the brain is through accelerating the breakdown of Abeta after it is produced. The article by White AR *et al* in The Journal of Biochemistry, attached hereto as **Exhibit 3,** illustrates this phenomenon. Here the authors again show that by using CQ to deliver copper to several cell types which express APP, the level of Abeta in the culture medium is dramatically reduced. The authors show that this reduction in Abeta occurs because the copper transferred into the cells by CQ promotes a biochemical cascade which results in the increased production of matrix-metalloprotease enzymes which act to degrade the Abeta that is secreted into the culture medium. In this paper, the presence of copper in the culture medium is insufficient in

itself to influence these events and it is the ionophore property of CQ that is required to deliver the metal across the cell membrane.

15. As one of ordinary skill in the art may conclude, a drug having greater ionophoric ability relative to a second drug would be more likely to confer greater Abeta reduction in the brain.

16. I have conducted an experiment to determine the ionophoric properties of the Carissimi compound (CC) and the compounds 1033 and 1051 of the present specification, compared to a positive control compound, CQ, in an ionophore test.

17. These experiments described herein were either conducted by me or under my direct supervision and control.

18. The protocol was conducted as follows in accordance with the following procedure:

M17 human neuroblastoma cells were plated out on 6 well tissue culture plates and left overnight. Sufficient cells were provided to achieve approximately 70 % confluence (1 million cells). Cells were incubated in a media of 1 ml of Opti-MEM (Invitrogen) with added 10% FBS, Sodium Pyruvate, NEAA, and PenStrep and 10 μM of $CuCl_2$ for 5 hr at 37°C. The cells were also incubated with or without the various test compounds (CC, 1033 or 1051 or CQ for a positive control). A 10 μM concentration of each of these test compounds was added to each set of cultured cells. At the conclusion of the incubation, the media were removed using a vacuum aspirator, and 1 ml of PBS was added to dislodge the cells. Cells were then transferred to microfuge tubes and pelleted. The PBS was discarded and the remaining cell pellets were frozen at -20 C. The cell pellets were assayed for metal content using inductively coupled plasma mass spectrometry (ICPMS) analysis.

The cell pellets were prepared as follows:

50 ul of concentrated Nitric Acid (Aristar, BDH) was added to each cell pellet, and the samples were allowed to digest overnight. Following this procedure, the samples were heated for 20 min at 90°C to complete the digestion. The volume of each sample was reduced to ~45 µl after digestion, to which a further 1 ml of 1% Nitric Acid diluent was added.

Measurements of the metal content of the neuroblastoma cells were performed using a Varian UltraMass ICPMS instrument under operating conditions suitable for routine multi-element analysis.

19. The results of these experiments for each test compound is provided in the bar graph below:

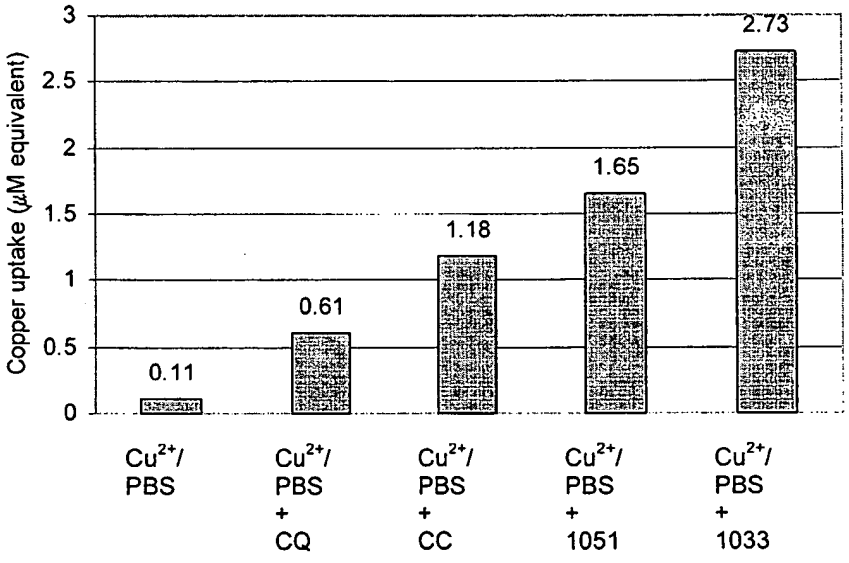

20. The vertical axis of the graph indicates the concentration of copper in micromolar per $1x10^6$ cells taken up by the cultured neuronal cells. Further, it is understood that the term

"equivalent" as used on the vertical axis, signifies that the results have been normalized over more than one assay.

21. The control experiment without drug (Cu/PBS) indicated there was some uptake of copper by the cells when the test compound was absent. As shown by the data depicted in the graph above, when CQ was added, the amount of copper taken up was 0.61 μM; for CC, the amount of copper taken up was 1.18 μM; for 1051, the amount of copper taken up was 1.65 μM; and for 1033, the amount of copper taken up was 2.73 μM.

22. Thus, in the ionophore test, as described in Paragraphs 18-21 herein,1033 exhibits greater than a two-fold rise in ionophore performance over CC, while 1051 exhibits a significant rise in ionophore performance over CC. More specifically, 1033 provides a 231% rise and 1051 provides a 39.8% rise in ionophore performance, respectively relative to CC.

23. Based on the data, it is my opinion that one of ordinary skill in the art would conclude that 1051, and especially 1033, exhibit a significantly enhanced capability relative to CC to reduce the levels of Abeta, a common target protein of Alzheimer disease therapies.

24. I declare that all statements made herein of my own knowledge are true and that all statements made on information and belief are believed to be true; and that those statements were made with the knowledge that willful false statements and the like so made are punishable by fine or imprisonment, or both, under Section 1001 of Title 18 of the United States Code, and that such willful false statements may jeopardize the validity of the application or any patent issuing thereon.

By: _____ Dated: 16/09/08

Robert Cherny

CURRICULUM VITAE

DR ROBERT ALAN CHERNY

PART A: BACKGROUND

Academic background

Degrees

1980	BSc	Monash University (majored in Biochemistry & Immunology)
1990	PhD	Prince Henry's Hospital Medical Research Institute, Monash University, Australia Thesis Title: Stromal - epithelial interactions in the ovine endometrium

Scholarships

1988-1990	The William Buckland Foundation Postgraduate Scholarship

Current and Previous appointments

Current Position/s	**Address**
1995-2005 Lecturer and Senior Research Officer (Hon since 2006)	Dept of Pathology, The University of Melbourne
1995-present Senior Research Fellow and Co-Head Oxidation Disorders (Neuropathology Laboratory	The Mental Health Research Institute of Victoria

Previous Appointments	**Address**
1992-1994 Research Officer	Centre for Animal Biotechnology, The University of Melbourne
1990-1992 Research Officer	Department of Physiology, Monash University

1987-1990 PhD student	Prince Henry's Institute of Medical Research (Monash University, Department of Anatomy
1985- 1987 Graduate Research Assistant	Prince Henry's Institute of Medical Research
1982-1985 Graduate Research Assistant, Research and development	Teva Pharmaceuticals Pty Ltd, Jerusalem, Israel; Veterinary products section

Postgraduate Training

I have over 20 years of research experience with a strong leaning to translational research My skill set is broad based. Between 1982 and 1985 my immunology background was applied to veterinary vaccine R&D for a large pharmaceutical company (Teva Pharmaceuticals) where I introduced a new spinner jar method for culturing viruses to replace the traditional roller bottles. Upon my return to Australia in 1985 I was employed as a graduate research assistant where I gained expertise in the areas of cell biology and endocrinology. During my PhD studies at Prince Henry's Institute of Medical Research I became expert at protein analysis by 2D gel electrophoresis, radio-immunoassay, immunohistochemistry and cell and embryo culture techniques. I developed a bicameral chamber for the analysis of vectorial protein secretion by polarised cells and a technique for separating stromal and epithelial cell populations by differential tryspsinisation. This method remains in use to the present day. I was also the first to describe the pattern of oestrogen receptor expression in the uterus of the sheep using immunohistochemistry. My first post-doctoral appointment was in the laboratory of Dr Geoffrey Schwartz in the Department of Physiology, Monash University, investigating the interactions between the various cell types comprising the anterior pituitary and their influence upon cells isolated from the adrenal cortex. This work was reviewed in an article published in Endocrine Reviews (Impact factor 17.3) in 1992. With the completion of this project I joined A/Prof Mal Brandon and Prof Alan Trounson at the Centre for Animal Biotechnology to support a grant to develop bovine embryonic stem cells for accelerating improvement of Victorian dairy herd genetics. Having established that classical stem cell techniques could not be applied to cattle I developed a novel method for extracting pluripotential primordial germ cells from foetal bovine gonads which I demonstrated could integrate into the inner cell mass of a bovine embryo. This technique offered an alternative to embryo splitting for rapid expansion of a high quality genetic stock. The finding was patented and the rights purchased by a commercial entity (Stem Cell Sciences) which grew out of the project.

With the conclusion of that project in 1995 I was approached by Professor Colin Masters to take charge of the Neuropathology laboratory at the Mental Health Research Institute of Victoria (MHRI). This laboratory had been the site of some crucial discoveries in the area of Alzheimer's disease (AD), especially with respect to the expression and biology of the Alzheimer's amyloid precursor protein APP, and its toxic cleavage product Aβ. I took responsibility for rebuilding MHRI AD research which had suffered a steep decline following the movement of

key personnel to laboratories in the USA. These individuals included Dr Ashley Bush with whom I began an extremely fruitful collaboration regarding the role of transition metals in the achitecture and toxicity of the Aβ protein. During the last twelve years I have developed expertise in protein chemistry and extraction techniques, metallochemistry, free-radical biology and oxidative stress in the context of neurodegenerative disorders. My collaborations with the pahramceutical industry have provided me with experience in rational drug design, pharmacokinetics, blood-brain barrier physiology, high throughput assay development, identification of SAR, project management, intellectual property, design and analysis of animal trials and the design phase of clinical trials.

CONTRIBUTION TO THE DISCIPLINE

The last five years have been particularly productive, highlighted by major papers in the Journal of Biological Chemistry (impact factor 6.5), Annals of Neurology (impact factor 7.7), Neuron (impact factor 14.1) and The Lancet (impact factor 18.3), several of which have achieved high to very high citation rates (50 to 300). While I have been keen to establish my academic and scientific credentials, my experience in industry led me to appreciate the key role afforded by commercial interests in translating basic science into therapeutic reality. Thus a feature of my career has always been to concentrate a significant proportion of my efforts on translational science. Since 1999 I have been intimately involved in the process of commercialisation of our research which culminated in an agreement between The University of Melbourne and a public-listed company Prana Biotechnology Pty Ltd and since March 2000 I have been Senior Project Manager for the Prana Biotechnology-University of Melbourne Research Agreement with responsibility for developing *in vitro* screening assays and animal trials. Over the past three years a successful animal trial of a drug for AD for which I had primary responsibility has translated into a positive Phase II human clinical trial of one drug with a Phase II trial of a second generation drug in progress. In addition to the commercial support I have been successful in attracting substantial funds from Government, institutional and philanthropic sources and currently manage a budget in excess of $1.5 million per annum.

Research Profile

National and International Profile:

The high citation rates of my publications attest to the influence of my work in the Alzheimer's research community and I am frequently called upon to review manuscripts and grant applications. In 2002 I was invited to address the International Alzheimer's conference in Philadelphia. I maintain productive collaborations with groups in Chile (Prof Nibaldo Inestrosa, *University of*

Santiago), South Korea (Prof Jae Koh, *University of Ulsan College of Medicine, Seoul*), the USA (Prof Julie Anderson, *Buck Institute for Aging Research, Novato, California*). A proportion of my research commitment during the last five years has been subject to commercial confidentiality however at the recent International Conference on Alzheimer's Disease and Related Disorders in Madrid, Spain, I was senior or presenting author on four presentations and co-author on a further 14 (including two with collaborating labs). I was responsible for coordinating and reviewing the 16 poster and oral presentations of the largest single delegation from an individual laboratory to attend this large and prestigious conference. I have been invited to speak at several local research institutes (Howard Florey, NARI etc) and have been particularly active disseminating current research in Alzheimer's disease to community service groups (eg Rotary, Lions) and to lay interest groups (eg Alzheimer's Association of Australia).

International Collaborations:

- Prof Ashley Bush: *Former Head of the Laboratory for Oxidation Biology, Massachusetts General Hospital, Boston, USA; currently Unit Head, the Oxidation Disorders Laboratory, The Mental Health Research Institute of Victoria and Professor, Department of Pathology, University of Melbourne.* Prof Bush is a long-time collaborator. Typically, his group at Massachusetts General was responsible for generating *in vitro* data and my group in Melbourne applied that information to AD tissue and animal models for AD. Prof Bush returned to Melbourne in 2005 to take up an ARC Federation Fellowship. I continue to partner him in managing the Melbourne laboratory on a day to day basis.
- Assistant Prof Xudong Huang: *Department of Psychiatry, Massachusetts General Hospital, Boston, USA.* Dr Huang has worked with me to translate basic discoveries regarding the redox potential of the Aβ-Cu complex into a practical assay for drug development and screening.
- Dr Lee Goldstein: *Brigham and Womens Hospital Harvard Medical School, Boston, USA.* Dr Goldstein noted that a unique form of previously undiagnosed cataract seemed to be present in the lenses of AD sufferers. We collaborated to detect deposits of Aβ in the excised lenses of AD patients.
- Dr Avi Friedlich: *Bedford Veteran's Affairs Hospital, Boston, USA.* My group worked with Dr Friedlich to explain how the perivascular deposits of Aβ, which are a feature of AD cerebrovasculature, are influenced by the local zinc milieu.
- Dr Mahmoud Kiaei: *Cornell University, New York, USA.* Our lab has worked with Dr Kiaei to investigate the influence of copper on the course of disease in an animal model for Amyotrophic Lateral sclerosis.
- Prof Julie Anderson: *Buck Institute for Aging Research, Novato, California, USA.* Our collaboration has revolved around the role of metals in Parkinson's disease and the potential of metal chelating agents to attenuate neuronal damage in animal models of PD.
- Prof Jae Koh: *University of Ulsan College of Medicine, Seoul, Republic of*

Korea. We have been studying the role of zinc in the formation of amyloid plaques.

- Prof Nibaldo Inestrosa: *University of Santiago, Chile.* Prof Inestrosa's group is studying the influence of copper upon Aβ expression in a transgenic c.elegans model. Our role in the collaboration has been to measure metal levels and consult on experimental design.
- A/Prof Takaomi Saido: *RIKEN Brain Science Institute, Saitama, Japan;* Prof Yoshi Kato: *School of Human Science and Environment, University of Hyogo, Japan;* and Prof Alex Roher: *Sun Health Research Institute, Arizona, USA.* We are studying the effects of oxidative processes upon the expression of oxidatively modified forms of Abeta in the AD brain.

National Collaborations:

- Prof Colin Masters: As former Chairman of the Department of Pathology and long-time head of our neurodegeneration group, Professor Masters has been supervisor, mentor and scientific collaborator. Our particular area of interest is identification of the 'toxic principle' in Alzheimer's disease.
- Prof Catriona McLean: *Head, Neuropathology, Alfred Hospital.* Prof Mclean and I have worked together to characterise the abundance and pathological relevance of soluble and insoluble Abeta in human AD brain.
- Dr Qiao Xin Li: *Department of Pathology, University of Melbourne.* Our collaboration involved ascertaining the distribution of soluble and insoluble Aβ species in a non-amyloidogenic animal model for Alzheimer's disease.
- Dr. Roberto Cappai: *Department of Pathology, University of Melbourne.* Our collaborations include metal binding to recombinant prion species, structure-function relationships in the Abeta metal binding site and investigations into the chemical basis of the aggregation of α synuclein
- Dr Kevin Barnham: *Department of Patholog,y University of Melbourne.* Our collaboration revolves around the physico-chemical properties of the Aβ-metal complex and oxidative modifications to Aβ resulting from the redox activity of the Aβ-copper interaction.
- Dr Anthony White: *Department of Biochemistry, University of Melbourne.* Our collaboration is concerned with the amelioration of the toxic effects of Abeta and metals in cell culture
- Dr Wah Chin Boon: *Prince Henry's Institute of Medical Research.* Our ongoing collaboration involves the role of estrogen in Aβ amyloid deposition in an Alzheimer's mouse model.
- Dr Victor Villemagne (2005-present): Dr Villenagne is a Nuclear Medicine practitioner recruited by Prof Masters to establish imaging techniques for the diagnosis of AD. I have worked closely with Dr Villemagne in working up methods for the evaluation of potential imaging agents in animals and post mortem human tissue.

- Prof Ralph Martins: *Macusker Foundation for Alzheimer's Research, Perth.* Plasma samples from a large ageing cohort were analysed for metal content.

The Biometals Analysis Facility, Department of Pathology, University of Melbourne

I founded and manage the Biometals Analysis Facility at the University of Melbourne. Since its inception in 2000 the BAF has become an invaluable and unique resource not duplicated elsewhere in Australia. The unit, which consists of an Inductively Coupled Plasma Mass Spectrometer and dedicated operator situated in the School of Medicine, has provided a gateway to numerous collaborations, both national and international which has had a dramatic effect on our research output. This resource is freely available to all members of the wider neurodegeneration research group and is heavily used by that group.

International collaborations which have employed our facility in the area of neurodegenerative disorders include the following:

- Prof Julie Anderson: *Buck Institute for Aging Research, Novato, California, USA.* Our collaboration has revolved around the role of metals in Parkinson's disease and the potential of metal chelating agents to attenuate neuronal damage in animal models of PD.
- A/Prof Simon Melov: *Buck Institute for Aging Research, Novato, California, USA.* Metal involvement in ageing and oxidative stress.
- Prof Jae Koh: *University of Ulsan College of Medicine, Seoul, Republic of Korea.* Studying the role of zinc in the formation of amyloid plaques.
- Assist Prof Xudong Huang: *Department of Psychiatry, Massachusetts General Hospital, Boston, USA.* Translating basic discoveries regarding the redox potential of the Aβ-Cu complex into a practical assay for drug development and screening.
- Dr Lee Goldstein: *Brigham and Womens Hospital, Harvard Medical School, Boston, USA.* Dr Goldstein noted that a unique form of previously undiagnosed cataract seemed to be present in the lenses of AD sufferers. We collaborated to detect deposits of Aβ and associated metals in the excised lenses of AD patients.
- Dr Avi Friedlich: *Bedford Veteran's Affairs Hospital, Boston, USA.* Explaining how the perivascular deposits of Aβ which are a feature of AD cerebrovasculature are influenced by the local zinc milieu.
- Dr Mahmoud Kiaei: *Cornell University, New York, USA.* Investigating the influence of copper upon the course of disease in an animal model for

Amyotrophic Lateral sclerosis.

- Dr Lenore Launer: *National Institutes of Mental Health, USA.* The correlation of CSF metals with Aβ levels in a large cohort of AD and age-matched patients.

Most Significant Papers

Cherny, R.A., Legg, J.T., McLean, C.A., Fairlie, D.P., Huang, X., Atwood, C.S., Tanzi, R.E, Masters, C.L. and Bush, A.I. (1999) Aqueous dissolution of Alzheimer's disease Aβ amyloid deposits by biometal depletion. J.Biol. Chem **274**: 23223-23228. **(163 citations)**

•In this work I demonstrated that the metals known to be associated with the amyloid plaques in AD brains play a crucial structural role in the deposits. I showed that application of a copper-zinc chelator of suitable affinity prepared in physiological buffer could dissolve amyloid deposits which hitherto were considered intractable under all but the most stringent conditions. This series of observations gave rise to the possibility that such agents if suitably non-toxic and bioavailable may be the basis of a novel therapeutic approach to the treatment of AD.

McLean, C.A.*, **Cherny, R.A.***, Fraser, F.W., Fuller, S.J., Smith, M.J., Beyreuther, K, Bush, A.I. and Masters, C.L. (1999) Soluble Aβ as a determinant of severity of neurodegeneration in Alzheimer's disease. Ann. Neurol.**46**: 860-866. **(318 citations)**

• It was commonly held that insoluble Aβ in the form of fibrils making up the amyloid plaques of AD were the primary neurotoxic agents in the disease. The work described here showed that the minor population of soluble Aβ and not the predominating fibrillar Aβ which correlates with neurodegeneration. This finding signalled a paradigm change in the search for the toxic principle in AD and has led to identification of soluble oligomers of Aβ as novel therapeutic targets.

* equal contribution

Cherny, R.A., Atwood, C.S., Xilinas, M.E., Gray, D.N., Jones, W.D., McLean, C.A., Barnham, K.J., Volitakis, I., Fraser, F.W., Kim, Y-S., Huang, X., Goldstein, L.E., Moir, R.D., Lim, J.T., Zheng, H., Tanzi, R.E., Masters, C.L. and Bush, A.I. (2001) Treatment with a copper-zinc chelator markedly and rapidly inhibits ß-amyloid accumulation in Alzheimer's disease transgenic mice. Neuron **30**: 665-676. **(318 citations)**

• The findings described in this article represent the first practical demonstration of the therapeutic potential of metal complexing agents for the treatment of Alzheimer's disease as first proposed in my 1999 paper (J.Biol. Chem **274**: 23223-23228)

Kaur, D., Yantiri, F., Mo, J.Q., Viswanath, V., Boonplueang, R., Jacobs, R., Yang, L., Flint-Beal, M., DiMonte, D., **Cherny, R.A.**, Bush, A.I. and Andersen, J.K. (2003) Non-toxic genetic or pharmacological iron chelation prevents MPTP-induced neurotoxicity

in vivo: A novel therapy for Parkinson's Disease. Neuron, **37**: 899-909 **(115 citations)**

• This work demonstrated that the copper/zinc chelator clioquinol is dramatically effective in reducing the symptoms of Parkinson's disease as well as Alzheimer's disease. This pivotal paper underlines our fundamental view that the major diseases of protein aggregation in the CNS are linked by a common pathophysiological mechanism.

Craig W Ritchie, Andrew Mackinnon, Steve Macfarlane , **Robert Cherny**, Qiao-Xin Li , Amanda Tammer, Darryl Carrington , Christine Mavros , Irene Volitakis, Konrad Beyreuther, Stephen Davis and Colin L Masters (2003) Metal – protein attenuation with iodochlorhydroxyquin (clioquinol) targeting Aβ amyloid deposition and toxicity in Alzheimer's disease: a pilot Phase 2 clinical trial.(2003) Arch Neurol. **60**: 1685-1691 **(134 citations)**

• This article presents results of the first clinical trial of clioquinol in Alzheimer's disease patients. The trial provided crucial clinical support for the hypothesis of metal dependent Abeta neurotoxicity in AD and reinforced the validity of the in-vitro and animal based screens for AD drug development.

Cherny, R.A., Barnham, K.J., Bush, A.I., Cappai, R., Gautier, E.C.L., Masters, C.L., Carrington, D., Kocak, G., Volitakis, I., Kok, G.B. (2006) PBT2, a novel MPAC for the treatment of Alzheimer's disease. Alzheimer's and Dementia: 2 (Supplement) S646
• This is the first description of a novel Alzheimer's drug developed using the Structure-Activity Relationship derived from our medicinal chemistry screening program. This drug has completed Phase I safety trials and in 2007 proceeded to a Phase II biomarker and efficacy study in AD patients.

APPENDIX 2

Ionophore assay protocol

At the end of the incubation, the media was removed and replaced with 1 ml PBS to dislodge the cells, which were then put into Eppendorf tubes and pelleted.

M17 human neuroblastoma cells are plated out on 6 well tissue culture plates and left overnight. Sufficient cells are provided to achieve approximately 70 % confluence (1 million cells).

Cells were incubated in a media of 1 ml of Opti-MEM (Invitrogen) with added 10% FBS, Sodium Pyrvate, NEAA, and PenStrep and 10 mM of Cu2+ for 5 hr at 37_C. The cells are also incubated with or without the various test compounds.

At the conclusion of the incubation the media is removed using a vacuum aspirator and 1 ml of PBS is added to dislodge the cells. Cells are then transferred to microfuge tubes and pelleted. The PBS is discarded and the remaining cell pellets are frozen at -20 C.

The cell pellets were then used for inductively coupled plasma mass spectrometry (ICPMS) analysis of metal content.

The cell pellets are prepared as follows:
50 ul of concentrated Nitric Acid (Aristar, BDH) is added to each cell pellet and the samples allowed to digest overnight. Following this procedure the samples are heated for 20 min at 90°C to complete the digestion. The volume of each sample is reduced to ~45 ul after digestion.to which a further 1 ml of 1% Nitric Acid diluent is added. (referred to as the "preparation solution" samples).

Measurements are performed using a Varian UltraMass ICPMS instrument under operating conditions suitable for routine multi-element analysis.

The instrument is calibrated using Blank, 10, 50 and 100 ppb samples of a certified multi-element ICPMS standard solution (ICP-MS- CAl2-1, Accustandard) for

Fe, Cu and Zn in 1% nitric acid. A certified internal standard solution containing 100 ppb Yttrium (Y 89) is included as an internal control (ICP-MS- IS-MIX1-1, Accustandard).

The metal content of the samples is represented as the molar concentration of metal per cell pellet.

The ICPMS based analysis is as previously described in Maynard et al., 2006.

APPENDIX 3

Figure 1

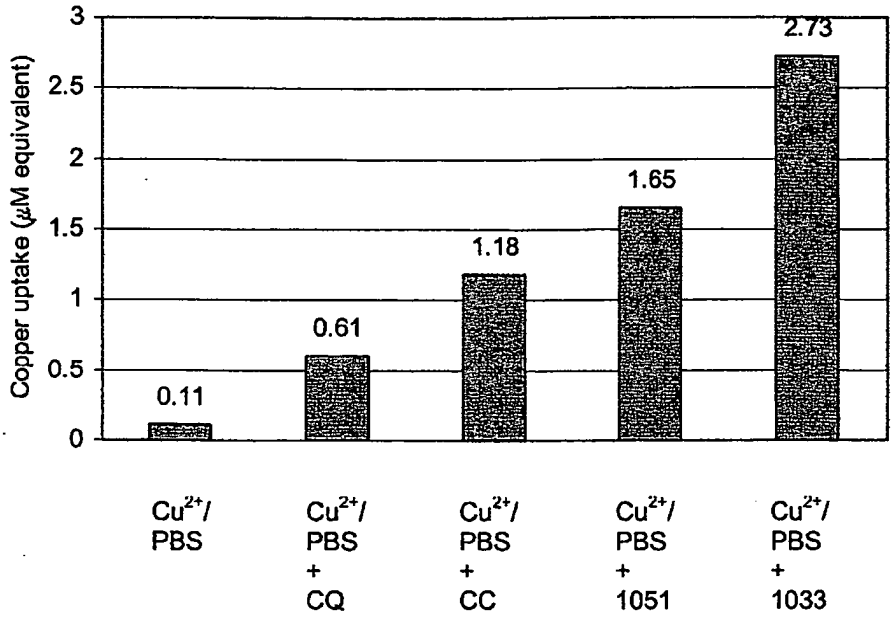

APPENDIX 4

White A.R. et al Journal of Biochemistry (attached printed copy)

Cater M.A.et al, Journal of Biochemistry (attached printed copy)

BJ www.biochemj.org

BJ Cell

Biochem. J. (2008) 412, 141–152 (Printed in Great Britain) doi:10.1042/BJ20080103

Intracellular copper deficiency increases amyloid-β secretion by diverse mechanisms

Michael A. CATER*, Kelly T. McINNES†, Qiao-Xin LI‡, Irene VOLITAKIS*, Sharon LA FONTAINE†, Julian F. B. MERCER† and Ashley I. BUSH*‡[1]

*Oxidation Biology Laboratory, Mental Health Research Institute of Victoria, Parkville, Victoria 3052, Australia, †Centre for Cellular and Molecular Biology, Deakin University, Burwood, Victoria 3125, Australia, and ‡Department of Pathology, University of Melbourne, Parkville, Victoria 3010, Australia

In Alzheimer's disease there is abnormal brain copper distribution, with accumulation of copper in amyloid plaques and a deficiency of copper in neighbouring cells. Excess copper inhibits Aβ (amyloid β-peptide) production, but the effects of deficiency have not yet been determined. We therefore studied the effects of modulating intracellular copper levels on the processing of APP (amyloid precursor protein) and the production of Aβ. Human fibroblasts genetically disposed to copper accumulation secreted higher levels of sAPP (soluble APP ectodomain)α into their medium, whereas fibroblasts genetically manipulated to be profoundly copper deficient secreted predominantly sAPPβ and produced more amyloidogenic β-cleaved APP C-termini (C99). The level of Aβ secreted from copper-deficient fibroblasts was however regulated and limited by α-secretase cleavage. APP can be processed by both α- and β-secretase, as copper-deficient fibroblasts secreted sAPPβ exclusively, but produced primarily α-cleaved APP C-terminal fragments (C83). Copper deficiency also markedly reduced the steady-state level of APP mRNA whereas the APP protein level remained constant, indicating that copper deficiency may accelerate APP translation. Copper deficiency in human neuroblastoma cells significantly increased the level of Aβ secretion, but did not affect the cleavage of APP. Therefore copper deficiency markedly alters APP metabolism and can elevate Aβ secretion by either influencing APP cleavage or by inhibiting its degradation, with the mechanism dependent on cell type. Overall our results suggest that correcting brain copper imbalance represents a relevant therapeutic target for Alzheimer's disease.

Key words: Alzheimer's disease (AD), amyloid, amyloid precursor protein (APP), copper, Menkes protein (ATP7A), neuron.

INTRODUCTION

AD (Alzheimer's disease) is characterized by three main pathologies in the brain: extraneuronal senile plaques, intraneuronal neurofibrillary tangles and diffuse loss of neural synapses (reviewed in [1]). The principal constituent of the senile plaque is aggregated Aβ (amyloid β-peptide) [2,3]. Aβ is normally secreted by cells and found in biological fluids. Considerable evidence indicates that the formation of senile plaques is mediated by endogenous biometals [4–7]. Copper and zinc are both enriched in Aβ plaques and co-purify with Aβ from post-mortem AD brain [6–8]. Metal chelation has also been shown to dissolve Aβ aggregates extracted from post-mortem AD brain [5] and inhibit Aβ accumulation in transgenic mouse models *in vivo* [9,10]. Aβ binds copper [11], and by catalysing its reduction can generate H_2O_2 from oxygen [8,12]. Therefore copper–Aβ complexes could contribute to AD disease progression. Perturbed metal homeostasis may foster Aβ aggregation in the AD brain.

Soluble Aβ is derived from intracellular proteolytic cleavage of APP (amyloid precursor protein) [13]. APP localizes to the constitutive secretory pathway within cells and is orientated with a large N-terminal ectodomain that is either luminal [TGN (*trans*-Golgi network)/vesicles] or exofacial (plasma membrane) and a short cytoplasmic C-terminal region. APP undergoes intramolecular cleavage by α-, β- and γ-secretases (Figure 1). Apart from within the Aβ region, APP contains a second histidine-based copper-binding site located in the N-terminal ectodomain, which is homologous with APLP (amyloid precursor-like protein)2 [14]. There is growing evidence for physiological interactions between APP (or its proteolytic fragments) and copper metabolism. APP and APLP2 knockout mice accumulate copper in tissues, notably in brain and liver [15,16], whereas transgenic mice overexpressing the Swedish mutant of APP or just the last 100 C-terminal residues have a decreased level of brain copper [17,18]. Copper levels modulate APP transcription [19] and may modify APP protein processing. In one report, APP processing was sensitive to extracellular copper levels, with an elevation in copper reducing the level of Aβ production while increasing the secretion of APP ectodomain in cultured cells [20]. In addition, mutation of ATP7B (Wilson protein), which significantly increases liver and brain copper, has been shown to decrease brain and plasma Aβ levels [18].

Copper homeostasis is heavily dependent on the activities of the copper transporters ATP7A (Menkes protein) and ATP7B, which are defective in the genetic disorders of Menkes and Wilson disease respectively (reviewed in [21]). ATP7A is expressed in most tissues (except the liver), whereas ATP7B is expressed in liver hepatocytes, brain, breast and placenta. These copper ATPases translocate cytosolic copper across membranes and into secretory compartments. To remove excess intracellular copper, both proteins relocate from the TGN to exocytic vesicles [22,23]. Previously, ATP7A was found to generate vesicular copper that is

Abbreviations used: Aβ, amyloid β-peptide; AD, Alzheimer's disease; APLP, amyloid precursor-like protein; APP, amyloid precursor protein; APP695, 695 residue APP; ATP7A, Menkes protein; ATP7B, Wilson protein; BACE1, β-site amyloid precursor protein-cleaving enzyme 1; BCS, bathocuproinedisulfonic acid; BME, basal Eagle's medium; C83, α-cleaved APP C-terminal fragment; C99, β-cleaved APP C-terminal fragment; CHO, Chinese-hamster ovary; CT, C-terminus; DAPT, *N*-[*N*-(3,5-difluorophenacetyl)-L-alanyl]-(*S*)-phenylglycine t-butyl ester; FCS, fetal calf serum; NP40, Nonidet P40; NT, N-terminus; PBST, PBS containing 0.05 % Tween 20; RT–PCR, reverse transcription–PCR; sAPP, soluble APP ectodomain; SOD1, superoxide dismutase 1; TBST, Tris-buffered saline with Tween 20; TGN, *trans*-Golgi network; wt, wild-type.

[1] To whom correspondence should be addressed (email abush@mhri.edu.au).

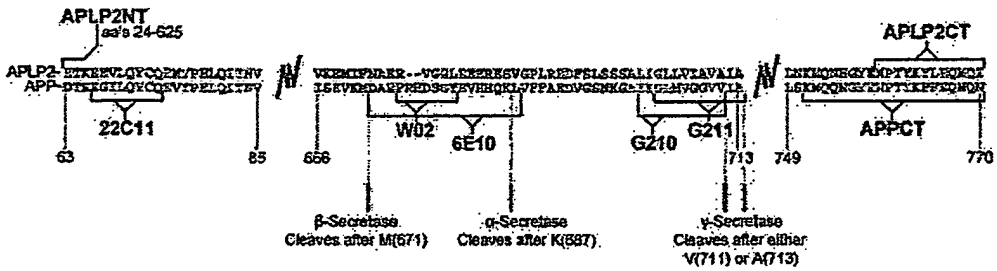

Figure 1 Schematic representation of antibody epitopes and secretase cleavage sites

Amino acid sequence alignment between the regions of APP and APLP2 recognized by the antibodies used in this study. Antibodies are shown in bold and their epitopes are indicated by horizontal brackets. APP/APLP2 regions are shown by their amino acid numbers under solid vertical lines. The main secretase cleavage sites are also shown.

released into the synaptic cleft from the post-synaptic neuron on NMDA (*N*-methyl-D-aspartate) stimulation [24]. Therefore APP, Aβ and ionic copper are co-localized to the glutamatergic synaptic cleft where amyloid pathology first occurs.

Information about the impact of intracellular copper on APP processing is limited. While increasing copper in cell culture [20] and in transgenic mice [18,25] is associated with decreased Aβ levels, the mechanism for this is unclear. Moreover, nothing is known about the effect of copper deficiency on Aβ production, which is important because AD brain tissue is copper deficient [26–29]. To address this, we have studied human fibroblast cell lines with genetically modified levels of the copper-efflux proteins ATP7A and ATP7B to determine how changes in the level of intracellular copper influence APP and APLP2 processing and Aβ production. We further investigated the influence of copper modulation on APP and APLP2 proteolysis in human neuroblastoma cells.

EXPERIMENTAL

Cells and reagents

Immortalized human fibroblast cell lines [GM2069 (normal), A12-H9, Me32a, C3-C1 and WND16] with different copper phenotypes were generated as described previously [30]. The details of these cell lines and their characterization are shown in Figure 2. Fibroblasts were cultured at 37 °C and 5 % CO_2 as a monolayer in BME (basal Eagle's medium; Trace BioSciences, Noble Park, VIC, Australia), supplemented with 10 % (v/v) FCS (fetal calf serum; Commonwealth Serum Laboratories, Broadmeadows, VIC, Australia), 2 mM L-glutamine, 12 mM $NaHCO_3$ and 100 mM Hepes (Thermo Electron). The fibroblast cell lines transfected with *ATP7A* or *ATP7B* were cultured in medium containing 500 μg/ml G418 to maintain transgene expression [30]. The human SY5Y neuroblastoma line was cultured at 37 °C as a monolayer in RPMI 1640 medium (Trace BioScience) supplemented with 20 % (v/v) FCS (Commonwealth Serum Laboratories), 2 mM L-glutamine, 12 mM $NaHCO_3$, 100 mM Hepes, 1 mM pyruvate (Thermo Electron) and 0.5 μM uridine (Sigma). The SY5Y cell line transfected with wt (wild-type) APP695 (695 residue APP) was cultured in medium supplemented with 2 μg/ml puromycin to maintain transgene expression.

Synthetic Aβ [Aβ(1–40) and Aβ(1–42)] were purchased from the W.M. Keck Foundation Laboratory (Yale University, New Haven, CT, U.S.A.) and was dissolved in 50 mM Tris/HCl (pH 6.8), 150 mM NaCl and 0.5 % (v/v) NP40 (Nonidet P40). The γ-secretase inhibitor DAPT {*N*-[*N*-(3,5-difluorophenacetyl)-L-alanyl]-(*S*)-phenylglycine t-butyl ester} was purchased from Merck. The goat polyclonal anti-ATP7A and anti-ATP7B antibodies (designated R17 and NC36 respectively) have been characterized previously [31,32], The following antibodies were supplied by the Department of Pathology, University of Melbourne (Melbourne, VIC, Australia): mouse monoclonal antibody WO2 [33], mouse monclonal anti-Aβ(1–40) antibody (G210) [33], mouse monoclonal anti-Aβ(1–42) antibody (G211) [33], rabbit polyclonal anti-APLP2NT antibody [34] (where NT is N-terminus) and mouse monoclonal antibody 22C11 [35]. Mouse monoclonal antibody 6E10, rabbit polyclonal anti-APPCT (where CT is C-terminus) and anti-APLP2CT antibodies were purchased from Merck, and mouse monoclonal anti-β-actin was purchased from Sigma. The epitopes recognized by the APP- and APLP2-specific antibodies are shown in Figure 1. All other reagents were supplied by Sigma unless specified otherwise.

Culturing conditions and transfection

Culturing conditions were optimized to allow the concurrent examination of both whole-cell lysates and conditioned medium by Western-blot analysis. In a 12-well tray, each fibroblast line was seeded into separate wells ($\sim 1.6 \times 10^5$ cells) and cultured in 2 ml of medium (see above) for 24 h. The medium was then replaced with 400 μl of fresh basal medium or medium containing 2 μM DAPT and/or 10 μM cyclohexamide, or 100 μM or 200 μM $CuCl_2$ (see the Results section for details) and the fibroblasts were further cultured for 16 h overnight. The conditioned medium was removed and retained, and the cells were quickly washed with ice-cold PBS before the addition of 150 μl of ice-cold lysis buffer [50 mM Tris/HCl (pH 6.8), 150 mM NaCl, 0.5 % (v/v) NP40 and protease inhibitor cocktail] to each well. The tray was rocked on ice at 4 °C for 10 min and then the cell lysates were transferred into 1.5 ml tubes. Lysates and conditioned medium were centrifuged at 9503 *g* for 10 min at 4 °C to remove cellular debris. These conditions were optimized so that 40–50 μg of total protein (lysate) was analysed by Western blot. SY5Y cells overexpressing wtAPP695 were cultured to $\sim$80 % confluency in 25 cm^2 flasks. The medium (see above) was then replaced with 2.5 ml of fresh basal medium or medium containing treatment (2 μM DAPT, 100 μM or 200 μM $CuCl_2$; see the Results section for details) and the cells were further incubated for 16 h overnight. For copper chelation treatment, cells were cultured in medium supplemented with 200 μM BCS (bathocuproinedisulfonic acid) and 200 μM D-penicillamine for an initial 56 h period. Cell lysates and conditioned medium was prepared as described above for the fibroblasts; however, the cells were lysed in 500 μl of ice-cold lysis buffer.

The generation of the mammalian expression construct encoding wtAPP695 (pIRESpuro2-based) has been described

A

Cell lines	Characteristics	Copper Phenotype*
GM2069	Normal (control) fibroblasts.	Normal
Me32a	Fibroblasts derived from Menkes disease patient. Accumulate copper due to lacking ATP7A and ATP7B expression.	~650% increase
A12-H9	Me32a cells transfected with ATP7A. Enhanced capacity to efflux copper due to ATP7A overexpression.	~65% decrease
WND16	Me32a cells transfected with ATP7B. Partially rescues Menkes patient fibroblasts. ATP7B sequesters copper into exocytic vesicles.	~100% increase

* Intracellular copper levels compared to normal fibroblasts (GM2069) calculated from results shown in Figure C

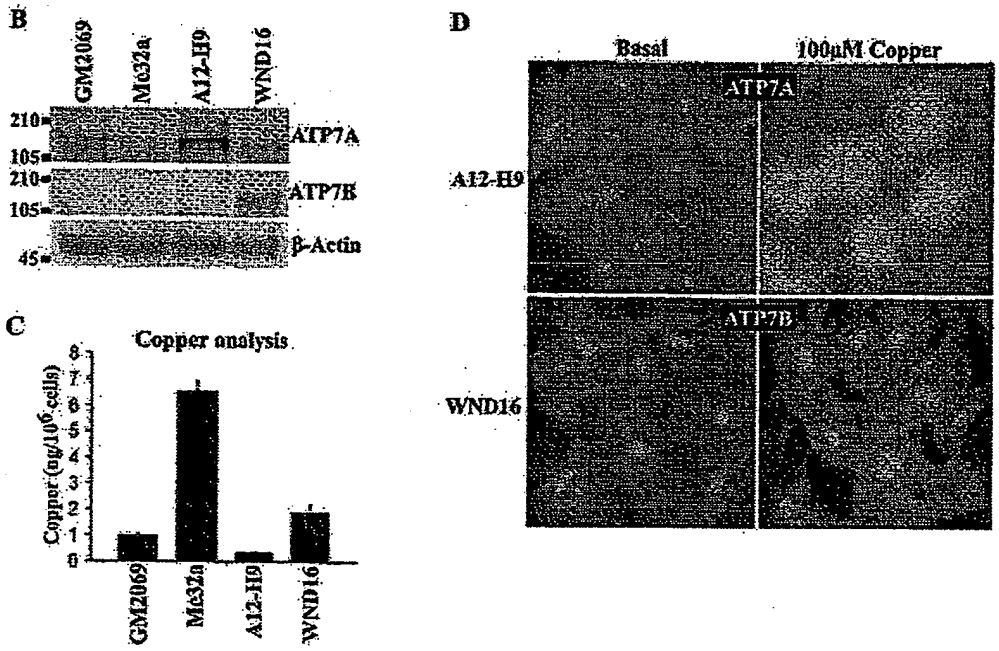

Figure 2 Characterization of immortalized human fibroblast cell lines with genetically modified intracellular copper levels

(A) Description of each fibroblast line including the relative level of intracellular copper compared with the control fibroblast line (GM2068). (B) Western-blot analysis comparing the level of ATP7A and ATP7B expression in each fibroblast line, with anti-β-actin antibody used as a control. Molecular-mass-markers are indicated on the left (in kDa). (C) Copper content of each fibroblast line. Results are normalized means ± S.D. ($n = 3$) for each cell line and are ng of copper per 1×10^6 cells. (D) Immunofluorescence microscopy showing the copper-dependent subcellular localization of ATP7A and ATP7B in A12-H9 and WND16 fibroblasts respectively. The fibroblasts were cultured in either basal medium (0.5–1 μM Cu) or 100 μM $CuCl_2$-supplemented medium for 2 h at 37 °C before fixation.

previously [36]. Transient transfection of GM2069 and A12-H9 fibroblasts with the plasmid encoding wtAPP695 was performed using FuGENE®HD (Roche) following the manufacturer's recommendations. Stable transfection of SY5Y cells with the plasmid encoding wtAPP695 was performed using Lipofectamine™ (Invitrogen) following the manufacturer's instructions. The cells were recovered overnight in RPMI 1640 medium containing 20% (v/v) FCS before transfectants were isolated by treatment with 2 μg/ml puromycin for 30 days.

Western-blot analysis and densitometry

Cell lysates and conditioned media were fractionated by electrophoresis on Novex® pre-cast gels (10% or 10–20% gradient gels) using the Xcell Surelock™ mini-cell system (Invitrogen). Samples were prepared for electrophoresis by the addition of Novex® Tricine SDS sample buffer (Invitrogen) and 10% (v/v) 2-mercaptoethanol, and were heated at 90 °C for 5 min. Following electrophoresis (125 V for ~90 min), proteins were transferred on to nitrocellulose (Amersham) using the XCellII™ blot module and the Xcell Surelock™ mini-cell system (Invitrogen) according to the manufacturer's instructions. The nitrocellulose membrane was then blocked using 5% (w/v) non-fat dried skimmed milk powder in TBST (Tris-buffered saline with Tween 20) buffer [10 mM Tris/HCl (pH 8.0), 150 mM NaCl and 0.1% (v/v) Tween 20] for 1 h at room temperature (22 °C). The membrane was then incubated with primary antibody diluted in TBST at 4 °C overnight or for 2 h at room temperature. The following primary antibodies were used: anti-ATP7A (R17, 1:1000 dilution), anti-ATP7B (NC36, 1:1000 dilution), anti-β-actin (1:10000 dilution), WO2 (1:25 dilution), 22C11 (1:100 dilution), 6E10 (1:100 dilution), APLP2NT (1:1500 dilution), APLP2CT (1:5000 dilution) and APPCT (1:20000 dilution) antibodies. After three washes, each for 10 min with TBST, the appropriate HRP (horseradish peroxidase)-conjugated secondary antibody (Dako; 1:10000 dilution in TBST) was applied to the membrane for 1 h at room temperature. Analysis was carried out using ECL (enhanced chemiluminescence) reagent (Amersham),

following the manufacturer's instructions and images were captured using the LAS-3000 imaging suite and analysed using Multi Gauge software (Fuji).

Densitometry was used to evaluate immunolabelled protein intensity and was expressed as a percentage comparison with the control experiment. Pixel intensities (arbitrary units) were quantified using Multi Gauge software (Fuji) and their levels were normalized relative to β-actin controls. The average of three independent experiments for each condition (as detailed in the Results section) was used for comparison. We also determined whether the correlation between the level of Aβ and pixel intensity was linear (results not shown). Incremental amounts of synthetic Aβ(1–40) were subjected to densitometry and their pixel intensity values (arbitrary units) were compared in order to determine linearity [gradient (m)]. We found that provided the amount of Aβ was below 100 pg then a linear relationship was maintained ($m = 1$). However, if the level exceeded 100 pg, then this linearity was lost. We therefore assumed linearity in the densitometry evaluation of the Aβ bands shown in Figure 5C, because their intensity was less than that of 100 pg Aβ(1–40). The linearity of β-actin densitometry measurements was also evaluated and a linear relationship existed when 60 μg or less of total cellular lysate was used (results not shown).

Antibody-capture ELISA for Aβ quantification

The level of Aβ in culture medium was quantified using DELFIA® double-capture ELISA as described previously [36,37]. Briefly, separate wells (of a 96-well plate) were coated with the mouse monoclonal anti-Aβ(1–40) antibody (G210, 0.4 μg/well) or anti-Aβ(1–42) antibody (G211, 0.6 μg/well) and then blocked with casein buffer [0.5 % (w/v) casein with PBST (PBS containing 0.05 % (v/v) Tween 20)] for 2 h at 37 °C. Plates were washed with PBST before biotinylated WO2 together with culture medium or synthetic Aβ standards [Aβ(1–40) and Aβ(1–42)] was added to each well and incubated overnight at 4 °C. The plates were again washed with PBST and then streptavidin-labeled europium (PerkinElmer) was applied to each well. Enhancement solution (PerkinElmer) was then added and the absorbance (A) was measured using a Wallac VICTOR^2 1420 Multilabel plate reader (PerkinElmer; $\lambda_{ex} = 340$ nm and $\lambda_{em} = 613$ nm). Results obtained with the Aβ standards generated a standard curve, which was then used to calculate the Aβ concentration in the culture media (expressed as ng/ml). Each sample was measured in triplicate wells and averaged. Results are normalized means ± S.D. ($n = 3$) for each condition.

Immunofluorescence microscopy

The A12-H9 and WND16 fibroblast cell lines were cultured in 75 cm^2 flasks to ~90 % confluency before being harvested with 3 ml of trypsin solution [0.05 % (v/v) trypsin and 0.02 % (v/v) EDTA] and adjusted to 10 ml with serum-containing medium [10 % (v/v) FCS]. In a 24-well tray, aliquots (100 μl) of the 10 ml cell suspensions (~8×10^4 cells) were seeded on to flamed 13 mm glass coverslips and were cultured with 1 ml medium until the cells reached ~80 % confluency. The medium was then replaced with either basal (0.5–1 μM $CuCl_2$) or supplemented (100 μM $CuCl_2$) medium and the fibroblasts were incubated for a further 2 h. After treatment, the cells were fixed by incubation in 4 % (w/v) paraformaldehyde in PBS for 10 min at room temperature, permeabilized using 0.1 % (v/v) Triton X-100 in PBS for 10 min at room temperature and then blocked in 1 % (w/v) BSA and 1 % (w/v) gelatin in PBS at 4 °C overnight. In between each step, the cells were washed four times with blocking solution. The coverslips were then incubated with either anti-ATP7A antibody (R17, 1:2000 dilution) or anti-ATP7B (NC36, 1:5000 dilution) for 1 h at room temperature. Following four washes with blocking solution, the coverslips were then incubated with donkey anti-goat Alexa Fluor® 488 (Chemicon; 1:2000 dilution in blocking solution) for 1 h at room temperature. Coverslips were mounted on to glass microslips using 2.6 % (w/v) 1,4-diazadicyclo[2.2.2]octane (Sigma) in 90 % (v/v) glycerol. Immunolabelled cells were analysed using Olympus PROVIS AX70 microscope and a × 60 oil objective lens.

Intracellular metal analysis

The fibroblast cell lines were each split into triplicate 75 cm^2 flasks containing 20 ml of medium and incubated for 24 h. The medium was then replaced with fresh medium (see above) and the cells were incubated for a further 16 h. The medium was then discarded and the cells washed with 2 ml of trypsin solution [0.025 % (v/v) trypsin and 0.02 % (v/v) EDTA] before being harvested with 1.6 ml of trypsin solution. Cells were counted using a haemocytometer and 1.5 ml of the cell suspension was centrifuged at 1000 g for 5 min at room temperature to pellet the cells, after which the supernatant was removed and the pellet was stored at −20 °C until it was analysed for copper content. Analysis of the level of copper, zinc and iron in the SY5Y overexpressing wtAPP695 cells was performed as described above; however, these cells were cultured for 56 h before the medium was replaced for 16 h overnight treatment. For copper chelation treatment, the cells were also cultured in medium supplemented with 200 μM BCS and 200 μM D-penicillamine for the initial 56 h period. Cellular metal concentration was measured using inductive-coupled plasma MS (UltraMass 700, Varian). The average of triplicate determinations for each cell line and condition was used for comparison.

RT–PCR (reverse transcription–PCR)

The generation of cDNA from the four fibroblast cell lines was achieved using the SuperScript™ III CellsDirect cDNA synthesis system (Invitrogen) following the manufacturer's protocol. Oligonucleotides used to amplify APP, APLP2 and β-actin were designed for specificity and complemented the human sequence. The APP-specific oligonucleotides are capable of amplifying all *APP* alternatively-spliced products. The sequences of these primers are as follows: APP#1 (forward) 5′-AATGTGGATTCTGCTGATGCGGAG-3′, APP#2 (reverse) 5′-CCCATTCTCTCATGACCTGGGA-3′, APLP2#1 (forward) 5′-TCGCTTTGTTACACCTTTC-3′, APLP2#2 (reverse) 5′-TAGCTTGAAGCTCTGCCTCT-3′, β-actin#1 (forward) 5′-GGCGGCAACACCATGTACCCT-3′ and β-actin#2 (reverse) 5′- AGGGGCCGGACTCGTCATACT-3′. The PCR reaction contained 1 × PCR buffer, 0.2 mM of each dNTP, 2 mM $MgCl_2$, 0.2 μM of each primer, 2.5 units Platinum Taq DNA polymerase and 3 μl of cDNA (Invitrogen). Reactions were run on an Eppendorf Epgradient S Mastercycler on the following program: one cycle of 94 °C for 2 min, 38 cycles of 94 °C for 45 s, 57 °C for 60 s and 72 °C for 60 s, followed by one cycle of 72 °C for 2 min. The PCR reactions were resolved on 1.8 % (w/v) agarose gels using standard electrophoresis procedures.

RESULTS

Human fibroblasts with altered intracellular copper levels

Human fibroblast cell lines with genetically modified levels of the copper-efflux proteins ATP7A and ATP7B, and therefore different copper phenotypes (Figure 2A), were used to determine if

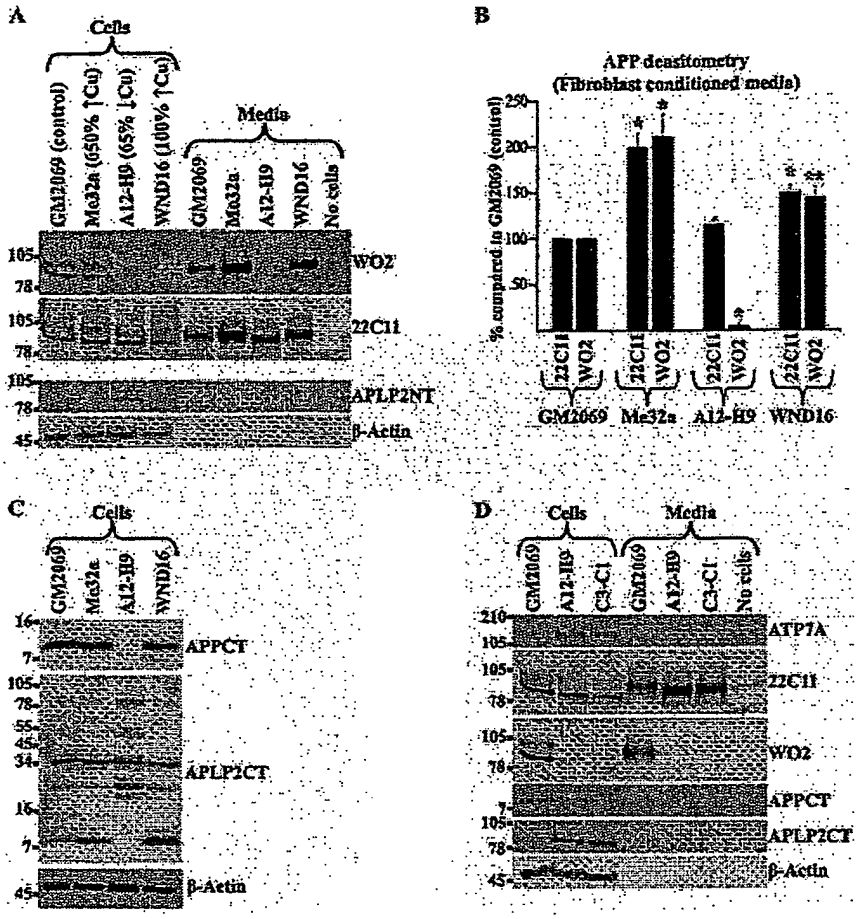

Figure 3 Intracellular copper levels dramatically influence APP and APLP2 metabolism

(**A**) Western-blot analysis of APP and APLP2 in whole-cell lysates and conditioned medium from the indicated fibroblast cell lines. Whole-cell lysates and medium were Western blotted using WO2, 22C11 and APLP2NT antibodies, with anti-β-actin antibody as a control. The percentage increases and decreases in parenthesis refer to the change in copper levels compared with the control cell line. (**B**) Densitometric analysis of the level of APP secreted into medium conditioned by the fibroblast cell lines. The experiment shown in (**A**) was repeated three times and the pixel intensity of the immunolabelled sAPPα and sAPPβ detected were evaluated and normalized against β-actin controls. Results are the percentage of secreted APP [total sAPP (22C11) and sAPPα (WO2)] compared with the control cell line (GM2069). Results were analysed using the Student's *t* test (*, $P < 0.01$; **, $P < 0.05$). (**C**) Western-blot analysis of the α- and β-secretase-cleaved APPCT and APLP2CT in the indicated fibroblast cell lines by Western blotting with APPCT and APLP2CT antibodies, with anti-β-actin antibody used as a control. (**D**) Western-blot analysis of APP and APLP2 in whole-cell lysates and conditioned medium from normal fibroblast cells (GM2069) and two copper-deficient fibroblast cell lines (A12-H9 and C3-C1). Whole-cell lysates and medium were Western blotted using the, 22C11, WO2, APPCT, APLP2CT and anti-ATP7A antibodies, with anti-β-actin antibody used as a control. All Western blots shown are representative of three independent experiments. Molecular-mass-markers are indicated on the left (in kDa).

changes in intracellular copper levels influence APP metabolism. Ordinarily ATP7A is endogenously expressed in fibroblasts (Figure 2B) and is primarily responsible for maintaining a homeostatic level of intracellular copper [21]. Fibroblasts derived from a Menkes disease patient (Me32a), which are devoid of functional ATP7A (Figure 2B) [30], accumulate ~650% more copper than normal fibroblasts (GM2069) (Figures 2A and 2C). In contrast, when ATP7A is overexpressed in the same Menkes patient cell line (A12-H9; Me32a cells transfected with ATP7A) (Figure 2B), the intracellular level of copper is drastically depleted, with cells containing ~65% less copper than normal fibroblasts (GM2069) (Figures 2A and 2C). The copper accumulation phenotype of the Menkes patient line (Me32a) can also be partially corrected by exogenous expression of ATP7B (WND16) (Figures 2A and 2C) [30]. However, this fibroblast line (WND16) still contains ~100% more copper than normal fibroblasts (GM2069) (Figures 2A and 2C), indicating that there may be inadequate expression of ATP7B to completely compensate for ATP7A disruption (Figure 2B). ATP7A eliminates excess intracellular copper directly across the plasma membrane [38], whereas ATP7B sequesters excess copper into exocytic vesicles [22]. This mechanistic difference becomes apparent when cells are exposed to an elevated level of copper, which stimulates the trafficking of only ATP7A to the cell periphery (Figure 2D). We utilized these cell lines to explore the influence of intracellular copper level on APP metabolism.

Copper depletion switches APP secretase cleavage from α-cleavage to β-cleavage

Western-blot analysis and densitometry were used to investigate the expression profile of APP in the fibroblast cell lines (Figure 3). Two antibodies (WO2 and 22C11) were used to differentiate between sAPP (soluble APP ectodomain) α and sAPPβ (see

Figure 1). The 22C11 antibody detects cleaved APP ectodomain generated through either the non-amyloidogenic (α-cleaved) or the amyloidogenic (β-cleaved) pathway. The WO2 antibody detects only sAPPα, as β-secretase activity cleaves upstream of its epitope. Fibroblasts with normal (GM2069) or an elevated level of intracellular copper (Me32a and WND16) produced similar levels of intracellular APP, as detected by both WO2 and 22C11 antibodies (Figure 3A). These cells also secreted an abundant amount of sAPPα into their medium, as determined by WO2 detection (Figure 3A). Medium conditioned by copper-accumulating Me32a and WND16 fibroblasts had a marked and significant increase in the level of sAPPα compared with medium conditioned by normal fibroblasts (GM2069) ($\sim$100% and $\sim$48% increases respectively) (Figure 3B). These results indicate that an elevation in intracellular copper increases APP production and subsequent sAPPα secretion, although the steady-state intracellular level of APP is unchanged (Figure 3B). Copper-deficient fibroblasts (A12-H9) expressed and secreted an sAPP species that was detectable by using the 22C11 antibody, but not with the WO2 antibody (Figure 3A), and migrated at a slightly lower molecular-mass (Figure 3A). These results are consistent with profound copper-depletion switching APP proteolysis from α-secretase cleavage (sAPPα secretion) to β-secretase cleavage (sAPPβ secretion). Additionally, the copper-depleted fibroblasts (A12-H9) secreted a level of total sAPP similar to that secreted by control (GM2069) fibroblasts (Figure 3B). These results indicate that there is a basal amount of total sAPP secretion that is maintained even under copper-deficient conditions, whereas total sAPP secretion rises under conditions of copper excess. Analysis of APLP2 in these fibroblast cell lines revealed that APLP2 also increased its steady-state expression under conditions of copper deficiency (A12-H9) (Figure 3A). Full-length APLP2 was only detected in the copper-depleted (A12-H9) fibroblasts. No secreted APLP2 was detected in the medium.

To further investigate APP cleavage in these fibroblast cell lines, an anti-APPCT antibody was used to assay any C-terminal APP cleavage fragments (see Figure 1). Fibroblasts with normal (GM2069) or elevated (Me32a and WND16) intracellular copper levels contained a similar steady-state level of an APP C-terminal fragment (10 kDa in size) consistent with C83 (α-cleaved APP C-terminal fragment) (Figure 3C). No C-terminal fragment was detected in the copper-deficient fibroblasts (A12-H9) (Figure 3C), despite the cells abundantly secreting β-cleaved APP ectodomain (sAPPβ) (Figures 3A and 3B), suggesting that C99 (β-cleaved APP C-terminal fragment) is rapidly turned over. Use of an anti-APLP2CT antibody (raised against the last 12 amino acids of APLP2) demonstrated that only full-length APLP2 and not its C-terminal cleavage fragment(s) could be detected in the copper-deficient A12-H9 cells, but the C-terminal fragment(s) were present in the other fibroblast cell lines (Figure 3C). This suggested that APLP2 cleavage is inhibited by copper deficiency and there is consequently no C-terminal fragment generated. In summary, these results indicate that processing of both APP and APLP2 is sensitive to changes in intracellular copper concentrations.

To demonstrate that the differences in the cleavage of APP and APLP2 seen in the copper-deficient A12-H9 cells were not due to the transfection procedure itself (e.g. gene interruption by transgene integration), an independently derived clonal line (C3-C1) was also examined (Figure 3D). The C3-C1 fibroblast cell line was previously shown to have very similar characteristics to the A12-H9 fibroblast cell line [30], including the level of ATP7A overexpression and copper status. Indeed, this fibroblast line exhibited a similar APP and APLP2 Western blot profile to the A12-H9 cells (Figure 3D).

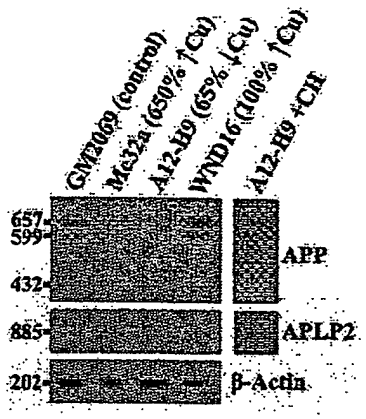

Figure 4 Copper deficiency modulates APP and APLP mRNA levels

RT–PCR amplification of APP and APLP2 in the indicated fibroblast cell lines. Amplification from A12-H9 cells treated with cycloheximide (CH) is also shown. The percentage increases and decreases in parenthesis refer to the change in copper levels compared with the control cell line. Note that fibroblasts transcribe the 770, 751 and 695 bp alternatively spliced *APP* mRNA as shown (657 bp, 599 bp and 432 bp products respectively). The sizes of the amplified products are indicated on the left in bp.

Copper depletion changes APP and APLP2 transcription/translation

It was reported previously that copper depletion in A12-H9 fibroblasts significantly down-regulates *APP* gene expression, as determined by Northern-blot analysis [19]. To validate this finding, we examined the level of *APP* mRNA in the fibroblast cell lines using RT–PCR (Figure 4). In addition, we also investigated *APLP2* mRNA levels. Fibroblasts with normal (GM2069) or elevated (Me32a and WND16) intracellular copper levels contained a steady-state level of both *APP* and *APLP2* mRNA (Figure 4). However, we could not amplify either *APP* or *APLP2* mRNA from the copper-deficient A12-H9 cells. Since these cells produce both APP and APLP2 protein (Figure 3), the inability to detect their respective mRNA transcripts was puzzling. We hypothesized that in these copper-deficient cells, the existence of *APP*/*APLP2* mRNA is low and transient and therefore any transcript produced is rapidly translated to protein. To demonstrate that copper-deficient A12-H9 cells do indeed produce mRNA transcripts for both *APP* and *APLP2*, the cells were treated with cycloheximide to prevent protein translation (Figure 4). Consequently, *APP* and *APLP2* mRNA molecules were faintly detected in the cycloheximide treated A12-H9 cells (Figure 4). Because steady-state APP protein levels are not decreased in the copper-deficient A12-H9 fibroblasts and medium compared with normal fibroblasts (GM2069) (Figures 3A and 3B), our findings of low APP mRNA message in A12-H9 cells indicate that copper deficiency either accelerates the translation of APP or inhibits the degradation of APP.

Amyloidogenic processing of APP is elevated in copper-deficient fibroblasts

An alternative approach to studying the processing of APP involves capturing the C-terminal fragments of APP by inhibiting γ-secretase activity and determining their levels through Western-blot analysis [39,40]. To capture the C-terminal fragments produced by normal (GM2069) and copper-deficient (A12-H9) fibroblasts, these cell lines were treated with the γ-secretase inhibitor DAPT [39] (Figures 5A and 5B). Inhibiting γ-secretase activity in normal fibroblasts (GM2069) had no effect on the levels of intracellular APP or secreted sAPPα

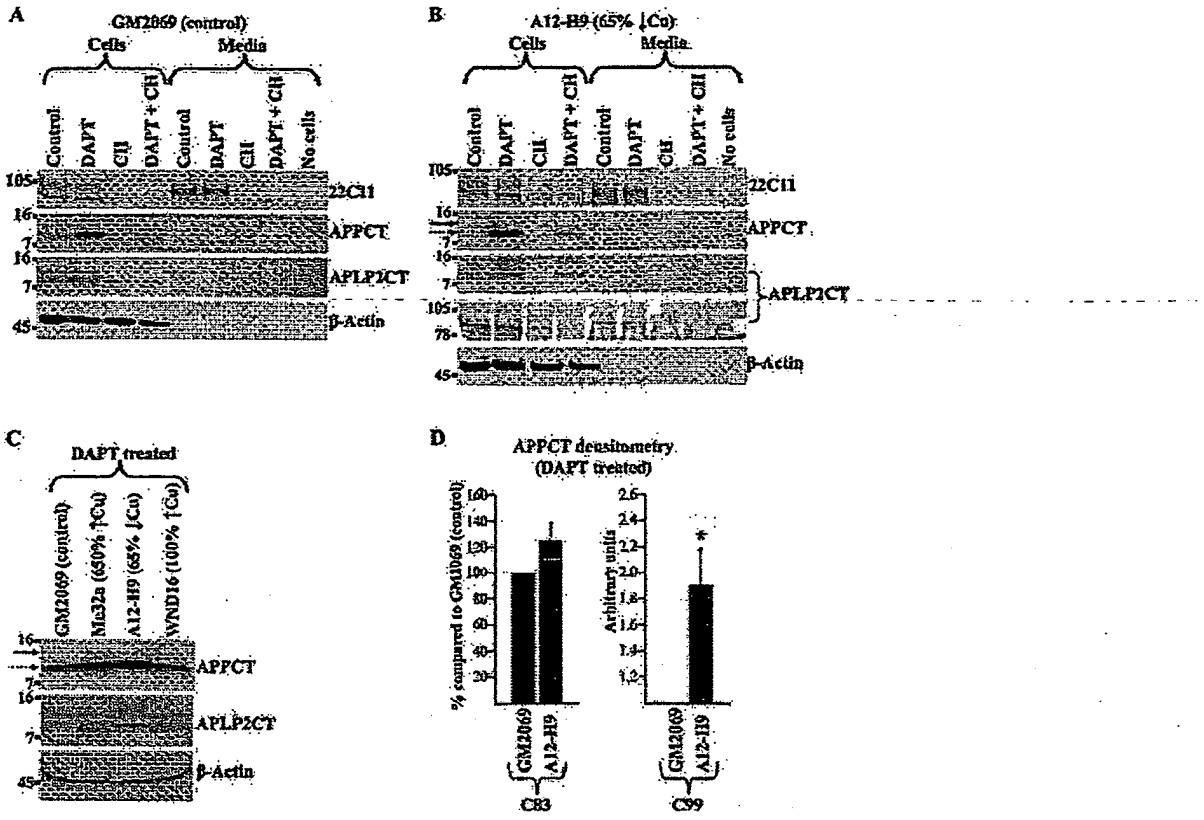

Figure 5 Copper deficiency increases γ-secretase cleavage of APP

(**A**) Western-blot analysis demonstrating that DAPT treatment prevents γ-secretase cleavage of *de novo* APP/APLP2 in normal fibroblasts (GM2069). GM2069 fibroblasts were cultured for 16 h in fresh basal medium (Control) or medium supplemented with 2 μM DAPT (DAPT), 10 μM cycloheximide (CH) or both 2 μM DAPT and 10 μM cycloheximide (DAPT + CH). Unconditioned medium (No cells) was also analysed. Lysates and medium were Western blotted using 22C11, APPCT and APLP2CT antibodies, with anti-β-actin antibody as a control. (**B**) Western-blot analysis demonstrating that DAPT treatment prevents γ-secretase cleavage of *de novo* APP/APLP2 in copper-deficient fibroblasts (A12-H9) was performed as in (**A**), but using the copper-deficient A12-H9 cell line. C99 (solid arrow) and C83 (dotted arrow) are indicated on the left. The percentage decrease in parenthesis refers to the change in copper level compared with the control cell line. (**C**) Western-blot analysis of DAPT-captured APP and APLP2 C-terminal fragments in the indicated fibroblast lines. The fibroblast cell lines were cultured for 16 h in medium supplemented with 2 μM DAPT and whole-cell lysates were Western blotted using APPCT and APLPCT antibodies, with anti-β-actin antibody used as a control. The percentage increases and decreases in parenthesis refer to the change in copper levels compared with the control cell line. C99 (solid arrow) and C83 (dotted arrow) are indicated on the left. (**D**) Densitometric analysis of the level of DAPT-captured C83 and C99 fragments in control (GM2069) and copper-deficient (A12-H9) fibroblasts. The experiment was repeated three times and the pixel intensity of the immunolabelled C83/C99 bands (detected by anti-APPCT antibody) were evaluated and normalized against β-actin controls. The level of C83 is expressed as a percentage compared with the control cell line (GM2069), whereas the level of C99 is expressed as arbitrary units, as there was no C99 detection in the control cell line (GM2069). Results were analysed using the Student's *t* test (*, $P = 0.031$). All Western blots shown are representative of three independent experiments. Molecular-mass-markers are indicated on the left (in kDa).

(Figure 5A). However, DAPT treatment markedly increased the level of C83 (Figure 5A). These results demonstrated that DAPT treatment did not perturb the production and subsequent secretion of sAPPα (and by inference did not influence α-secretase-mediated cleavage of APP), but only obstructed downstream γ-secretase processing. This is consistent with previous observations [39,40]. Inhibiting γ-secretase also increased the amount of APLP2 C-terminal fragment (Figure 5A). To establish if DAPT prevented γ-secretase-mediated cleavage of either *de novo* APP or existing intracellular APP molecules, cycloheximide was used in conjunction with DAPT treatment to prevent new protein synthesis (Figure 5A). Cycloheximide treatment alone markedly diminished the level of both intracellular APP and secreted sAPPα (Figure 5A) and reduced the amount of C-terminal fragments captured by DAPT treatment (Figure 5A), indicating that DAPT predominantly prevents γ-secretase cleavage of *de novo* APP. Taken together, these experiments demonstrate that DAPT treatment captures APP C-terminal fragments without affecting APP transcription or translation.

These experiments were repeated using the copper-deficient A12-H9 fibroblast line (Figure 5B). It is important to note that A12-H9 cells secrete only sAPPβ (Figure 3) and therefore these cells are predicted to produce C99 and therefore more Aβ. Inhibiting γ-secretase (DAPT treatment) in the copper-depleted fibroblasts (A12-H9) had no effect on the levels of intracellular APP or secreted sAPPβ (Figure 5B). DAPT treatment also had no effect on the intracellular level of full-length APLP2 (Figure 5B). However, DAPT treatment captured two C-terminal fragments (Figure 5B): a predominant fragment corresponding to C83 (~10 kDa) and a faint larger fragment corresponding to C99 (~12 kDa). Therefore despite copper-depleted fibroblasts (A12-H9) secreting only sAPPβ (Figure 3), this did not result in the production of only C99. In fact, the majority of the C-terminal fragments produced by A12-H9 cells were still C83, with C99 molecules being an increased product (Figure 5B). The activities of α- and β-secretase are therefore not mutually exclusive, and in copper-depleted fibroblasts each APP molecule was processed by both secretases producing sAPPβ and C83.

Furthermore, the predicted sAPPα product was not detectable in the medium and therefore must be either relatively low in abundance or rapidly degraded. In addition, γ-secretase inhibition captured APLP2 C-terminal fragments (Figure 5B). A12-H9 cells, when left untreated, exhibited only full-length APLP2 and no C-terminal cleavage product below 15 kDa (Figures 3C and 3D). Therefore APLP2 is still processed in copper-deficient A12-H9 fibroblasts, although possibly more slowly, leading to an increase in full-length APLP2.

To determine if the level of APP C-terminal fragment(s) produced in the copper-deficient A12-H9 cells is comparable with that produced by the other fibroblast cell lines, each cell line was treated with DAPT and their level of APP C-termini captured directly compared (Figures 5C and 5D). Copper-deficient fibroblasts (A12-H9) treated with DAPT produced as much or more C83 and C99 compared with the other cell lines (GM2069, Me32a and WND16). This was surprising since, in contrast to the other cell lines, A12-H9 fibroblasts did not exhibit any APP C-terminal fragments (C83 or C99) under non-DAPT conditions (Figures 3C and 3D). In other words, A12-H9 cells produce more C-terminal APP fragments (C83 and C99), but they can only be detected when cells are treated with the γ-secretase inhibitor DAPT (Figures 5B–5D). Therefore the processing of the C-terminus by γ-secretase must be markedly increased in the copper-depleted A12-H9 fibroblasts compared with fibroblast cell lines with normal or elevated copper. Western-blot analysis revealed that presenilin-1 expression level was not increased in copper-deficient A12-H9 cells (results not shown).

As shown with DAPT treatment, a small percentage of the C-terminal fragments generated by A12-H9 cells were amyloid-harbouring C99 fragments (Figures 5B and 5C). We hypothesized that when A12-H9 cells are not treated with DAPT, these C99 fragments would be cleaved by γ-secretase, liberating the Aβ peptide, and therefore the copper-deficient fibroblasts (A12-H9) should exhibit increased production of Aβ. The Aβ secreted endogenously by A12-H9 cells was below detection limits (results not shown). Therefore we overexpressed wtAPP695 in normal (GM2069) and copper-deficient (A12-H9) fibroblasts to test whether copper deficiency caused an increase in the production of Aβ (Figure 6A). In normal fibroblasts (GM2069), wtAPP695 overexpression resulted in the abundant secretion of sAPPα, which was detected by WO2 (Figure 6A). Unlike non-transfected cells that exclusively secreted sAPPβ (Figure 3), A12-H9 fibroblasts overexpressing wtAPP695 secreted abundant sAPPα (Figure 6A). This suggests that wtAPP695 expression exceeded the capacity of the A12-H9 fibroblasts to process APP via the β-cleavage pathway (sAPPβ) (Figures 3A and 3B) and, as a consequence, much of the APP was processed by α-secretase (Figure 6A). Nevertheless, overexpression of APP permitted sufficient production of Aβ for it to be detected by WO2 (Figure 6A) and 6E10 (Figure 6B) antibodies. When transfected with wtAPP695, the copper-deficient fibroblasts (A12-H9) clearly generated more Aβ than normal fibroblasts (GM2069) (Figures 6A and 6B). The level of wtAPP695 expressed in both fibroblast cell lines was equivalent, indicating that a difference in expression level was not responsible for the elevated Aβ production seen in copper-deficient fibroblasts. Therefore copper depletion caused by ATP7A overexpression increases β- and γ-secretase activities in human fibroblasts.

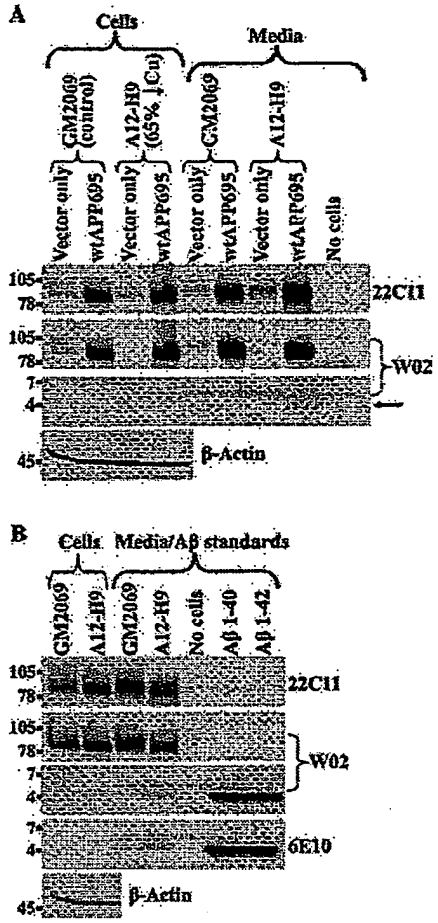

Figure 6 Copper deficiency in fibroblasts increases the generation of Aβ

(A) Western-blot analysis of normal (GM2069) and copper-deficient (A12-H9) fibroblasts transfected with *wtAPP695*, with transfection with vector only as a control. Unconditioned medium was also analysed as a control. Whole-cell lysates and medium were Western blotted using 22C11 and W02 antibodies, with anti-β-actin antibody as a control. The percentage decrease in parenthesis refers to the change in copper level compared with the control cell line. (B) Western-blot analysis confirming Aβ secretion from copper-deficient fibroblasts overexpressing wtAPP695. GM2069 fibroblasts were used as a control cell line. Synthetic Aβ1–40 and Aβ1–42 standards (100 pg) were run concurrently with whole-cell lysate and medium samples. Samples were Western blotted using 22C11, W02 and 6E10 antibodies, with anti-β-actin antibody used as a control. All Western blots shown are representative of three independent experiments. Molecular-mass-markers are indicated on the left (in kDa).

Copper depletion in human neuronal cells increases Aβ secretion

To ascertain if the level of intracellular copper influences APP metabolism in neuronal cells, we investigated a human SY5Y neuroblastoma line overexpressing wtAPP695 (SY5Y-wtAPP695). We found that we were unable to transfect these cells with ATP7A; therefore, in order to deplete these cells of copper they were cultured in medium supplemented with BCS (200 μM) and D-penicillamine (200 μM), which chelate Cu^{1+} and Cu^{2+} respectively. This approach reduced intracellular copper by ~27% (Figure 7A). Alternatively, to elevate the level of intracellular copper, the culture medium was supplemented with 200 μM $CuCl_2$. This relatively high concentration of $CuCl_2$ was necessary to counteract the inherent copper-sequestering nature of serum [20% (v/v) FCS] and increased intracellular copper by ~600% (Figure 7A). The copper-modulating treatments had no significant effect on the level of intracellular zinc, but treatment with copper chelators elevated intracellular iron levels by ~29% (Figure 7A), which is consistent with the inhibition of ceruloplasmin activity [41].

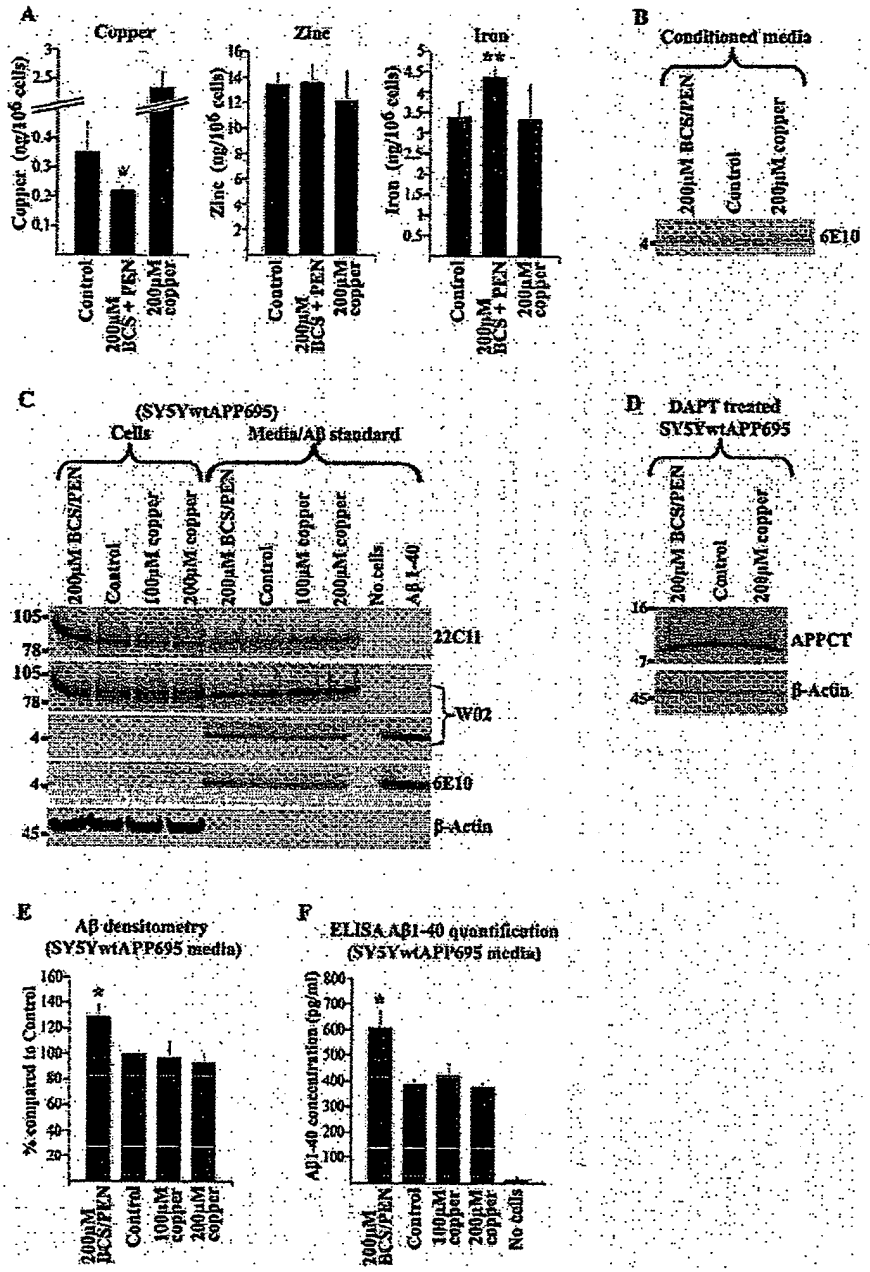

Figure 7 Copper deficiency increases Aβ secretion from human neuronal cells

(**A**) Copper, zinc and iron content of SY5YwtAPP695 cells was measured using inductive-coupled plasma MS. The neuronal cells were cultured in basal medium (Control), medium supplemented with either 200 μM BCS and D-penicillamine (BCS + PEN), or with 200 μM $CuCl_2$. Results are normalized means $\pm$ S.D. ($n = 3$) and are shown as ng of metal per 1×10^6 cells. Results were analysed using the Student's t test (*, $P = 0.039$; **, $P = 0.018$). (**B**) Western-blot analysis demonstrating that copper supplementation or chelation does not directly affect the detection of secreted Aβ. Conditioned medium from SY5YwtAPP695 cells was Western blotted using the 6E10 antibody. Molecular-mass-markers are indicated on the left (in kDa). (**C**) Western-blot analysis demonstrating that copper deficiency increases the level of Aβ secreted from human neuronal cells. SY5YwtAPP695 cells were cultured in basal medium (Control), 200 μM BCS and D-penicillamine (BCS/PEN), 100 μM $CuCl_2$ or 200 μM $CuCl_2$. Whole-cell lysates and medium were Western blotted using 22C11, W02 and 6E10 antibodies, with anti-β-actin antibody as a control. Unconditioned medium (no cells) and synthetic Aβ1–40 standard were also analysed. Molecular-mass-markers are indicated on the left (in kDa). (**D**) Western-blot analysis demonstrating that modulating medium copper levels does not alter APP processing in human neurons. SY5YwtAPP695 cells were cultured in 200 μM BCS and D-penicillamine (BCS/PEN) or 200 μM $CuCl_2$ after treatment with 2 μM DAPT. Anti-β-actin antibody was used as a control. Molecular-mass-markers are indicated on the left (in kDa). (**E**) Copper deficiency significantly increases the level of Aβ secreted from human neuronal cells as determined by densitometry. The experiment shown in (**C**) was repeated three times and the pixel intensity of the immunolabelled Aβ bands were evaluated and normalized against β-actin controls. Results are the level of secreted Aβ as a percentage compared with the control sample. Results were analysed by the Student's t test (*, $P = 0.028$). (**F**) ELISA-based quantification confirmed that copper deficiency increases the level of Aβ secreted from human SY5YwtAPP695 neuronal cells. The concentration of Aβ1–40 secreted into the medium from SY5YwtAPP695 cells cultured in 200 μM BCS and D-penicillamine (BCS/PEN), 100 μM $CuCl_2$ or 200 μM $CuCl_2$ was measured by ELISA. Background Aβ measurements in non-conditioned medium were also made (No cells). Results are normalized means $\pm$ S.D. ($n = 3$) and were analysed using the Student's t test (*, $P = 0.006$).

Copper promotes Aβ cross-linking, whereas metal chelators have been shown to dissolve Aβ aggregates both *in vitro* and *in vivo* [5,9]. Therefore it was possible that copper supplementation or chelation could cause secreted Aβ to oligomerize or dissolve into monomers respectively. To determine if this was the case, medium conditioned by SY5YwtAPP695 cells was divided evenly and incubated in equal volumes with either the chelators (BCS and D-penicillamine), PBS (control) or 200 μM $CuCl_2$ (Figure 7B). An equivalent level of Aβ was observed in all three conditions, indicating that these treatments do not directly affect the detection of monomeric Aβ in this time frame. This is probably because of agents in the medium that scavenge H_2O_2 generated by Aβ [8,12]. Therefore modulation of copper in our experiments does not alter the amount of monomeric Aβ detected in the cell-free medium.

We next investigated the impact of copper deficiency and copper accumulation on the production and secretion of Aβ from neuronal cells (Figure 7C). Modulating intracellular copper in SY5Y cells transfected with wtAPP695 had no observable effect on the steady-state level of intracellular APP or on the level of sAPP secretion, as shown by detection with 22C11 and WO2 antibodies (Figure 7C). Nevertheless, copper deficiency did noticeably increase the level of secreted Aβ in comparison with the other conditions tested. This was established by Western blotting with both WO2 and 6E10 antibodies (Figure 7C). These results demonstrate that, as with fibroblasts, copper deficiency increases neuronal Aβ secretion.

To determine if modulating intracellular copper had an impact on the processing of APP, the SY5Y wtAPP695 cells were treated with either 200 μM $CuCl_2$ or copper-chelating agents (BCS and D-penicillamine) and then with the γ-secretase inhibitor DAPT to capture the C-terminal fragments (Figure 7D). Western-blot analysis demonstrated that there is no difference in the amount of C83 or C99 produced by the cells under any of the copper conditions tested (Figure 7D). Incubating the neuronal cells in medium containing the copper chelators for 5 or 7 days and/or inducing differentiation by culturing with 20 μM retinoic acid had no effect on C83/C99 production (results not shown). We tested whether this lack of response to copper modulation may have been the result of overexpression of APP by assaying untransfected parental SY5Y cells for C-terminal fragments. Neither $CuCl_2$ nor copper chelation affected the levels of the APP C-terminal fragments in non-transfected SY5Y cells (results not shown). These results suggest that modulating copper has no effect on APP processing in neuronal SY5Y cells, but does increase the level of Aβ secreted. In order for this to occur, there is most likely some variation in the degradation of Aβ, with copper deficiency decreasing Aβ breakdown as reported previously [36].

Densitometry was used to measure and compare the levels of Aβ secreted by the SY5YwtAPP695 cells under each copper condition (based on detection with the 6E10 antibody) (Figure 7E). Copper deficiency resulted in ~30% more Aβ in the SY5YwtAPP695 conditioned medium, whereas elevated intracellular copper had no significant effect (Figure 7E). To confirm this observation and to determine which Aβ species is being secreted, the levels of both Aβ(1–40) and Aβ(1–42) in the medium were further quantified by ELISA (Figure 7F) [36,37]. Verifying the densitometry results, ELISA quantification demonstrated that copper deficiency caused SY5YwtAPP695 cells to secrete an elevated concentration of Aβ(1–40) (~36% increase) (Figure 7F). The level of Aβ(1–42) in the conditioned medium was below detection limits. These results demonstrate that copper deficiency in neuronal SY5Y cells increases Aβ(1–40) secretion.

DISCUSSION

In the AD brain, copper is sequestered in senile plaques by direct co-ordination to Aβ peptides [5–8], but there is a net decrease in tissue copper levels in neocortical tissue [26–28], reflected by diminished activities of copper-dependent enzymes such as cytochrome c oxidase [42–44] and SOD1 (superoxide dismutase 1) [45,46]. Therefore copper collects outside of the cortical cells, which are themselves copper deficient. We found that copper deficiency increased the level of Aβ secretion from both human fibroblast and neuroblastoma cells. These observations have implications for AD progression, as elevated Aβ production and subsequent aggregation (plaque formation) could further perpetuate localized neural copper deficiency by seizing available copper. This in turn, according to our results, could increase Aβ secretion and generate a vicious cycle.

In fibroblasts, an elevation in intracellular copper levels increased the production and subsequent secretion of α-cleaved APP (sAPPα), whereas copper-deficient cells secreted increased β-cleaved APP (sAPPβ) (Figures 3A and 3B). These results are consistent with previous observations using CHO (Chinese-hamster ovary) cells, where excess copper increased the secretion of APP ectodomain and correspondingly reduced the level of Aβ production [20]. We have confirmed the previous findings of Bellingham et al. [19], who showed that sAPPα cannot be detected by Western blot in the copper-deficient A12-H9 cells (Figure 3A). However, we have extended these findings by showing that these fibroblasts actually secrete sAPPβ instead (Figures 3A and 3B). Since these cells still produce some C83 (Figures 5B and 5C), it is possible that sAPPα is rapidly cleaved or cleared under these conditions, making it undetectable. Indeed, sAPPα could be detected when A12-H9 cells were transfected with APP (Figures 6A and 6B). This demonstrates that APP molecules can be cleaved by both α- and β-secretase pathways concurrently and therefore the two activities are not mutually exclusive as previously considered [47,48]. Importantly, the level of sAPPβ production does not therefore directly correlate with the level of Aβ production.

Our results also demonstrate that copper deficiency in fibroblasts increases the cleavage of APP C-terminal fragments by γ-secretase. APP C-terminal fragments were undetectable in copper-depleted A12-H9 fibroblasts, but were abundant in the other fibroblast cell lines (Figures 3C and 3D). However, inhibition of γ-secretase (with DAPT) revealed that A12-H9 fibroblasts actually produced an elevated level of C83 (Figure 5A). Therefore the C-terminus of APP must be processed more rapidly under conditions of copper deficiency. Our results show that copper deficiency may also increase the activity of BACE1 (β-site amyloid precursor protein-cleaving enzyme 1). The intracellular signalling mechanisms involved are not yet clear, but a Cu^{1+} binding site has been identified on the cytoplasmic C-terminus of BACE1 [49], which mediates an interaction with the copper chaperone for SOD1. This raised the hypothesis that copper levels can influence BACE1 activity or trafficking.

Another important observation is the differential modulation of APP and APLP2 processing by copper. Both APP and APLP2 mRNA levels dropped markedly under copper-deficient conditions (Figure 4), consistent with copper-dependent transcriptional regulation for both genes. Nonetheless, rapid translation of both proteins was still evident when γ-secretase processing was inhibited (Figure 5C). Despite both proteins being cleaved by BACE1 and γ-secretase [50,51], our current results show that under copper-deficient conditions, APP processing shifts from α-cleavage to β-cleavage, whereas APLP2 processing is generally attenuated and consequently there is more

steady-state full-length protein (Figures 3A, 3C and 3D). There may also be an increase in β-cleavage fragments of APLP2 (Figure 5C). The purpose of this differential processing of APP compared with APLP2 under copper-deficient conditions is not clear, but it is interesting to note that a recent report described a significant decrease in the ratio of cerebrospinal fluid sAPPα to soluble APLP2 in mild cognitive impairment and AD [52]. This finding is consistent with the effect of cellular copper deficiency that we have observed *in vitro*. Furthermore, with APP and APLP2 both contributing to [16] and being affected by copper homeostasis, it will be interesting to explore the contribution of both proteins and their processing to the pathophysiology of Menkes and Wilson diseases.

Contrary to results obtained using fibroblasts, changes in APP processing were not observed in copper-deficient neuroblastoma cells (Figures 7C and 7D). There are several possible explanations for this difference. The processing of APP may be cell-type dependent or depend on which spliced variant of APP is predominantly expressed (as APP770 is the prevalent form in fibroblasts; Figure 4). The lowering of intracellular copper by chelation in the neuroblastoma cells (~27% decrease) may have been insufficient to match the response seen in the more profoundly copper-deficient fibroblasts (~65% decrease). Lowering intracellular copper levels in fibroblasts by chelation also had no observable effect on APP processing (results not shown). Again, the decrease in copper that could be achieved in fibroblasts by chelation was only ~20% (results not shown). Finally, there may be a specific requirement for the copper deficiency to be induced by ATP7A. Despite the level of intracellular copper in neuroblastoma cells having no obvious effect on secretase cleavage of APP (Figures 7C and 7D), copper deficiency did raise the level of Aβ secretion by at least 30% (Figures 7E and 7F). This response was also observed using human M17 neuroblastoma cells transfected with wtAPP695 (results not shown). These results suggest that, in neuroblastoma cells, copper deficiency down-regulates the degradation of Aβ and subsequently the concentration of secreted Aβ increases.

Aβ can be degraded *in vitro* and *in vivo* by numerous metalloproteinases including neprilysin, matrix-metalloproteases and insulin-degrading enzyme (reviewed in [1]). Recently, White et al. [36] demonstrated using CHO cells that clioquinol liganded to Cu^{2+} selectively up-regulated matrix-metalloprotease activity and consequently increased the degradation of Aβ by elevating intracellular copper (clioquinol alone had no effect). However, these authors found that increasing copper alone ($CuCl_2$ without clioquinol) in the medium induced a 35% increase in Aβ(1–40) secretion [36]. These results appear to conflict with results obtained by Borchardt et al. [20] using the same cell type (CHO), and also with our results using human neuroblastoma cells (Figure 7). This inconsistency might be explained by the presence of a serum factor or a copper carrier (such as clioquinol) modifying the behaviour of copper. Indeed, results from White et al. [36] indicate that clioquinol-liganding of Cu^{2+} induced opposite effects (decreased Aβ) in cell culture compared with the effects of free Cu^{2+} (increased Aβ). In serum, copper will complex to several ligands including α-fetoprotein (fetal albumin) and amino acids. The copper studies conducted by White et al. [36] were carried out in serum-free conditions unlike Borchardt et al. [20] or our present study. Nevertheless, results obtained in APP transgenic mice on the effect of elevated brain copper on Aβ levels *in vivo* support the conclusion that elevated cellular copper decreases Aβ levels [18,25]. TgCRND8 AD model mice (expressing human APP containing both Swedish and Indiana mutations) crossed with the toxic milk (tx) mouse, a model for Wilson disease that accumulates copper in the brain and liver, have reduced Aβ plaques and diminished plasma Aβ levels [18]. Similarly, APP23 AD model mice (expressing human APP containing the Swedish mutation) on three months of dietary copper supplementation had significantly reduced Aβ production [25]. Notably, Tg2576 mice (expressing APP containing the Swedish mutation) treated with clioquinol have reduced brain Aβ burden, but levels of brain copper rise with this treatment [9]. In contrast, the addition of copper to the drinking water of cholesterol-fed rabbits induced immunoreactive Aβ accumulation in the neocortex and neurological impairment [53]. Aβ–copper complexes recruit cholesterol to generate neurotoxic chemical species [54], so under particular circumstances, such as in a high-cholesterol environment, a reaction of Aβ with copper ions may foster neurotoxicity and pathology. We have recently found that Aβ and copper are enriched in the cholesterol-rich lipid raft compartment of neuronal cells even under conditions of copper deficiency (Y. Hung and A.I. Bush, unpublished work). This may explain the mechanism leading to the co-mingling of copper and Aβ in copper-deficient tissue.

In summary, our results are consistent with brain copper deficiency elevating Aβ concentrations. Therefore the ionophoric properties of molecules like clioquinol that can redistribute copper from Aβ aggregates to neighbouring copper-deficient cells may be essential to their potential therapeutic benefit.

This work was supported by funds from the Australian Research Council (Federation Fellowship and Discovery Project Grant DP0664068) and the Alzheimer's Association Zenith Award 04-1002 to A.I.B.

REFERENCES

1 Adlard, P. and Bush, A. (2006) Metals and Alzheimer's disease. J. Alzheimers Dis. **10**, 145–163
2 Glenner, G. and Wong, C. (1984) Alzheimer's disease and Down's syndrome: sharing of a unique cerebrovascular amyloid fibril protein. Biochem. Biophys. Res. Commun. **122**, 1131–1135
3 Masters, C., Simms, G., Weinman, N., Multhaup, G., McDonald, B. and Beyreuther, K. (1985) Amyloid plaque core protein in Alzheimer's disease and Down's syndrome. Proc. Natl. Acad. Sci. U.S.A. **82**, 4245–4249
4 Bush, A., Pettingell, W., Multhaup, G., d Paradis, M., Vonsattel, J., Gusella, J., Beyreuther, K., Masters, C. and Tanzi, R. (1994) Rapid induction of Alzheimer A β-amyloid formation by zinc. Science **265**, 1464–1467
5 Cherny, R., Legg, J., McLean, C., Fairlie, D., Huang, X., Atwood, C., Beyreuther, K., Tanzi, R., Masters, C. and Bush, A. (1999) Aqueous dissolution of Alzheimer's disease Aβ-amyloid deposits by biometal depletion. J. Biol. Chem. **274**, 23223–23228
6 Lovell, M., Robertson, J., Teesdale, W., Campbell, J. and Markerbery, W. (1998) Copper, iron and zinc in Alzheimer's disease senile plaques. J. Neurol. Sci. **158**, 47–52
7 Dong, J., Atwood, C., Anderson, S., Siedlak, M., Smith, S. and Carey, P. (2003) Metal binding and oxidation of amyloid-β within isolated senile plaque cores: Raman microscopic evidence. Biochemistry **42**, 2768–2773
8 Opazo, C., Huang, X. and RA, C. (2002) Metalloenzyme-like activity of Alzheimer's disease β-amyloid. Cu-dependent catalytic conversion of dopamine, cholesterol, and biological reducing agents to neurotoxic H_2O_2. J. Biol. Chem. **277**, 40302–40308
9 Cherny, R., Atwood, C., Xilinas, M., Gray, D., Jones, W., McLean, C., Barnham, K., Volitakis, I., Fraser, F., Kim, Y. et al. (2001) Treatment with a copper-zinc chelator markedly and rapidly inhibits β-amyloid accumulation in Alzheimer's disease transgenic mice. Neuron **30**, 665–676
10 Lee, J., Friedman, J., Angel, I., Kozac, A. and JY, K. (2004) The lipophillic metal chelator DP-109 reduces amyloid pathology in brains of human β-amyloid precursor protein transgenic mice. Neurobiol. Aging **25**, 1315–1321
11 Atwood, C., Scarpa, R., Huang, X., Moir, R., Jones, W., Fairlie, D., Tanzi, R. and Bush, A. (2000) Characterization of copper interactions with Alzheimer amyloid β-peptides: identification of an attomolar-affinity copper binding site on amyloid β1-42. J. Neurochem. **75**, 1219–1233
12 Huang, X., Atwood, C. and Hartshorn, M. (1999) The Aβ peptide of Alzheimer's disease directly produces hydrogen peroxide through metal ion reduction. Biochemistry **38**, 7609–7616

13 Seubert, P., Vigo-Pelfrey, C., Esch, F., Lee, M., Dovey, H., Davis, D., Sinha, S., Schlossmacher, M., Whaley, J., Swindlehurst, C. et al. (1992) Isolation and quantification of soluble Alzheimer's β-peptide from biological fluids. Nature **359**, 268–269
14 Barnham, K., McKinstry, W., Multhaup, G., Galatis, D., Morton, C., Curtain, N., Williamson, A., White, A., Hinds, M., Norton, R et al. (2003) Structure of the Alzheimer's disease amyloid precursor protein copper binding domain. A regulator of neuronal copper homeostasis. J. Biol. Chem. **278**, 17401–17407
15 Bellingham, S., Ciccotosto, G., Needham, B., Fodero, A., White, A., Masters, C., Cappai, R. and Camakaris, J. (2004) Gene knockout of amyloid precursor protein and amyloid precursor-like protein-2 increases cellular copper levels in primary mouse cortical neuron and embryonic fibroblasts. J. Neurosci. **91**, 423–428
16 White, A., Reyes, R., Mercer, F., Camakaris, J., Zheng, H., Bush, A., Multhaup, G., Beyreuther, K., Masters, C. and Cappai, R. (1999) Copper levels are increased in the cerebral cortex and liver of APP and APLP2 knockout mice. Brain Res. **842**, 439–444
17 Maynard, C., Cappai, R., Volitakis, I., Cherny, R., White, A., Beyreuther, K., Masters, C., Bush, A. and Li, Q.-X. (2002) Overexpression of Alzheimer's disease amyloid-β opposes the age-dependent elevations of brain copper and iron. J. Biol. Chem. **277**, 44670–44676
18 Phinney, A., Drisaldi, D., Schmidt, S., Lugowski, S., Coronado, V., Liang, Y., Horne, P., Yang, J., Sekoulidis, J., Coomaraswamy, J., et al. (2003) *In vivo* reduction of amyloid-β by a mutant copper transporter. Proc. Natl. Acad. Sci. U.S.A. **100**, 14193–14198
19 Bellingham, S., Lahiri, D., Maloney, B., La Fontaine, S., Multhaup, G. and Camakaris, J. (2004) Copper depletion down-regulates expression of the Alzheimer's disease amyloid-β precursor protein gene. J. Biol. Chem. **279**, 20378–20384
20 Borchardt, T., Camakaris, J., Cappai, R., Masters, C., Beyreuther, K. and Multhaup, G. (1999) Copper inhibits β-amyloid production and stimulates the non-amyloidogenic pathway of amyloid-precursor-protein secretion. Biochem. J. **344**, 461–467
21 Cater, M. and Mercer, J. (2005) Molecular biology of metal homeostasis and detoxification. In Topics in Current Genetics (Tamas, J. and Martinoia, E., eds.), pp. 101–129, Spinger, Berlin
22 Cater, M., La Fontaine, S., Shield, K., Deal, Y. and Mercer, J. (2006) ATP7B mediates vesicular sequestration of copper: insight into biliary copper excretion. Gastroenterology **130**, 493–506
23 Nyasae, L., Bustos, R., Braiterman, L., Eipper, B. and Hubbard, A. (2006) Dynamics of endogenous ATP7A (Menkes protein) in intestinal epithelial cells: copper-dependent redistribution between two intracellular sites. Am. J. Physiol. Gastrointest. Liver Physiol. **292**, 1181–1194
24 Schlief, M., Craig, A. and Gitlin, J. (2005) NMDA receptor activation mediates copper homeostasis in hippocampal neurons. J. Neurosci. **25**, 239–246
25 Bayer, T., Schafer, S., Simons, A., Kemmling, A., Kamer, T., Tepest, R., Eckert, A., Schussel, K., Eikenberg, O., Sturchler-Pierrat, C. et al. (2003) Dietary Cu stabilizes brain superoxide dismutase 1 activity and reduces amyloid Aβ production in APP23 transgenic mice. Proc. Natl. Acad. Sci. U.S.A. **100**, 14187–14192
26 Deibel, M., Ehmann, W. and Markesbery, W. (1996) Copper, iron and zinc imbalances in severely degenerative brain regions in Alzheimer's disease: possible relation to oxidative stress. J. Neurol. Sci. **143**, 137–142
27 Loeffler, D., LeWitt, P., Juneau, P., Sima, A., Nguyen, H., DeMaggio, A., Brickman, C., Brewer, G., Dick, R., Troyer, M. and Kanaley, L. (1996) Increased regional brain concentrations of ceruloplasmin in neurodegenerative disorders. Brain Res. **738**, 265–274
28 Rao, K., Rao, R., Shanmugavelu, P. and Menon, R. (1999) Trace elements in Alzheimer's disease brain: A new hypothesis. Alzheimers Rep. **2**, 241–246
29 Religa, D., Strozyk, D., RA, C., Volitakis, I., Haroutunian, V., Winblad, B., Naslund, J. and Bush, A. (2006) Elevated cortical zinc in Alzheimer disease. Neurology **67**, 69–75
30 La Fontaine, S., Firth, S., Camakaris, J., Englezou, A., Theophilos, M., Petris, M., Howie, M., Lockhart, P., Greenough, M., Brooks, H. et al. (1998) Correction of the copper transport defect of Menkes patient fibroblasts by expression of the Menkes and Wilson ATPases. J. Biol. Chem. **273**, 31375–31380
31 Cater, M., Forbes, J., La Fontaine, S., Cox, D. and Mercer, J. (2004) Intracellular trafficking of the human Wilson protein: the role of the six N-terminal metal binding sites. Biochem. J. **380**, 805–813
32 Ke, B., Llanos, R., Wright, M., Deal, Y. and Mercer, J. (2006) Alteration of copper physiology in mice overexpressing the human Menkes protein ATP7A. Am. J. Physiol. Regul. Integr. Comp. Physiol. **290**, 1460–1467
33 Ida, N., Hartmann, T., Pantel, J., Schröder, J., Zerfass, R., Förstl, H., Sandbrink, R., Masters, C. and Beyreuther, K. (1996) Analysis of heterogeneous βA4 peptides in human cerebrospinal fluid and blood by a newly developed sensitive Western blot assay. J. Biol. Chem. **271**, 22908–22914
34 White, A., Zheng, H., Galatis, D., Maher, F., Hesse, L., Multhaup, G., Beyreuther, K., Masters, C. L. and Cappai, R. (1998) Survival of cultured neurons from amyloid precursor protein knock-out mice against Alzheimer's amyloid-toxicity and oxidative stress. J. Neurosci. **18**, 6207–6217
35 Weidemann, A., Konig, G., Bunke, D., Fischer, P., Salbaum, M., Masters, C. and Beyreuther, K. (1989) Identification, biogenesis, and localization of precursors of Alzheimer's disease A4 amyloid protein. Cell **57**, 115–126
36 White, R., Du, T., Laughton, K., Volitakis, I., Sharples, R., Xilinas, M., Hoke, D., Holsinger, D., Evin, G., Cherny, R. et al. (2006) Degradation of the Alzheimer disease amyloid β-peptide by metal-dependent up-regulation of metalloprotease activity. J. Biol. Chem. **281**, 17670–17680
37 Li, Q., Laughton, K., Mclean, C., Volitakis, I., Cherny, R., Cheung, N., White, A. and Masters, C. (2006) Overexpression of Aβ is associated with acceleration of onset of motor impairment and superoxide dismutase 1 aggregation in amyotrophic lateral sclerosis mouse models. Aging Cell **5**, 153–165
38 Petris, M. J., Mercer, J. F. B., Culvenor, J. G., Lockhart, P., Gleeson, P. A. and Camakaris, J. (1996) Ligand-regulated transport of the Menkes copper P-type ATPase efflux pump from the Golgi apparatus to the plasma membrane: a novel mechanism of regulated trafficking. EMBO J. **15**, 6084–6095
39 Dovey, H., John, V., Anderson, J., Chen, L., de Saint Andrieu, P., Fang, L. Y., Freedman, S. B., Folmer, B., Goldbach, E., Holsztynska, E. J. et al. (2001) Functional γ-secretase inhibitors reduce β-amyloid peptide levels in brain. J. Neurochem. **76**, 173–181
40 Sastre, M., Steiner, H., Fuchs, K., Capell, A., Multhaup, G., Condron, M., Teplow, D. and Haass, C. (2001) Presenilin-dependent γ-secretase processing of β-amyloid precursor protein at a site corresponding to the S3 cleavage of Notch. EMBO Rep. **2**, 835–841
41 De Domenico, A., Ward, D., Di Patti, M., Jeong, S., David, S., Musci, G. and Kaplan, J. (2007) Ferroxidase activity is required for the stability of cell surface ferroportin in cells expressing GPI-ceruloplasmin. EMBO J. **26**, 2823–2831
42 Cottrell, D., Blakely, E., Johnson, M., Ince, P. and Turnbull, D. (2001) Mitochondrial enzyme-deficient hippocampal neurons and choroidial cells in AD. Neurology **57**, 260–264
43 Maurer, I., Zierz, S. and Moller, H. (2000) A selective defect of cytochrome c oxidase is present in brain of Alzheimer disease patients. Neurobiol. Aging **21**, 455–465
44 Sullivan, P. and Brown, M. (2005) Mitochondrial aging and dysfunction in Alzheimer's disease. Prog. Neuropsychopharmacol. Biol. Psychiatry **29**, 407–410
45 De Deyn, P., Hiramatsu, M., Borggreve, F., Goeman, J., D'Hooge, R., Saerens, J. and Mori, A. (1998) Superoxide dismutase activity in cerebrospinal fluid of patients with dementia and some other neurological disorders. Alzheimer Dis. Assoc. Disord. **12**, 9–12
46 Omar, R., Chyan, Y., Andorn, A., Poeggeler, B., Robakis, N. and Pappolla, M. (1999) Increased expression but reduced activity of antioxidant enzymes in Alzheimer's disease. J. Alzheimers Dis. **1**, 139–145
47 Vassar, R., Bennet, B., Babu-Khan, S., Kahn, S., Mendiaz, E., Denis, P., Teplow, D., Ross, B., Amarante, P., Loeloef, R. et al. (1999) β-Secretase cleavage of Alzheimer's amyloid precursor protein by the transmembrane aspartic protease BACE. Science **286**, 735–741
48 Yan, R., Belnkowski, M., Shuck, M., Miao, H., Tory, M., Pauley, A., Brashler, J., Stratman, N., Mathews, W., Buhl, A. et al. (1999) Membrane-anchored aspartyl protease with Alzheimer's disease activity. Nature **402**, 533–537
49 Angeletti, B., Waldron, K., Freeman, K., Bawagan, H., Hussain, I., Miller, C., Lau, K.-F., Tennant, M., Dennison, C., Robinson, N. and Dingwall, C. (2005) BACE1 cytoplasmic domain interacts with the copper chaperone for superoxide dismutase-1 and binds copper. J. Biol. Chem. **280**, 17930–17937
50 Pastorino, L., Ikin, A., Lamprianou, S., Vacaresse, N., Revelli, J., Platt, K., Paganetti, P., Mathews, P., Harroch, S. and Buxbaum, J. (2004) BACE (β-secretase) modulates the processing of APLP2 *in vivo*. Mol. Cell. Neurosci. **25**, 642–649
51 Scheinfeld, M., Ghersi, E., Laky, K., Fowlkes, B. and D'Adamio, L. (2002) Processing of β-amyloid precursor-like protein-1 and -2 by γ-secretase regulates transcription. J. Biol. Chem. **277**, 44194–44201
52 Post, A., Ackl, N., Rucker, M., Schreiber, Y., Binder, E. B., Ising, M., Sonntag, A., Holsboer, F. and Almeida, O. F. (2006) Toward a reliable distinction between patients with mild cognitive impairment and Alzheimer-type dementia versus major depression. Biol. Psychiatry. **59**, 858–862
53 Sparks, D. and Schreurs, B. (2003) Trace amounts of copper in water induce β-amyloid plaques and learning deficits in a rabbit model of Alzheimer's disease. Proc. Natl. Acad. Sci. U.S.A. **100**, 11065–11069
54 Puglielli, L., Friedlich, A. L., Setchell, K. D., Nagano, S., Opazo, C., Cherny, R. A., Barnham, K. J., Wade, J. D., Melov, S., Kovacs, D. M. and Bush, A. I. (2005) Alzheimer disease β-amyloid activity mimics cholesterol oxidase. Clin. Invest. **115**, 2556–2563

Received 11 January 2008/29 January 2008; accepted 4 February 2008
Published as BJ Immediate Publication 4 February 2008, doi:10.1042/BJ20080103

THE JOURNAL OF BIOLOGICAL CHEMISTRY VOL. 281, NO. 26, pp. 17670–17680, June 30, 2006

Degradation of the Alzheimer Disease Amyloid β-Peptide by Metal-dependent Up-regulation of Metalloprotease Activity*

Received for publication, March 16, 2006, and in revised form, April 28, 2006 Published, JBC Papers in Press, April 28, 2006, DOI 10.1074/jbc.M602487200

Anthony R. White[‡§¶1], Tai Du[‡§¶], Katrina M. Laughton[‡§], Irene Volitakis[‡§], Robyn A. Sharples[‡§‖], Michel E. Xilinas[§], David E. Hoke[‡§2], R. M. Damian Holsinger[‡§], Geneviève Evin[‡§], Robert A. Cherny[‡§], Andrew F. Hill[‡§‖**], Kevin J. Barnham[‡§], Qiao-Xin Li[‡§], Ashley I. Bush[‡§3], and Colin L. Masters[‡§¶]**

From the Departments of [‡]Pathology and [‖]Biochemistry and the [¶]Centre for Neuroscience, University of Melbourne, Victoria 3010, Australia and the [§]Mental Health Research Institute and the [**]Bio21 Molecular Biology and Biotechnology Institute, Parkville, Victoria 3052, Australia

Biometals play an important role in Alzheimer disease, and recent reports have described the development of potential therapeutic agents based on modulation of metal bioavailability. The metal ligand clioquinol (CQ) has shown promising results in animal models and small phase clinical trials; however, the actual mode of action *in vivo* has not been determined. We now report a novel effect of CQ on amyloid β-peptide (Aβ) metabolism in cell culture. Treatment of Chinese hamster ovary cells overexpressing amyloid precursor protein with CQ and Cu^{2+} or Zn^{2+} resulted in an ~85–90% reduction of secreted Aβ-(1–40) and Aβ-(1–42) compared with untreated controls. Analogous effects were seen in amyloid precursor protein-overexpressing neuroblastoma cells. The secreted Aβ was rapidly degraded through up-regulation of matrix metalloprotease (MMP)-2 and MMP-3 after addition of CQ and Cu^{2+}. MMP activity was increased through activation of phosphoinositol 3-kinase and JNK. CQ and Cu^{2+} also promoted phosphorylation of glycogen synthase kinase-3, and this potentiated activation of JNK and loss of Aβ-(1–40). Our findings identify an alternative mechanism of action for CQ in the reduction of Aβ deposition in the brains of CQ-treated animals and potentially in Alzheimer disease patients.

Alzheimer disease (AD)[4] is characterized by progressive neuronal dysfunction, reactive gliosis, and the formation of amyloid plaques in the brain. The major constituent of AD plaques is the amyloid β-peptide (Aβ), which is cleaved from the membrane-bound amyloid precursor protein (APP) (1). Aggregated or oligomeric Aβ can induce neurotoxicity through pathways involving free radical production and increased neuronal oxidative stress (2). Among the factors capable of promoting Aβ aggregation *in vivo*, recent evidence supports a central role for biometals such as Cu^{2+} and Zn^{2+} in this process (3).

An important factor in controlling Aβ accumulation in AD patients is the activity of Aβ-degrading enzymes. Recent studies have identified several candidate proteases that may contribute to catabolism of Aβ in the brain. Neprilysin, insulin-degrading enzyme, angiotensin-converting enzyme, and matrix metalloproteases (MMPs) have all demonstrated Aβ-degrading activity *in vitro* and/or *in vivo* (4–6). Reduced activity of these or other Aβ-degrading proteases with age may play a role in promoting accumulation and deposition of Aβ in AD patients. Development of strategies to enhance clearance of Aβ may lead to novel therapeutic treatments for AD patients.

Promoting Aβ clearance may be achieved through modulating metal sequestration or metal-protein interactions. 5-Chloro-7-iodo-8-hydroxyquinoline or clioquinol (CQ), a disused antibiotic, has received considerable attention as a potential metal ligand in AD and Parkinson disease patients (7–9). Preliminary studies revealed that CQ rapidly and potently dissolved aggregates of synthetic or AD brain-derived Aβ *in vitro* (10). In subsequent animal studies, a 9-week oral treatment with CQ resulted in a 49% reduction of Aβ levels and significantly increased Cu^{2+} and Zn^{2+} levels in brains of Tg2576 mice (10). Small clinical trials of CQ have demonstrated a significant slowing of cognitive decline together with a lowering of plasma Aβ-(1–42) levels in a subset of AD patients compared with matched placebo controls (8).

The mechanism of action by CQ was suggested to be via metal sequestration, resulting in Aβ dissolution. However, CQ could also act by alternative pathways involving modulation of cellular biometal metabolism, APP expression, or Aβ processing (11). To investigate this, Chinese hamster ovary (CHO) cells overexpressing APP were treated with CQ in the presence or absence of physiological levels of biometals. When CQ was added to cells in the presence of Cu^{2+} or Zn^{2+}, the secreted levels of Aβ-(1–40) and Aβ-(1–42) were dramatically reduced. Analogous effects were seen in N2a neuroblastoma cells. Subsequent investigation revealed that this effect was associated with uptake of Cu^{2+} and Zn^{2+} and loss of Aβ through increased MMP-mediated degradation. These findings identify a novel mechanism for the therapeutic efficacy of CQ in which CQ·Cu^{2+} or CQ·Zn^{2+} complexes promote Aβ degradation.

EXPERIMENTAL PROCEDURES

Materials—CQ, bacitracin, puromycin, Me_2SO, ascorbate, LY-294,002, wortmannin, bathophenanthroline disulfonate (BPS), *cis*-diamminedichloroplatinum (cisplatin), LiCl, SP600125, staurosporine, thior-

* This work was supported in part by the National Health and Medical Research Council of Australia. The costs of publication of this article were defrayed in part by the payment of page charges. This article must therefore be hereby marked "*advertisement*" in accordance with 18 U.S.C. Section 1734 solely to indicate this fact.
[1] Supported by an R. D. Wright fellowship from the National Health and Medical Research Council of Australia. To whom correspondence should be addressed: Dept. of Pathology, University of Melbourne, Cnr. Grattan St. and Royal Parade, Victoria 3010, Australia. Tel.: 61-3-8344-1805; Fax: 61-3-9349-4004; E-mail: arwhite@unimelb.edu.au.
[2] Supported by Ruth L. Kirschstein National Research Service Award Individual Fellowship AG05887 from NIA, National Institutes of Health.
[3] Supported by NIA Grant R01-AG12686 from the National Institutes of Health, the Alzheimer's Association, the American Health Assistance Foundation, and the Australian Research Council.
[4] The abbreviations used are: AD, Alzheimer disease; Aβ, amyloid β-peptide; APP, amyloid precursor protein; MMPs, matrix metalloproteases; CQ, clioquinol; CHO, Chinese hamster ovary; BPS, bathophenanthroline disulfonate; GSK, glycogen synthase kinase; MnTMPyP, Mn(III) tetrakis(1-methyl-4-pyridyl)porphyrin pentachloride; JNK, c-Jun N-terminal kinase; ERK, extracellular signal-regulated kinase; ICP-MS, inductively coupled plasma mass spectrometry; PI3K, phosphoinositol 3-kinase; MEK, mitogen-activated protein kinase/extracellular signal-regulated kinase kinase; ELISA, enzyme-linked immunosorbent assay; PBS, phosphate-buffered saline; Tricine, *N*-[2-hydroxy-1,1-bis(hydroxymethyl)ethyl]glycine; MAPK, mitogen-activated protein kinase.

phan, and PD 98,059 were purchased from Sigma (Sydney, Australia). SB 203580, bestatin, GM 6001, phosphoramidon, glycogen synthase kinase (GSK) Inhibitor IX, MMP Inhibitor I (broad-spectrum MMP inhibitor), MMP-2 Inhibitor I, MMP-3 Inhibitor I, MMP-9 Inhibitor I, Mn(III) tetrakis(1-methyl-4-pyridyl)porphyrin pentachloride (MnTMPyP), and serine/cysteine protease inhibitor mixture (EDTA-free) were obtained from Merck Biosciences (Victoria, Australia). Anti-APP antibody 22C11 was obtained from Chemicon International, Inc. (Temecula, CA). Antibody 369 (APP-(656–695) epitope) was a kind gift from Dr. Sam Gandy (Thomas Jefferson University, Philadelphia, PA). Antibodies to total or phospho-specific forms of Akt, JNK, ERK1/2, p38, and GSK3 were obtained from Cell Signaling Technology, Inc. (Beverly, MA).

Generation of APP-transfected CHO and N2a Neuroblastoma Cells—APP-CHO and APP-N2a neuroblastoma cells were generated by expressing the 695-amino acid APP cDNA in the pIRESpuro2 expression vector (Clontech). Cells were transfected using Lipofectamine 2000 and cultured in RPMI 1640 medium supplemented with 1 mM glutamine and 10% fetal bovine serum (all from Invitrogen, Mount Waverley, Victoria). Transfected cells were selected and maintained using 7.5 μg/ml puromycin (Sigma).

Exposure of Cells to CQ and Metals—APP-overexpressing cells were passaged at a ratio of 1:6 and grown in 6- or 12-well plates for 2–3 days before experiments. CQ was prepared as a 10 mM stock solution in Me_2SO and added to serum-free RPMI 1640 medium supplemented with puromycin as described above. Basal metal levels in the medium were 0.5, 1.3, and 2.1 μM for Cu^{2+}, Zn^{2+}, and Fe^{2+}, respectively, as determined by inductively coupled plasma mass spectrometry (ICP-MS). Additional metals were added (10 μM unless stated otherwise), and the medium was briefly mixed by aspiration prior to addition to cells. Control cultures were treated with vehicle (Me_2SO) alone. Inhibitors of phosphoinositol 3-kinase (PI3K) (LY-294,002 and wortmannin), JNK (SP600125), MEK1/2 (PD 98,059), p38 (SB 203580), GSK3 (GSK Inhibitor IX), and metalloproteases (GM 6001, phosphoramidon, thiorphan, bestatin, MMP-2 Inhibitor I, and MMP-9 Inhibitor I) were prepared as 10 mM stock solutions in Me_2SO and added at the indicated concentrations. Ascorbate, MnTMPyP, bacitracin, BPS, LiCl, and MMP-3 Inhibitor I were prepared as 10 mM solutions in distilled H_2O. Serine/cysteine protease inhibitor mixture (EDTA-free) was prepared as a 10× solution in distilled H_2O. Where stated, vector only-transfected or wild-type (non-APP-overexpressing) cells were exposed to synthetic human Aβ-(1–40) with or without CQ, metals, and inhibitors (see below). Cultures were incubated for up to 6 h, and conditioned media were taken for measurement of Aβ levels by enzyme-linked immunosorbent assay (ELISA). Cell viability was determined by lactate dehydrogenase release following kit instructions (Promega Corp., Annandale, New South Wales, Australia). For immunoblotting, cells were harvested into PhosphoSafe extraction buffer (Novagen) containing Protease Inhibitor Cocktail III (Calbiochem) and stored at −80 °C until used. Alternatively, cells were washed three times with phosphate-buffered saline (PBS) and harvested for analysis of metal levels by ICP-MS.

ICP-MS—Cells were treated with CQ and/or metals for 6 h unless stated otherwise and washed three times with Chelex 100-treated PBS (pH 7.4). Cells were scraped into PBS; an aliquot was taken for protein determination (protein microassay, Bio-Rad); and the remaining cells were collected by centrifugation at 14,000 rpm for 2 min in a Hermle microcentrifuge (Labnet International, Inc., Edison, NJ). Metal levels were determined in cell pellets by ICP-MS as described previously (12) and converted to ng of metal/mg of protein.

Degradation of Synthetic Aβ-(1–40)—Human Aβ-(1–40) was purchased from the W. M. Keck Laboratory (Yale University, New Haven, CT) and dissolved in Me_2SO at 1 mg/ml. The dissolved peptide was further diluted into Chelex 100-treated distilled H_2O at 100 ng/ml before addition to vector only-transfected CHO cell cultures in serum-free medium at 10 ng/ml without aging. In separate experiments, Aβ-(1–40) was also added to N2a mouse neuroblastoma, SH-SY5Y human neuroblastoma, or HeLa human epithelial cells in serum-free Opti-MEM I (Invitrogen). After 6 h (with or without addition of inhibitors and 10 μM each CQ, Cu^{2+}, or CQ and Cu^{2+}), the medium was collected, and the remaining Aβ-(1–40) levels were determined by ELISA.

Double Antibody Capture ELISA for Aβ Detection—Aβ levels were determined in culture medium using the DELFIA® double capture ELISA (PerkinElmer Life Sciences, Melbourne, Australia). 384-Well plates (Greiner Bio-One GmbH, Frickenhausen, Germany) were coated with monoclonal antibody G210 in 15 mM Na_2CO_3 and 35 mM $NaHCO_3$ (pH 9.6) for Aβ-(1–40) detection. Plates were washed with PBS containing 0.05% Tween and blocked with 0.5% (w/v) casein. Biotinylated monoclonal antibody WO2 (Aβ-(5–8) epitope) and the culture medium or Aβ standards were added (50 μl) to each well and incubated overnight at 4 °C. Plates were washed with PBS containing 0.05% Tween, and streptavidin-labeled europium (PerkinElmer Life Sciences) was added. The plates were washed; enhancement solution (PerkinElmer Life Sciences) was added; and the plates were read in a Wallac VICTOR^2 plate reader with excitation at 340 nM and emission at 613 nM. Aβ-(1–40) and Aβ-(1–42) standards and samples were assayed in triplicate. The values obtained from the triplicate wells were used to calculate the Aβ concentration (expressed as ng/ml) based on the standard curve generated on each plate. We observed a good correlation between ELISA results and Western blot analysis of Aβ levels in CQ·Cu^{2+}-treated cultures. As the ELISA offered quantitative data on Aβ levels, we chose this as the preferred method for assessing changes to secreted Aβ levels.

Western Blot Analysis of Protein Expression and Phosphorylation—Cell lysates prepared in PhosphoSafe extraction buffer were mixed with SDS sample buffer (Novex) and separated on 12% Tris/glycine/SDS-polyacrylamide gels (Novex). Western blotting of Aβ in the conditioned medium was performed using 10–20% Tris/Tricine gels. Proteins were transferred to polyvinylidene difluoride membranes and blocked with milk solution in Tris-buffered saline/Tween before immunoblotting for total or phospho-specific proteins. Membranes were probed for 1 h with antiserum against Aβ (antibody WO2), C-terminal APP (antibody 369), or full-length APP (antibody 22C11) at 1:2000 dilution and with horseradish peroxidase-conjugated rabbit anti-mouse or goat anti-rabbit secondary antibody at 1:5000 dilution. For detection of signal transduction molecules, membranes were probed with polyclonal antiserum against actin, JNK, phospho-JNK, p38, phospho-p38, ERK1/2, phospho-ERK1/2, Akt, phospho-Akt, GSK3β, phospho-GSK3α/β, MMP-2, or MMP-6 at 1:5000 dilution. Horseradish peroxidase-conjugated goat anti-rabbit secondary antiserum was used at 1:10,000 dilution. Blots were developed by chemiluminescence (ECL Advance, Amersham Biosciences) and imaged on a GeneGnome chemiluminescence imager (Syngene, Cambridge, UK). We found that the expression of total levels of kinases (Akt, JNK, ERK, and p38) was unaffected by metal uptake in APP-CHO cells. In contrast, actin, tubulin, and other proteins normally used for equalizing protein loading were found to be altered depending on metal levels.[5] Therefore, equal sample loading and protein transfer

[5] A. R. White, T. Du, K. M. Laughton, I. Volitakis, R. A. Sharples, M. E. Xilinas, D. E. Hoke, R. M. D. Holsinger, G. Evin, R. A. Cherny, A. F. Hill, K. J. Barnham, Q.-X. Li, A. I. Bush, and C. L. Masters, unpublished data.

TABLE 1
Metal concentrations in APP-CHO cells treated with CQ and metals for 6 h

Treatment	Cellular metal levels (p value compared with vehicle control)		
	Cu^{2+}	Zn^{2+}	Fe^{2+}
		ng/mg protein	
Vehicle	4.6 ± 0.1	182 ± 8	53 ± 5
CQ (10 μM)	20 ± 3 (0.01)	313 ± 39 (0.05)	25 ± 1
Cu^{2+} (10 μM)	24 ± 1	169 ± 10	48 ± 2
Zn^{2+} (10 μM)	6 ± 1	190 ± 16	16 ± 7
Fe^{2+} (10 μM)	4 ± 2	108 ± 7	845 ± 129 (0.001)
CQ-Cu^{2+} (10 μM)	472 ± 46 (0.005)	85 ± 14	17 ± 2
CQ-Zn^{2+} (10 μM)	29 ± 2	1838 ± 64 (0.001)	17 ± 4
CQ-Fe^{2+} (10 μM)	3 ± 2	269 ± 27	889 ± 22 (0.001)

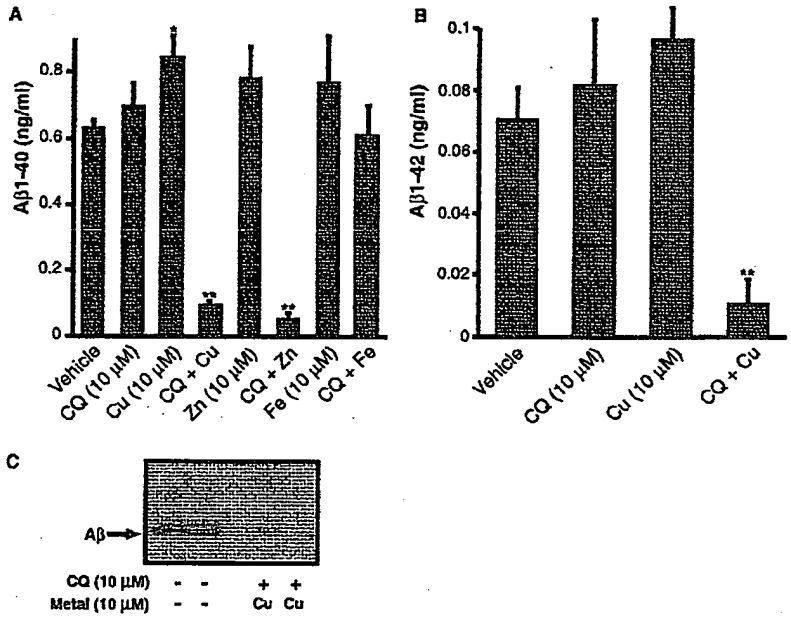

FIGURE 1. *A*, Aβ-(1–40) levels in medium from CQ-treated APP-CHO cells. Cultures were exposed to CQ (10 μM) with or without 10 μM Cu^{2+}, Zn^{2+}, or Fe^{2+} for 6 h, and Aβ-(1–40) levels were determined in culture medium by ELISA. Cu^{2+} alone induced a small but significant increase (*, $p < 0.01$) in Aβ-(1–40) secretion, whereas exposure to CQ-Cu^{2+} or CQ-Zn^{2+} significantly reduced Aβ-(1–40) levels (**, $p < 0.0001$). *B*, Aβ-(1–42) levels in medium from CQ-treated APP-CHO cells. Cultures were exposed to 10 μM CQ with or without 10 μM Cu^{2+} as described for *A*. CQ-Cu^{2+} induced a significant decrease in secreted Aβ-(1–42) levels (**, $p < 0.0001$). *Error* bars represent S.E. *C*, Immunoblotting of medium from CQ-Cu^{2+}-treated APP-CHO cells. Cultures were exposed to 10 μM CQ-Cu^{2+} for 6 h, and the conditioned medium was analyzed by Western blotting using anti-Aβ antiserum (antibody WO2). Aβ levels were significantly lower in cultures treated with CQ-Cu^{2+} compared with untreated controls.

were assessed by consistency of total kinase protein levels rather than unrelated protein levels on immunoblots.

Cell Adhesion Assay—Cell adhesion to collagen type IV was determined using an InnoCyte ECM cell adhesion assay (collagen type IV; Merck Biosciences). Cells were treated with CQ, Cu^{2+}, or CQ and Cu^{2+} (with or without inhibitors) for 4 h before harvesting with a rubber policeman into the culture medium. Cells were dissociated by aspiration, replated onto collagen type IV, and cultured for an additional 2 h. The medium was discarded, and cells were washed briefly with two changes of PBS before addition of calcein acetoxymethyl ester for 1 h (37 °C). Cell adhesion was determined by fluorescence spectrophotometry on a Wallac VICTOR^2 plate reader with excitation at 490 nM and emission at 535 nm.

MMP Assays—The activity of MMPs in the conditioned medium and cell lysates was determined using an EnzoLyte MMP fluorometric assay kit (AnaSpec, Inc., San Jose, CA). Briefly, the conditioned medium or cell lysates (freshly extracted without protease inhibitors) were incubated with MMP-specific peptide substrates following the kit instructions. The substrates used were QXL520-γAbu-Pro-Cha-Abu-*S*-methyl-L-cysteine-His-Ala-Dab(5-FAM)-Ala-Lys-HN_2 (where γAbu is γ-aminobutyric acid, Cha is D-cyclohexylalanine, Dab is 2,4-diaminobutyric acid, and 5-FAM is 5-carboxyfluorescein; broad-spectrum substrate), QXL520-Pro-Leu-Ala-Leu-Trp-Ala-Arg-Lys(5-FAM)-NH_2 (MMP-1), 5-FAM-Pro-LeuAla-Nva-Dap(QXL520)-Ala-Arg-NH_2 (where Nva is norvaline and Dap is diaminopropionic acid; MMP-2), QXL520-Pro-Tyr-Ala-Tyr-Trp-Met-Arg-Lys(5-FAM)-NH_2 (MMP-3), QXL520-Pro-Leu-Gly-Met-Trp-Ser-Arg-Lys(5-FAM)-NH_2 (MMP-2/9), and QXL520-Pro-Leu-Ala-Tyr-Trp-Ala-Arg-Lys(5-FAM)-NH_2 (MMP-8). No MMP-9-specific substrate was available. Cleavage of substrates by MMPs removed the quenching effect of QXL520 on 5-carboxyfluorescein, resulting in increased fluorescence with excitation at 490 nM and emission at 535 nm.

Statistical Analysis—All data described in graphical representations are means ± S.E. unless stated from a minimum of three separate experiments. Results were analyzed using Student's two-tailed *t* test.

RESULTS

CQ Mediates Uptake of Cu^{2+} and Zn^{2+} but Not Fe^{2+} in APP-CHO Cells—As CQ is a lipid-soluble metal ligand, we examined the effect of CQ on metal levels in APP695-transfected CHO cells (APP-CHO). Cultures were treated with CQ (10 μM) alone or in the presence of 10 μM Cu^{2+}, Zn^{2+}, or Fe^{2+} for 6 h, and cellular metal levels were assessed by ICP-MS. Basal Cu^{2+} levels were 4.6 ± 0.1 ng/mg of protein, and exposure to CQ alone increased this to 20 ± 3 ng/mg of protein ($p < 0.01$) (Table 1). Treatment with CQ and Cu^{2+} (CQ·Cu^{2+}) induced a dramatic 103-fold increase in cellular Cu^{2+} levels (472 ± 46 ng/mg of protein; $p < 0.005$) (Table 1). CQ also increased cellular Zn^{2+} levels from 182 ± 8 to 1838 ± 64 ng/mg of protein ($p < 0.001$) (Table 1). Measurement of cell survival (lactate dehydrogenase release) revealed no significant effect on cell viability after 6 h of exposure to 10 μM CQ and Cu^{2+} or Zn^{2+}. Treatment of cultures with Fe^{2+} alone (10 μM) resulted in a 16-fold

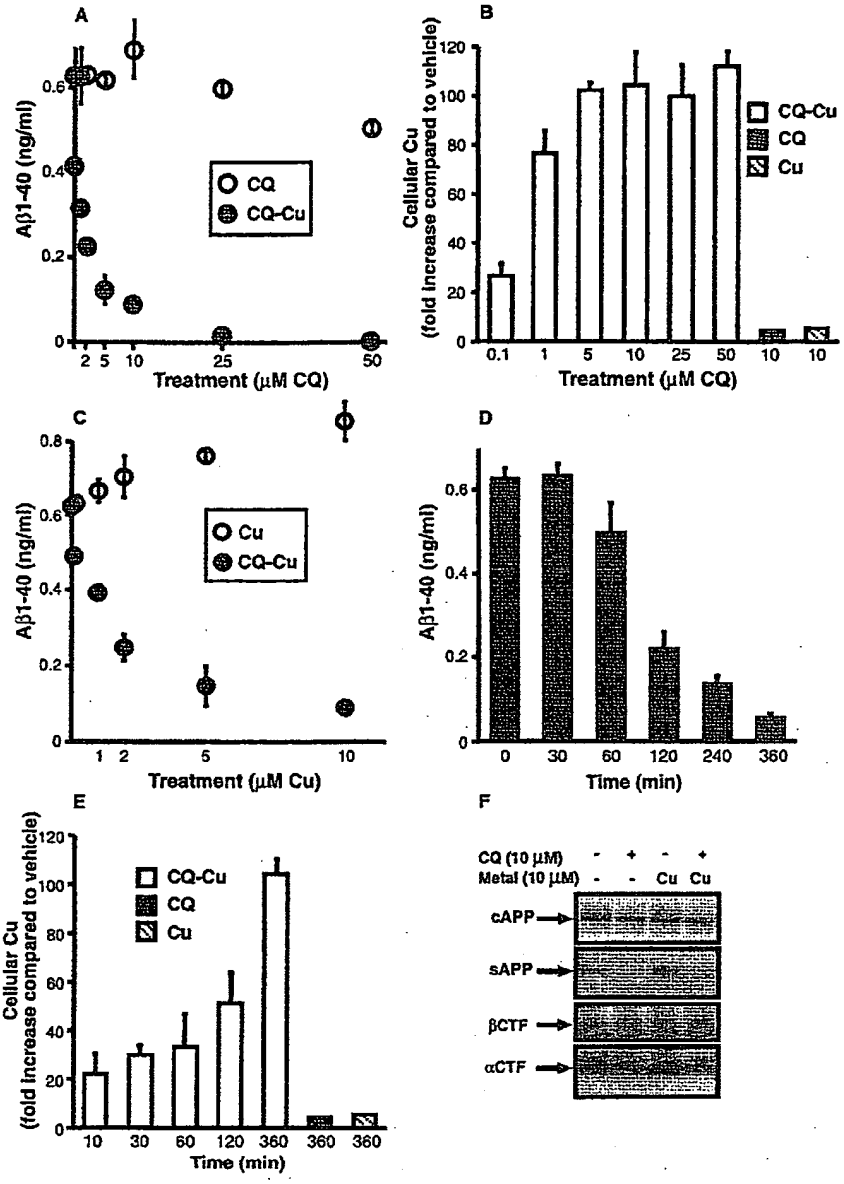

FIGURE 2. *A*, Aβ-(1–40) levels in medium from APP-CHO cells exposed to increasing concentrations of CQ. Cells were exposed to 0.1–50 μM CQ with or without 10 μM Cu^{2+} for 6 h. Aβ-(1–40) levels were determined in the culture medium by ELISA. All concentrations of CQ-Cu^{2+} tested (0.1–50 μM) induced a significant loss of secreted Aβ-(1–40) compared with CQ alone ($p < 0.001$–0.0001). *B*, cellular Cu^{2+} levels in APP-CHO cells exposed to Cu^{2+} and increasing concentrations of CQ. Cells were exposed to 10 μM Cu^{2+} and 0.1–50 μM CQ for 6 h. Cu^{2+} levels were determined in cell pellets by ICP-MS, revealing significantly increased cellular Cu^{2+} levels at all concentrations of CQ ($p < 0.001$–0.0001). The Cu^{2+} levels in vehicle-treated controls were equivalent to 1-fold Cu^{2+}. *C*, Aβ-(1–40) levels in medium from APP-CHO cells exposed to CQ and increasing concentrations of Cu^{2+}. Cells were treated with 10 μM CQ and 0.1–10 μM Cu^{2+} for 6 h. Cu^{2+} alone induced a small increase in secreted Aβ-(1–40) levels, but CQ-Cu^{2+} induced a dose-dependent decrease in secreted Aβ-(1–40) levels ($p < 0.01$–0.0001). *D*, Aβ-(1–40) levels in medium from APP-CHO cells exposed to CQ-Cu^{2+} for different time periods. Cells were treated with CQ-Cu^{2+} (10 μM) as described above, and Aβ-(1–40) levels were determined in the culture medium at time points up to 6 h after the start of treatment. Exposure to CQ-Cu^{2+} induced a time-dependent decrease in Aβ-(1–40) levels in the medium ($p < 0.05$–0.0001). *E*, cellular Cu^{2+} levels in APP-CHO cells exposed to CQ-Cu^{2+} for different time periods. Cells were exposed to CQ-Cu^{2+} (10 μM), and cellular Cu^{2+} levels were determined by ICP-MS in pellets at different time points up to 6 h after the start of treatment. CQ-Cu^{2+} induced a time-dependent increase in cellular Cu^{2+} levels ($p < 0.05$ at 120 min and $p < 0.001$ at 360 min). Relatively little change in cellular Cu^{2+} levels was induced by CQ or Cu^{2+} alone. The Cu^{2+} levels in vehicle-treated controls were equivalent to 1-fold Cu^{2+}. For all graphs, *error bars* represent S.E. *F*, APP levels in APP-CHO cells treated with CQ-Cu^{2+}. Cells were treated with 10 μM CQ with or without 10 μM Cu^{2+} for 6 h, and APP expression was determined by Western blotting in cell lysates and the conditioned medium. Equal protein loading was confirmed by immunoblotting for total JNK (not shown). CQ alone or CQ-Cu^{2+} decreased cellular APP (*cAPP*) expression and secreted APP (*sAPP*) levels in the conditioned medium. No change in APP β-C-terminal fragment (*βCTF*) C99 was observed with any treatment, whereas CQ-Cu^{2+} reduced expression of APP α-C-terminal fragment (*αCTF*) C83. Changes in APP expression did not correlate with secreted Aβ-(1–40) levels.

increase in cellular Fe^{2+} levels. However, co-treatment with CQ (10 μM) and Fe^{2+} did not further alter cellular Fe^{2+} levels. Analogous effects of CQ on cellular metal levels were also observed in vector only-transfected CHO cells. CQ-Cu^{2+} increased CHO cell Cu^{2+} levels by 94.5 ± 6-fold compared with untreated controls. Treatment with CQ-Zn^{2+} elevated Zn^{2+} levels by 10.5 ± 0.4-fold.

CQ and Cu^{2+} or Zn^{2+} Reduce Aβ Levels in Vitro—We examined whether CQ affects Aβ generation in APP-CHO cells. Treatment of APP-CHO cultures with 10 μM CQ alone for 6 h induced no significant change to Aβ-(1–40) levels in the culture medium (Fig. 1*A*). Interestingly, 10 μM Cu^{2+} alone for 6 h induced a 35% increase in Aβ-(1–40) levels ($p < 0.01$) (Fig. 1*A*).

When cultures were exposed to 10 μM CQ and 10 μM Cu^{2+}, we observed a potent reduction (~85%) of secreted Aβ-(1–40) levels ($p < 0.0001$) (Fig. 1*A*). An analogous effect was observed upon treatment with CQ and 10 μM Zn^{2+} (Fig. 1*A*). No significant changes were observed in Aβ-(1–40) levels when cells were treated with CQ plus Fe^{2+} (Fig. 1*A*). Potent inhibition of secreted Aβ-(1–42) levels also occurred with CQ-Cu^{2+}-treated cells (Fig. 1*B*). However, as Aβ-(1–42) levels in APP-CHO cells were near the detection limit of the ELISA, subsequent analysis of Aβ was restricted to Aβ-(1–40). The loss of secreted Aβ upon treatment with CQ-Cu^{2+} was confirmed by immunoblot analysis of the conditioned medium (Fig. 1*C*) and surface-enhanced laser desorption ionization mass spectrometry (data not shown).

Inhibition of Aβ Can Be Induced by Low Concentrations of CQ and Cu^{2+}—To examine the potency of CQ in inhibiting secreted Aβ levels, we treated cultures with 0.1–50 μM CQ with or without 10 μM Cu^{2+} for 6 h. Aβ-(1–40) was significantly decreased at 0.1 and 1.0 μM CQ plus Cu^{2+} (Fig. 2*A*). We also examined the effects of different concentrations of CQ on Cu^{2+} uptake in APP-CHO cells. 0.1 μM CQ induced an increase of ~25-fold in cellular Cu^{2+} levels (Fig. 2*B*). Increasing CQ concentrations resulted in further elevation of cellular Cu^{2+} levels, reaching 112-fold (at 50 μM) compared with control levels (Fig. 2*B*). The ability of low concentrations of CQ to increase cellular Cu^{2+} levels correlated with the potent reduction of secreted Aβ levels by CQ-Cu^{2+} (Fig. 2*A*). Although CQ has been reported

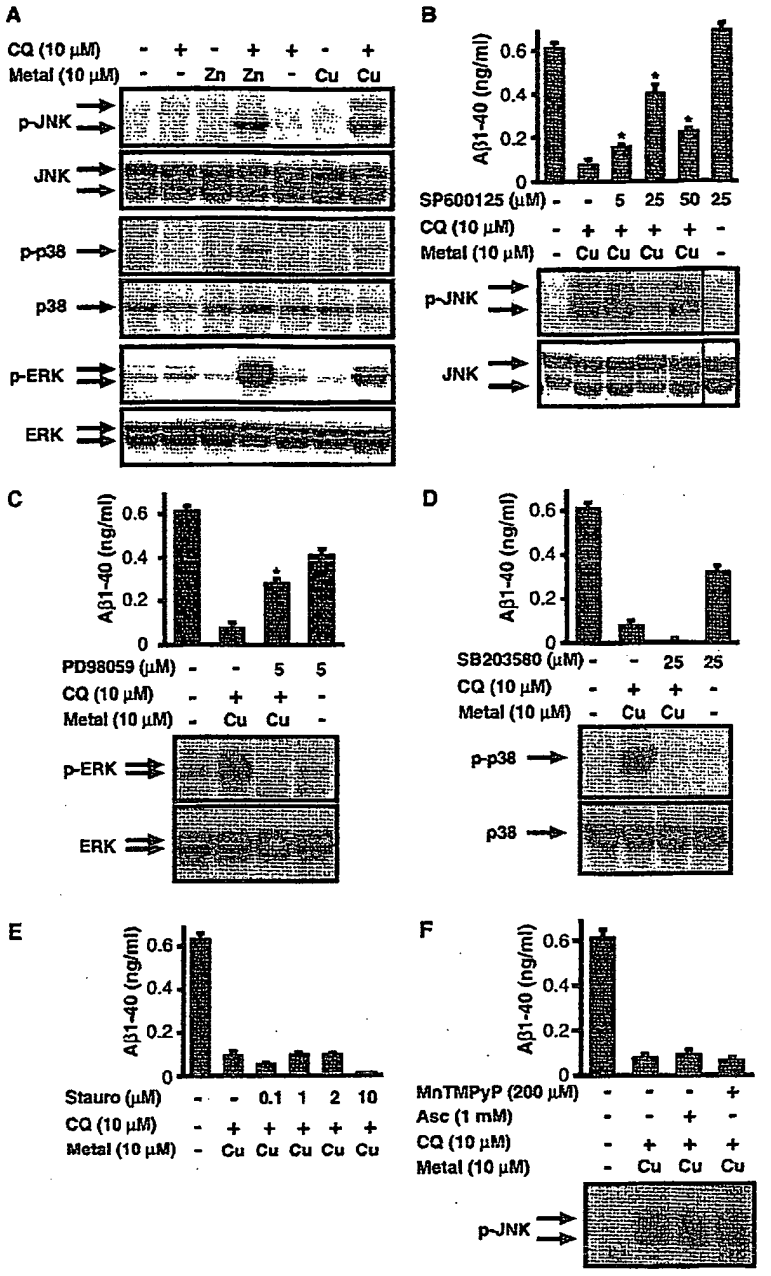

FIGURE 3. *A*, effects of CQ and metals on activation of MAPK pathways in APP-CHO cells. Cells were exposed to 10 μM CQ with or without 10 μM Cu^{2+} or Zn^{2+} for 6 h. Activation of MAPKs, including JNK, p38, and ERK1/2, was determined by Western blotting of cell lysates. CQ alone had no effect on the activity of MAPKs. In the presence of Cu^{2+} or Zn^{2+}, CQ induced activation of JNK, p38, and ERK1/2 (phospho-JNK, phospho-p38, and phospho-ERK1/2) *B*, JNK activation is associated with the loss of Aβ-(1–40) in APP-CHO cells treated with CQ-Cu^{2+}. Cells were exposed to 10 μM CQ-Cu^{2+} for 6 h in the presence or absence of the JNK inhibitor SP600125 (5–50 μM). Treatment of cells with CQ-Cu^{2+} induced activation of JNK with concurrent loss of Aβ-(1–40). Co-treatment of cells with SP600125 significantly inhibited both JNK activation and Aβ-(1–40) loss (*, $p < 0.001$). The dividing line represents removal of unrelated lanes. *C*, effect of the MEK1/2 inhibitor PD 98,059 on ERK1/2 activity and Aβ-(1–40) levels in APP-CHO cells treated with CQ-Cu^{2+}. Cells were treated with 10 μM CQ-Cu^{2+} for 6 h with or without addition of PD 98,059 (5 μM). Co-treatment with PD 98,059 abrogated ERK1/2 activation induced by CQ-Cu^{2+} and significantly inhibited Aβ-(1–40) loss (*, $p < 0.001$). *D*, the p38 inhibitor SB 203580 has no effect on the loss of Aβ-(1–40) induced by CQ-Cu^{2+}. APP-CHO cells were treated with 10 μM CQ-Cu^{2+} as described above with or without SB 203580 (25 μM). SB 203580 prevented p38 activation by CQ-Cu^{2+}, but did not prevent Aβ-(1–40) loss induced by CQ-Cu^{2+}. SB 203580 alone reduced Aβ-(1–40) levels. *E*, staurosporine does not inhibit the loss of Aβ-(1–40) induced by CQ-Cu^{2+}. APP-CHO cells were treated with 10 μM CQ-Cu^{2+} for 6 h in the presence or absence of the broad-spectrum protein kinase inhibitor staurosporine (*Stauro*; 0.1–10 μM). Co-treatment with staurosporine did not prevent the loss of Aβ-(1–40) by CQ-Cu^{2+}. *F*, JNK activation and Aβ-(1–40) loss by CQ-Cu^{2+} are not abrogated by antioxidants. APP-CHO cells were exposed to 10 μM CQ-Cu^{2+} for 6 h in the presence or absence of the free radical scavenger MnTMPyP (200 μM) or the antioxidant ascorbate (*Asc*; 1 mM). Co-treatment with MnTMPyP or ascorbate had no effect on JNK activation or Aβ-(1–40) loss. For all graphs, *error bars* represent S.E.

to optimally bind Cu^{2+} at a ratio of 2:1 (13), our titration studies showed no significant differences in Cu^{2+} uptake and inhibition of Aβ levels upon varying the CQ/Cu^{2+} ratios.

To determine the effects of Cu^{2+} concentration on secreted Aβ levels, cultures were exposed to 10 μM CQ with different concentrations of Cu^{2+}. 0.1 μM added Cu^{2+} significantly inhibited Aβ levels (Fig. 2*C*). Higher concentrations of added Cu^{2+} further decreased secreted Aβ levels (Fig. 2*C*). We also examined the time course of Aβ inhibition by CQ plus Cu^{2+} (10 μM each). We observed an initial decrease in Aβ levels from 30 to 60 min after addition of CQ-Cu^{2+}. A greater loss of Aβ was observed from 60 to 120 min after treatment (Fig. 2*D*). Examination of cellular metal levels revealed a 22-fold increase in Cu^{2+} after a 10-min exposure to CQ-Cu^{2+} (Fig. 2*E*). Cu^{2+} levels increased further at each time point, reaching a maximum level of 103-fold at 360 min (Fig. 2*E*).

Loss of Aβ by CQ-Cu^{2+} Does Not Correlate with Cellular APP Levels—To further understand how CQ-Cu^{2+} mediates Aβ loss, we determined whether there is a corresponding loss in APP expression. Exposure to CQ alone or to CQ-Cu^{2+} reduced both APP expression and secretion (Fig. 2*F*). However, as shown in Fig. 1*A*, only CQ-Cu^{2+} inhibited secreted Aβ levels. Interestingly, there was a reduction in the α-C-terminal 83-amino acid fragment of APP (C83) upon CQ-Cu^{2+} treatment, although no changes in APP β-C-terminal 99-amino acid fragment (C99) expression were found (Fig. 2*F*). This was consistent with our observation that the activity of BACE1 (beta-site APP-cleaving enzyme 1) in APP-CHO membrane preparations was unchanged after treatment with CQ-Cu^{2+}. Likewise, analysis of COS-7 cells transfected with a C-terminal APP construct (APP C99) (14) revealed no effect on γ-secretase cleavage of APP C99 by CQ-Cu^{2+}.[5] These findings demon-

strate that the loss of secreted Aβ upon treatment with CQ·Cu^{2+} is unlikely to result from altered APP processing.

Loss of Secreted Aβ by CQ·Cu^{2+} Is Mediated through Activation of JNK and ERK—Metal ligands can stimulate MAPK pathways (15, 16). To examine whether the effects of CQ·Cu^{2+} on Aβ occur via these pathways, we treated cultures with CQ and Cu^{2+} or Zn^{2+} (10 μM each) and measured activation of JNK, p38, and ERK1/2 in cell lysates. CQ with Cu^{2+} or Zn^{2+} induced substantial activation of JNK and ERK1/2, with moderate activation of p38 (Fig. 3*A*).

We then examined whether activation of these MAPK pathways is involved in the inhibitory action of CQ and metals on secreted Aβ levels. The JNK inhibitor SP600125 resulted in significant inhibition of JNK phosphorylation (Fig. 3*B*) and a significant elevation of Aβ-(1–40) levels compared with CQ·Cu^{2+} alone ($p < 0.001$) (Fig. 3*B*). The ERK1/2 phosphorylation inhibitor PD 98,059 (5 μM) prevented ERK activation after exposure to CQ·Cu^{2+} (Fig. 3*C*) and significantly inhibited Aβ loss ($p < 0.001$) (Fig. 3*C*). In contrast, the p38 inhibitor SB 203580 or the broad-spectrum protein kinase inhibitor staurosporine had no restorative effect on Aβ levels (Fig. 3, *D* and *E*).

JNK can be activated in response to cell stresses such as generation of reactive oxygen species or through growth factor-mediated pathways (17). Therefore, we examined whether JNK phosphorylation is mediated by generation of reactive oxygen species in the CQ·Cu^{2+}-treated cultures. APP-CHO cells were exposed to CQ·Cu^{2+} together with the reactive oxygen species scavenger MnTMPyP (200 μM) or the antioxidant ascorbate (1 mM). Treatment with these antioxidants did not inhibit JNK phosphorylation or prevent Aβ loss in CQ·Cu^{2+}-treated cultures (Fig. 3*F*). This is consistent with Zn^{2+} inducing effects analogous to those of Cu^{2+}, as Zn^{2+} is a redox-inactive metal and should not directly stimulate reactive oxygen species generation. Therefore, the results strongly suggest that activation of JNK by CQ·Cu^{2+} is not mediated through metal-induced oxidative stress.

Inhibition of Aβ by CQ·Cu^{2+} Requires Activation of the PI3K-Akt-GSK3 Pathway—Modulation of GSK3, a downstream target of PI3K and Akt activation, changes Aβ production in APP-CHO cells (18). Therefore, we examined whether the PI3K-Akt-GSK3 pathway is associated with the loss of Aβ production in CQ·Cu^{2+}-treated cells. Treatment of cells with CQ and Cu^{2+} (10 μM each) for 6 h resulted in significant activation of Akt (Fig. 4*A*). Co-treatment of cultures with the specific PI3K inhibitor LY-294,002 inhibited Akt phosphorylation induced by CQ·Cu^{2+} and significantly abrogated the decrease in secreted Aβ levels ($p < 0.0001$) (Fig. 4*A*).

Treatment of cultures with 10 μM CQ·Cu^{2+} for 6 h increased the phosphorylated forms of GSK3α/β, and this effect was blocked by LY-294,002 (Fig. 4*A*). There was also a small increase in total GSK3β levels in CQ·Cu^{2+}-treated cultures, which may partially account for the increased levels of phosphorylated GSK3.

We then investigated whether PI3K-Akt-GSK3 activation is upstream of MAPK activation. Treatment of cultures with 25 μM LY-294,002 (or 10 nM wortmannin; data not shown) inhibited phosphorylation of Akt as well as phosphorylation of both JNK and ERK1/2 (Fig. 4*B*). Conversely, treatment of cultures with inhibitors of JNK and ERK1/2 phosphorylation (SP600125 and PD 98,059 respectively) did not inhibit Akt phosphorylation (data not shown). These data demonstrate that PI3K-Akt activation is upstream of JNK and ERK activation.

Activation of the PI3K-Akt and JNK Pathways Alone Is Not Sufficient for Loss of Aβ—As inhibitors of PI3K and JNK pathways blocked the loss of Aβ by CQ·Cu^{2+}, we examined whether nonspecific up-regulation of these pathways also results in loss of Aβ in APP-CHO cells. Cultures exposed to 25–100 μM Cu^{2+} (without CQ) for 6 h revealed potent

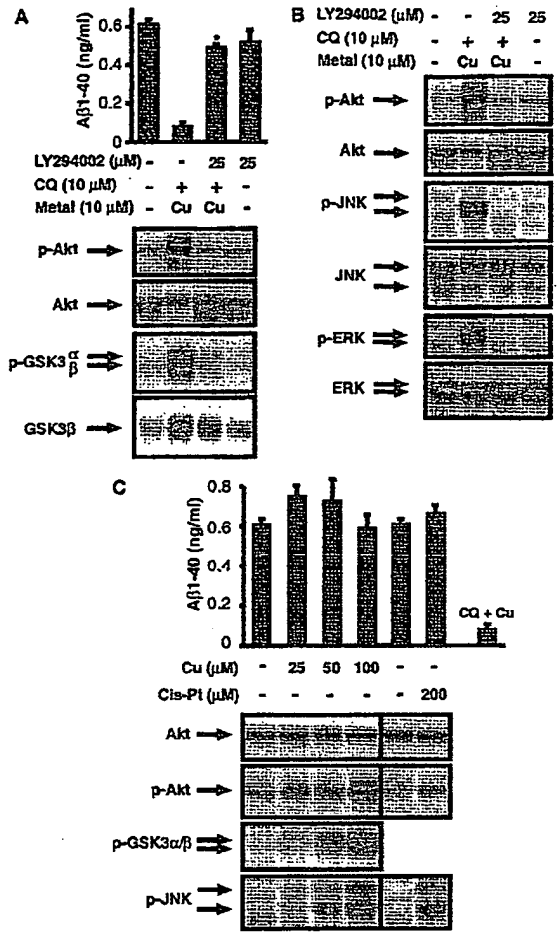

FIGURE 4. *A*, effect of PI3K inhibition on the loss of Aβ-(1–40) induced by CQ·Cu^{2+}. APP-CHO cells were treated with 10 μM CQ·Cu^{2+} with or without the PI3K inhibitor LY-294,002 (25 μM) for 6 h. Akt and GSK3 phosphorylation was determined by Western blotting of cell lysates, and Aβ-(1–40) levels were measured in the culture medium by ELISA. Treatment of cultures with CQ·Cu^{2+} induced activation of Akt and phosphorylation of GSK3α/β. Co-treatment with LY-294,002 inhibited Akt and GSK3 phosphorylation and abrogated Aβ-(1–40) loss induced by CQ·Cu^{2+} (*, $p < 0.0001$). *B*, effect of PI3K inhibition on MAPK signaling in APP-CHO cells treated with CQ·Cu^{2+}. Cultures were exposed to 10 μM CQ·Cu^{2+} with or without 25 μM LY-294,002 for 6 h. Co-treatment with LY-294,002 prevented activation of Akt, JNK, and ERK. *C*, activation of the PI3K and MAPK pathways is not sufficient alone for the loss of Aβ. APP-CHO cells were exposed to 25–100 μM Cu^{2+} or 200 μM cisplatin (*Cis-Pt*) for 6 h. 25–100 μM Cu^{2+} induced activation of Akt, and 50–100 μM Cu^{2+} induced phosphorylation of GSK3 and JNK. However, Cu^{2+} alone did not induce Aβ loss. Cisplatin (200 μM) did not activate the PI3K pathway, but induced phosphorylation of JNK. Cisplatin did not affect Aβ levels. Aβ levels induced by 10 μM CQ·Cu^{2+} are shown for comparison. For all graphs, *error bars* represent S.E.

activation of Akt, whereas 50 and 100 μM Cu^{2+} also induced phosphorylation of GSK3 and JNK (Fig. 4*C*). Moreover, cultures treated with the apoptotic agent cisplatin (200 μM) for 6 h revealed activation of JNK but not Akt (Fig. 4*C*). However, neither of these treatments (Cu^{2+} or cisplatin) reduced secreted Aβ levels, demonstrating that the PI3K-Akt and JNK pathways are necessary, but insufficient alone, for the loss of Aβ in APP-CHO cells.

GSK3 Phosphorylation Promotes Activation of JNK in Cultures Treated with CQ·Cu^{2+}—Our data suggested that phosphorylation of GSK3 in CQ·Cu^{2+}-treated cells may modulate downstream JNK activation. To examine this, we treated cultures with CQ·Cu^{2+} in the presence of LiCl (an inducer of GSK3 phosphorylation). In the presence of CQ·Cu^{2+}, 5 mM LiCl increased phosphorylated GSK3 levels compared with CQ·Cu^{2+} alone (Fig. 5*A*). LiCl had no effect on phospho-Akt levels, demonstrating that the effect was not mediated through increased PI3K

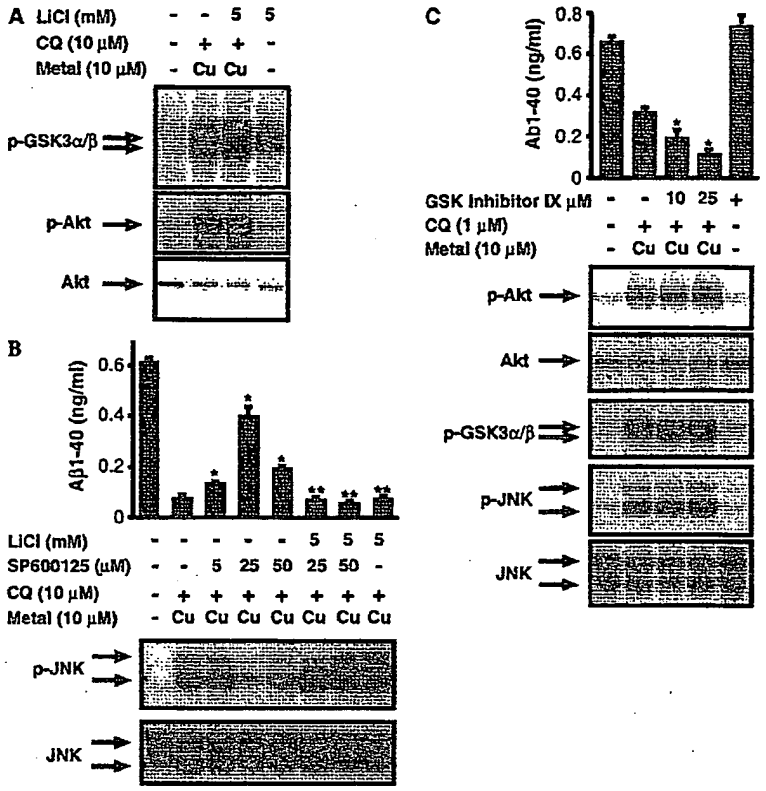

FIGURE 5. *A*, effect of LiCl on GSK3 phosphorylation in APP-CHO cells exposed to CQ·Cu^{2+}. Cells were treated with 10 μM CQ·Cu^{2+} with and without 5 mM LiCl for 6 h. Phosphorylation of GSK3α/β was determined by Western blotting of cell lysates. LiCl alone induced a low level of GSK3 phosphorylation, but, together with CQ·Cu^{2+}, greatly increased GSK3 phosphorylation without effect on Akt phosphorylation. *B*, effect of LiCl on Aβ-(1–40) in cultures treated with CQ·Cu^{2+}. APP-CHO cells were treated with 10 μM CQ·Cu^{2+} with or without the JNK inhibitor SP600125 (5, 25, or 50 μM) and/or LiCl (5 mM) for 6 h. CQ·Cu^{2+} induced JNK phosphorylation, and this was inhibited by co-treatment with SP600125. The loss of Aβ-(1–40) induced by CQ·Cu^{2+} was also inhibited by SP600125. Co-treatment with 5 mM LiCl substantially increased JNK activation even in the presence of the JNK inhibitor SP600125. Co-treatment with LiCl also restored the loss of Aβ-(1–40) induced by CQ·Cu^{2+}, overcoming the inhibitory action of SP600125 (*, $p < 0.001$ compared with control cultures, **, $p < 0.001$ compared with cultures treated with CQ·Cu^{2+} and SP600125). LiCl alone had no significant effect on Aβ-(1–40) levels (not shown). *C*, effect of GSK Inhibitor IX on GSK3, JNK, and Aβ levels in APP-CHO cells. Cultures were treated with 10 μM CQ·Cu^{2+} for 6 h with or without 10 or 25 μM GSK Inhibitor IX. GSK Inhibitor IX increased GSK3 and JNK phosphorylation induced by CQ·Cu^{2+}. GSK Inhibitor IX also potentiated the loss of Aβ-(1–40) (*Ab1–40*) induced by CQ·Cu^{2+} (*, $p < 0.001$). For all graphs, *error bars* represent S.E.

and Akt activities (Fig. 5*A*). LiCl potentiated JNK phosphorylation in cultures treated with CQ·Cu^{2+} (Fig. 5*B*). This potentiation was sufficient to overcome the inhibitory action of 25 or 50 μM SP600125 on JNK phosphorylation (Fig. 5*B*). Interestingly, potentiation of JNK phosphorylation by LiCl also overcame the ability of SP600125 to prevent Aβ loss in the medium (Fig. 5*B*). To confirm the potentiating effect of GSK3 phosphorylation on JNK activation, we treated cultures with 1 μM CQ and 10 μM Cu^{2+} in the presence of GSK Inhibitor IX (10 or 25 μM). This increased phosphorylation of GSK3 and JNK compared with CQ·Cu^{2+} alone (Fig. 5*C*). The increased GSK3 and JNK phosphorylation correlated with a down-regulation of Aβ levels in the culture medium (Fig. 5*C*). These results provide strong evidence that increased phosphorylation of GSK3 in CQ·Cu^{2+}-treated cultures promotes activation of JNK and leads to loss of secreted Aβ.

CQ·Cu^{2+} Induces Metalloprotease-dependent Loss of Aβ—Exposure of APP-CHO cells to CQ·Cu^{2+} for 6 h resulted in morphological changes consistent with altered cell adhesion (detachment of cells), but without an obvious role for cytotoxicity or oxidative stress (Fig. 3*F*). To examine this, we measured adhesion of cells to a collagen type IV matrix after treatment with 10 μM CQ and Cu^{2+}. As shown in Fig. 6*A*, CQ·Cu^{2+} inhibited APP-CHO cell adhesion to collagen type IV by ~50%. The loss of adhesion could be prevented by treatment with SP600125 or LY-294,002 (Fig. 6*A*). As loss of cell adhesion is commonly associated with activation of metalloproteases (19), we treated cells with broad-spectrum metalloprotease inhibitors. GM 6001 (10 μM), BPS (500 μM), and MMP Inhibitor I (20 μM) significantly inhibited CQ·Cu^{2+}-mediated loss of cell adhesion to collagen type IV (Fig. 6*A*).

To determine whether metalloproteases mediate Aβ loss, APP-CHO cells were treated with a range of metalloprotease inhibitors, and Aβ levels were measured after exposure to CQ·Cu^{2+}. All metalloprotease inhibitors tested except thiorphan (neprilysin inhibitor) significantly inhibited the decrease in secreted Aβ levels induced by CQ·Cu^{2+} (Fig. 6*B*). To confirm that the loss of secreted Aβ was mediated through increased metalloprotease-mediated degradation rather than altered APP processing, vector only-transfected CHO cell cultures were exposed to 10 ng/ml synthetic human Aβ-(1–40) for 6 h with or without CQ·Cu^{2+}. Measurement of Aβ-(1–40) levels in the conditioned medium revealed 0.89 ± 0.11 ng/ml remaining in the control medium after 6 h, indicating substantial clearance by cell uptake and/or degradation (Fig. 6*C*). Exposure of cultures to 10 μM CQ or 10 μM Cu^{2+} increased the levels of synthetic Aβ-(1–40) remaining in the medium after 6 h (Fig. 6*C*). However, treatment of cultures with CQ·Cu^{2+} significantly decreased Aβ-(1–40) levels by 56% compared with controls and by 77% compared with CQ alone (Fig. 6*C*). Interestingly, this effect was prevented by co-treatment of cultures with LY-294,002 (25 μM) or inhibitors of metalloproteases (Fig. 6*C*). The results clearly support a role for PI3K-mediated metalloprotease degradation of Aβ as the primary cause of Aβ loss in cultures treated with CQ·Cu^{2+}.

CQ·Cu^{2+} Induces Up-regulation of MMP-2 and MMP-3 through Activation of the PI3K and JNK Pathways—The efficacy of GM 6001 and MMP Inhibitor I against loss of Aβ and cell adhesion strongly supported a role for up-regulation of MMPs in CQ·Cu^{2+}-treated cultures. Therefore, we measured the activity of MMPs in cells treated with CQ·Cu^{2+} using MMP-specific fluorescent substrates. MMP assays of cell lysates or the conditioned medium after treatment with CQ·Cu^{2+} for 6 h revealed a significant elevation of the specific activities of MMP-2 and MMP-3 (Fig. 7*A*). No significant changes were observed in the activities of MMP-1, MMP-8, and MMP-9. Western blot analysis of cell lysates with antisera to MMP-2 and MMP-9 confirmed the results from the fluorescent substrate assay. Both latent and activated forms of MMP-2 were up-regulated in cultures exposed to CQ·Cu^{2+}, whereas MMP-9 revealed only a minimum change (Fig. 7*A*, *inset*).

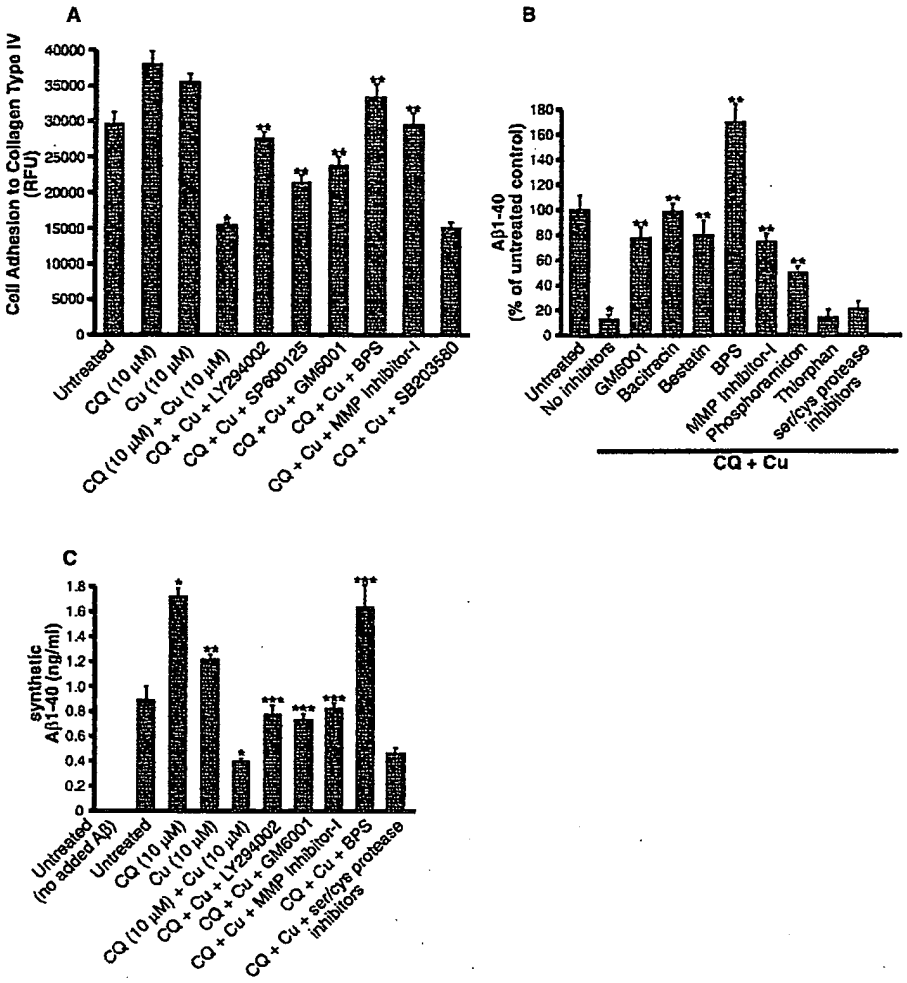

FIGURE 6. *A*, cell adhesion to a collagen type IV matrix. APP-CHO cells were exposed to CQ (10 μM), Cu^{2+} (10 μM), or CQ-Cu^{2+} with or without inhibitors, and adhesion to collagen type IV was determined by uptake of calcein acetoxymethyl ester by attached cells. Cells treated with CQ-Cu^{2+} revealed significantly lower adhesion to collagen type IV (*, $p < 0.0001$). The loss of adhesion was significantly inhibited (**, $p < 0.001$–0.0001) by co-treatment with LY-294,002 (25 μM), SP600125 (25 μM), GM 6001 (10 μM), BPS (500 μM), or MMP Inhibitor I (20 μM), but not by SB 203580 (25 μM). *RFU*, relative fluorescence units. *B*, Aβ loss is inhibited by metalloprotease inhibitors. APP-CHO cells were treated with 10 μM CQ-Cu^{2+} for 6 h with or without 10 μM GM 6001, 10 μM bacitracin, 10 μM bestatin, 500 μM BPS, 20 μM MMP Inhibitor I, 50 μM phosphoramidon, 25 μM thiorphan, or 1× serine/cysteine protease inhibitor mixture. Aβ(1–40) levels were measured in the culture medium by ELISA. CQ-Cu^{2+} induced a significant loss of Aβ(1–40) (*, $p < 0.0001$). Co-incubation with metalloprotease inhibitors significantly inhibited the loss of Aβ(1–40) induced by CQ-Cu^{2+} (**, $p < 0.001$ compared with CQ-Cu^{2+} alone). *C*, effect of CQ-Cu^{2+} on the loss of synthetic Aβ(1–40). Vector only-transfected CHO cells were exposed to CQ (10 μM), Cu^{2+} (10 μM), or CQ-Cu^{2+} for 6 h with or without LY-294,002 (25 μM), GM 6001 (10 μM), MMP Inhibitor I (20 μM), BPS (500 μM), or 1× serine/cysteine protease inhibitor mixture. Cultures were co-incubated with 10 ng/ml synthetic human Aβ(1–40) for 6 h, and the medium was assessed for remaining Aβ(1–40) by ELISA. Treatment of cultures with CQ or Cu^{2+} alone resulted in significantly increased levels of Aβ(1–40) remaining in the conditioned medium after 6 h (*, $p < 0.0001$; **, $p < 0.01$). Treatment with CQ-Cu^{2+} resulted in significantly decreased Aβ(1–40) levels compared with controls. The loss of Aβ(1–40) could be inhibited by addition of LY-294,002 or metalloprotease inhibitors (***, $p < 0.001$–0.0001 compared with CQ and Cu^{2+} alone). For all graphs, *error bars* represent S.E.

To further confirm activation of MMP-2 and MMP-3 by CQ-Cu^{2+}, cultures were treated with selective MMP inhibitors. Incubation of cultures with MMP-2 Inhibitor I prevented activation of MMP-2 by CQ-Cu^{2+}, but had no significant effect on MMP-3 activity (Fig. 7*B*). Likewise, MMP-3 Inhibitor I blocked activation of MMP-3, but did not affect MMP-2 activation by CQ-Cu^{2+} (Fig. 7*B*). An MMP-9 inhibitor had no effect on either MMP-2 or MMP-3 activation by CQ-Cu^{2+} (Fig. 7*B*). Moreover, we observed that LY-294,002 and SP600125 blocked activation of MMP-2 and MMP-3 (Fig. 7*B*).

Interestingly, the inhibitors of MMP-2 and MMP-3 significantly abrogated the loss of Aβ(1–40) caused by CQ-Cu^{2+} (Fig. 7*C*). These effects were consistent with a previous report that both MMP-2 and MMP-3 can cleave Aβ at several sites (10). In fact, surface-enhanced laser desorption ionization analysis of medium from our control cultures revealed Aβ cleavage products consistent with MMP-2-mediated degradation.[5] Unfortunately, few Aβ fragments of any size were observed in CQ-Cu^{2+}-treated cultures. This suggested that further degradation of the Aβ cleavage fragments may be occurring in these cultures, possibly through activation of aminopeptidases. This was supported by inhibition of Aβ loss by co-treatment with bestatin (aminopeptidase inhibitor) (Fig. 6*B*).

Finally, we examined alternative cell types for their ability to degrade Aβ when exposed to CQ-Cu^{2+}. Treatment of APP-overexpressing N2a murine neuroblastoma cells with 10 μM CQ and 10 μM Cu^{2+} for 6 h reduced Aβ levels from ~1.1 to 0.4 ng/ml ($p < 0.001$), whereas CQ or Cu^{2+} alone had no significant effect (Fig. 8*A*). In addition, non-transfected N2a, SH-SY5Y human neuroblastoma, and HeLa human epithelial cells were treated with 10 μM CQ and Cu^{2+} together with 10 ng/ml synthetic human Aβ-(1–40). Measurement of Aβ levels in the conditioned medium after 6 h revealed significantly reduced synthetic Aβ-(1–40) levels in all cell types after treatment with CQ-Cu^{2+}, and this could be prevented by co-treatment with GM 6001 (Fig. 8*B*). These results demonstrate that CQ-Cu^{2+} can modulate secreted Aβ levels via metalloproteases in different cell types, including neuroblastoma cells.

DISCUSSION

In this study, we have shown for the first time that the lipid-soluble metal ligand CQ modulates secreted Aβ levels *in vitro*. Whereas treatment of APP-expressing cells with CQ alone had little effect on Aβ levels in the culture medium, treatment with CQ complexed to Cu^{2+} or Zn^{2+} dramatically decreased extracellular Aβ levels. We have shown that this effect is closely related to the ability of CQ to mediate substantial increases in cellular Cu^{2+} or Zn^{2+} levels, resulting in selective up-regulation of MMP activity.

Interestingly, we found that even low concentrations of CQ or Cu^{2+} (0.1–1 μM each) could induce a significant loss of Aβ after only 6 h. The potency with which CQ-Cu^{2+} inhibited Aβ underscores the potential physiological relevance of our findings. A recent study reported human plasma levels of CQ at ~13–25 μM during small

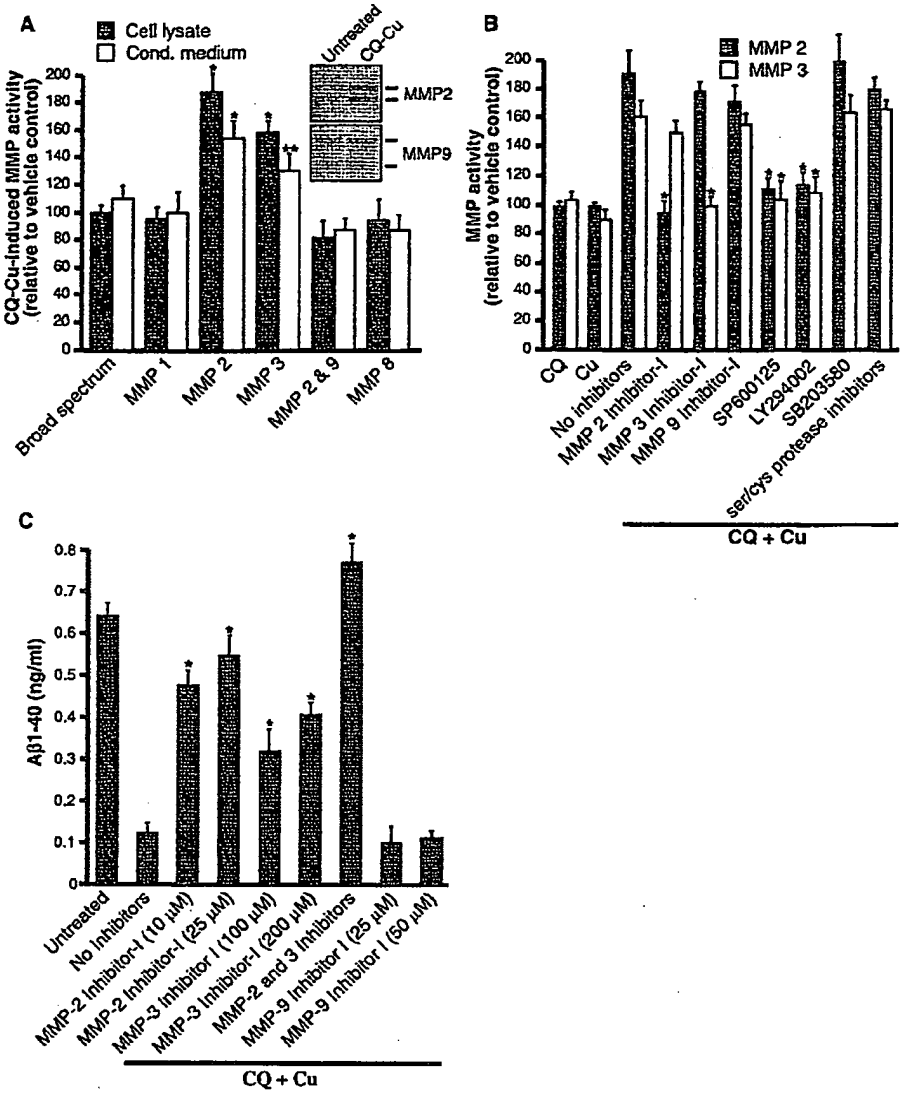

FIGURE 7. *A*, MMP activity induced by CQ-Cu^{2+}. APP-CHO cells were treated with 10 μM CQ-Cu^{2+} for 6 h, and MMP activity was assayed in cell lysates and the conditioned (*Cond.*) medium. MMP-1 and MMP-8 activities were not significantly altered in cells exposed to CQ-Cu^{2+}. MMP-2 and MMP-3 activities were significantly elevated by CQ-Cu^{2+} (*, $p < 0.001$; **, $p < 0.05$). No significant effects were observed using a broad-spectrum MMP substrate or a substrate recognized by both MMP-2 and MMP-9. *Inset*, Western blot analysis of cell lysates using antisera to MMP-2 and MMP-9. Western blotting confirmed that latent (*upper band*) and active (*lower band*) forms of MMP-2 were up-regulated in cultures treated with CQ-Cu^{2+} compared with controls. No change in latent MMP-9 (*upper band*) was observed in CQ-Cu^{2+}-treated cultures, although a slight increase in active MMP-9 (*lower band*) was seen. *B*, effect of inhibitors on MMP activity induced by CQ-Cu^{2+}. APP-CHO cells were exposed to CQ-Cu^{2+} (10 μM) for 6 h with or without MMP-2 inhibitor I (25 μM), MMP-9 inhibitor I (25 μM), LY-294,002 (25 μM), SB 203580 (25 μM), GM 6001 (10 μM), MMP-3 inhibitor I (200 μM), or 1× serine/cysteine protease inhibitor mixture. CQ-Cu^{2+} significantly activated both MMP-2 and MMP-3. MMP-2 activity induced by CQ-Cu^{2+} was significantly inhibited by co-treatment with MMP-2 inhibitor I, GM 6001, or LY-294,002. MMP-3 activity was significantly inhibited by MMP-3 inhibitor I, GM 6001, or LY-294,002 (*, $p < 0.001$–0.0001). *C*, effect of MMP inhibitors on the loss of Aβ-(1–40) in CQ-Cu^{2+}–treated cultures. APP-CHO cells were exposed to 10 μM CQ-Cu^{2+} for 6 h with or without MMP-2 inhibitor I (10 and 25 μM), MMP-3 inhibitor I (used at 100 and 200 μM, as this is a large, peptide-based inhibitor, not a small, lipid-soluble molecule), MMP-2 and MMP-3 inhibitors (25 and 200 μM), or MMP-9 inhibitor I (25 and 50 μM), and Aβ-(1–40) levels were measured in the culture medium by ELISA. MMP-2 inhibitor I and MMP-3 inhibitor I but not MMP-9 inhibitor I prevented the loss of Aβ-(1–40) induced by CQ-Cu^{2+} (*, $p <$ 0.0001). For all graphs, *error bars* represent S.E.

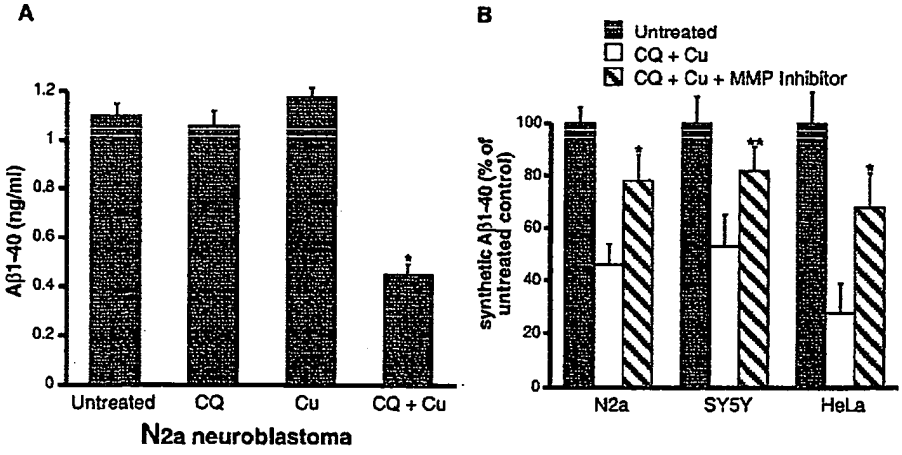

FIGURE 8. *A*, effect of CQ-Cu^{2+} on Aβ levels in APP-overexpressing N2a neuroblastoma cells. APP-N2a cells were treated with CQ or Cu^{2+} (10 μM each) or CQ-Cu^{2+} for 6 h. Aβ-(1–40) levels were determined in the conditioned medium by ELISA. Treatment with CQ-Cu^{2+} significantly reduced Aβ-(1–40) levels in APP-N2a cells (*, $p < 0.001$). *B*, loss of synthetic Aβ-(1–40) in different cell lines after treatment with CQ-Cu^{2+}. N2a, SH-SY5Y, or HeLa cells were exposed to 10 μM CQ-Cu^{2+} for 6 h with 10 ng/ml synthetic Aβ-(1–40). Treatment with CQ-Cu^{2+} significantly decreased synthetic Aβ-(1–40) levels in the conditioned medium of all cell types tested. Addition of the broad-spectrum MMP inhibitor GM 6001 (10 μM) significantly reduced the loss of Aβ-(1–40) (*, $p < 0.001$; **, $p <$ 0.01). For all graphs, *error bars* represent S.E.

phase clinical trials (8). CQ levels in the brain may reach 20% of serum levels, which equates to 2.6–5 μM (20). These concentrations were well within the range of CQ levels found to inhibit Aβ in our cultures if sufficient Cu^{2+} or Zn^{2+} was available. Cu^{2+} levels can range from 1.7 μM in the extracellular space of the brain to 250 μM in the synaptic cleft, whereas Zn^{2+} is also highly abundant in the brain, with synaptic levels reaching 300 μM (21). Further investigation is required to determine whether CQ can transport other metals (*i.e.*

nickel or cobalt) into cells and, if so, whether similar effects on APP metabolism are induced.

Although CQ is neurotoxic *in vitro* at low concentrations (22), cell lines are relatively more resistant to CQ than are primary neurons, and we found no evidence of increased cell death after 6 h of exposure to CQ and metals. Moreover, AD patients treated with 250 or 750 mg of CQ/day have not revealed complications that would indicate severe neurotoxicity (8). Similarly, mice treated with intraperitoneal injections of 28 mg/kg CQ also failed to show evidence of cytotoxicity (23). These findings suggest that the actions and toxicity of CQ *in vivo* are likely to be complex and dependent on the availability of "free" metals, antioxidants levels, and cellular resistance.

The mechanism of action by CQ-Cu^{2+} is via activation of the PI3K-Akt pathway and subsequent phosphorylation of JNK and ERK1/2. Although it is common to view PI3K-Akt and JNK/p38 as opposing pathways leading to cell survival and apoptosis, respectively (24), JNK activation can also be potentiated through PI3K activation (25, 26), as we have demonstrated here. Activation of both PI3K-Akt and JNK pathways has been reported in AD brain tissue, although the downstream consequences of this activity are not clear (27, 28).

PI3K is normally activated in response to cell stresses or growth factors, and metals can activate PI3K in some cell culture models (29). Particularly intriguing was our finding that activation of Akt and JNK by treatment with high Cu^{2+} levels alone (without CQ) or cisplatin had no effect on secreted Aβ levels, demonstrating that, although up-regulation of these pathways is required, by themselves, they are not able to decrease secreted Aβ levels. It is possible that, after exposure to CQ and metals, elevation of Cu^{2+} (or Zn^{2+}) levels in certain subcellular compartments results in specific modulation of multiple metal-dependent pathways, including PI3K activation (Fig. 9). This is consistent with reports that Zn^{2+} can activate gene expression by a PI3K- and JNK-dependent process (30). Alternatively, elevated metal levels could promote release of growth factors or other ligands that, in turn, activate PI3K, MAPK, and additional pathways. Interestingly, stimulation of MAPK pathways by metal-mediated growth factor release has been reported in lung epithelial cells (16, 31).

A common downstream signaling pathway controlled by PI3K activation involves phosphorylation of Akt and subsequent inhibition of GSK3 through phosphorylation (32). Treatment of cultures with LY-294,002 blocked phosphorylation of both Akt and GSK3α/β by CQ-Cu^{2+}. Inhibition (phosphorylation) of GSK3 can result in abrogation of Aβ production in APP-transfected cells (18), consistent with our findings. However, we found that phosphorylation of GSK3α/β correlated closely with increased JNK phosphorylation. Using inhibitors of GSK3 (LiCl and GSK Inhibitor IX), we demonstrated that increased phosphorylation of GSK3 potentiated JNK activation and subsequent Aβ loss. The mechanism behind this is not clear. As phosphorylation of GSK3 leads to its inactivation, the data suggest that activated GSK3 may inhibit or reduce JNK activation by certain stimuli. Similar effects have been reported previously, where a loss of GSK3 activity potentiated JNK activation by growth factors but not by cell stress (17, 33). This is consistent with our data suggesting that MAPK pathways are activated by CQ-Cu^{2+} via non-oxidative mechanisms. Down-regulation of GSK3 activity by CQ-Cu^{2+} could also affect tau phosphorylation, and this should be investigated in appropriate neuronal cell models.

Activation of cell signaling pathways by CQ-Cu^{2+} culminated in up-regulation of MMP activity and degradation of extracellular Aβ. Fig. 9 shows that the order of events are activation of PI3K-Akt, followed by phosphorylation of GSK3 as well as JNK and ERK. Inhibition of these

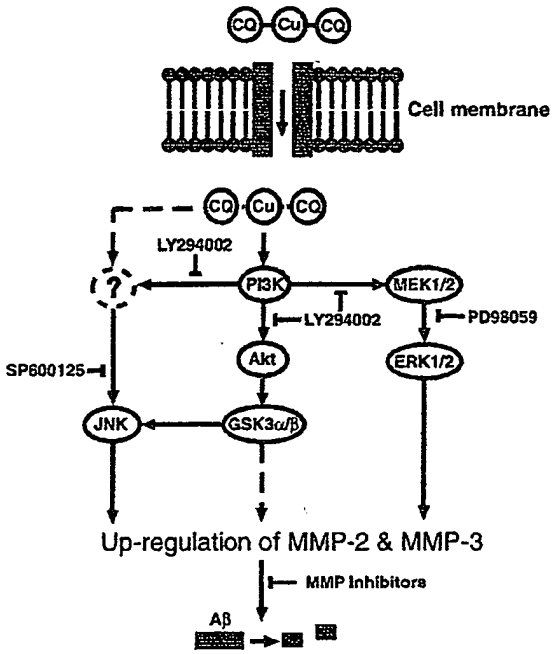

FIGURE 9. **Schematic of a proposed mechanism showing how CQ-Cu^{2+} mediates reduction of Aβ levels in APP-CHO cell cultures.** *Solid arrows* represent established pathways. *Dashed arrows* represent proposed pathways. CQ-Cu^{2+} complexes enter the cell by an unknown process. Cu^{2+} induces PI3K and additional cofactors (?) required for JNK activation. PI3K also activates Akt via phosphorylation, which, in turn, mediates phosphorylation of GSK3. PI3K activates MEK1/2 (not shown), resulting in phosphorylation of ERK1/2. Upon phosphorylation, GSK3 potentiates activation of JNK, which either alone or in concert with GSK3 or other signal factors, up-regulates the activities of MMP-2 and MMP-3. This induces an increase in degradation of extracellular or membrane-associated Aβ by these metalloproteases. Sites of inhibitor action are also shown.

kinases (Akt, JNK, and ERK) blocked activation of MMPs, so they are upstream of MMP activation. Moreover, inhibitors of the kinases and MMPs blocked the loss of Aβ, demonstrating that Aβ loss is downstream of these events. MMP activation is often associated with pathological changes to the cellular microenvironment in the brain, including tumor cell tissue invasion and migration and breakdown of blood-brain barrier permeability during cerebral ischemia. However, MMP activation can also have beneficial functions in the brain, including angiogenesis following ischemia and during axon guidance.

Up-regulation of MMP-2 and MMP-3 by Cu^{2+} or Zn^{2+} has been reported previously (16, 34), although excess Zn^{2+} can also inhibit MMP activity (35). In this study, we found that either Cu^{2+} or Zn^{2+} complexed to CQ induced activation of JNK, ERK, and p38 and loss of secreted Aβ. However, we investigated only CQ-Cu^{2+} complexes in detail, and it remains to be determined whether CQ-Zn^{2+} complexes mediate activation of the same MMPs.

Importantly, MMP-2 and MMP-3 levels can be increased through stimulation of the PI3K-Akt and MAPK (JNK and ERK) pathways (36, 37), which is consistent with our findings in CQ-Cu^{2+}-treated cells. Nonspecific Akt and JNK phosphorylation was unable to induce the decrease in secreted Aβ levels, indicating that CQ-delivered Cu^{2+} has a more complex effect on cell signaling pathways, resulting in up-regulation of MMPs. For example, there are a number of soluble inducers of MMP-2 and MMP-3, including transforming growth factor-β and epidermal growth factor, that could be released upon exposure to CQ and metals.

Aβ can be degraded *in vitro* and *in vivo* by several proteases, including metalloproteases, neprilysin, insulin-degrading enzyme, and MMPs (4, 6, 38). These metalloproteases may have important roles in clearance of Aβ in the brain, whereas reduced activity in AD patients could promote amyloid

deposition. As thiorphan (neprilysin inhibitor) had no effect on Aβ levels in CQ·Cu^{2+}-treated cultures, increased neprilysin activity is unlikely to be involved in Aβ loss. Although the inhibition of Aβ loss by bacitracin is consistent with insulin-degrading enzyme activity toward Aβ, immunoblot analysis of the culture medium revealed no increase in insulin-degrading enzyme levels after CQ·Cu^{2+} treatment (data not shown).

It has been shown previously that Aβ-(1–40) and Aβ-(1–42) can be degraded by MMP-2 (Lys^{16} ↓ Leu^{17}, Leu^{34} ↓ Met^{35}, and Met^{35} ↓ Val^{36}) and MMP-3 (Glu^{3} ↓ Phe^{4}) (4, 39). MMP-6 is also known to degrade Aβ at Lys^{16} ↓ Leu^{17}, Ala^{30} ↓ Ile^{31}, Leu^{34} ↓ Met^{35}, and Gly^{37} ↓ Gly^{38} (4, 39). Our study supports the MMP-mediated degradation of Aβ, as both MMP-2 and MMP-3 were up-regulated in response to CQ·Cu^{2+} treatment, and inhibition of these metalloproteases prevented the loss of secreted Aβ. Whether other MMPs (40) and proteases (*i.e.* aminopeptidases) are also involved in the loss of Aβ induced by CQ·Cu^{2+} is not known. Further investigation will be necessary to fully characterize the Aβ cleavage products in CQ·Cu^{2+}-treated cultures and to identify whether MMP-2- and MMP-3-mediated cleavage is a rate-limiting step in the rapid clearance of secreted Aβ.

Whether CQ enhances degradation of Aβ *in vivo* is not known. MMP expression and distribution are altered in AD brains, and up-regulation of MMP activity occurs in response to Aβ exposure *in vitro* (41). Although this may result from inflammatory processes, it could also be an attempt to increase Aβ degradation. Several recent studies have shown that increases in central nervous system Cu^{2+} levels result in lower Aβ levels and reduced plaque deposition (42, 43). Moreover, Cherny *et al.* (10) demonstrated that APP transgenic mice treated with CQ have elevated central nervous system Cu^{2+} and Zn^{2+} levels together with reduced Aβ deposition. These reports are consistent with our findings here that elevated Cu^{2+} or Zn^{2+} levels can reduce Aβ levels by increasing Aβ degradation. Interestingly, small phase clinical trials of CQ demonstrated lower plasma Aβ-(1–42) levels with elevated plasma Zn^{2+} levels in treated patients (8). This could reflect increased peripheral degradation of Aβ through elevated Zn^{2+} levels. If so, this would raise the possibility of targeting peripheral Aβ with metal ligands as a means of reducing the total Aβ load.

In summary, our studies indicate a potentially important therapeutic role for induction of MMP activation by metal ligands and subsequent Aβ degradation. If CQ also mediates clearance of Aβ *in vivo* through activation of Aβ-degrading MMPs, these findings will have important implications for the future direction of AD therapeutics based on modulation of metal bioavailability.

Acknowledgments—We thank Dr. Roberto Cappai for critically reading the manuscript and Dr. Ian Trounce for the APP-N2a cells.

REFERENCES

1. Masters, C. L., Simms, G., Weinman, N. A., Multhaup, G., McDonald, B. L., and Beyreuther, K. (1985) *Proc. Natl. Acad. Sci. U. S. A.* 82, 4245–4249
2. Barnham, K. J., Masters, C. L., and Bush, A. I. (2004) *Nat. Rev. Drug Discov.* 3, 205–214
3. Bush, A. I. (2003) *Trends Neurosci.* 26, 207–214
4. Roher, A. E., Kasunic, T. C., Woods, A. S., Ball, M. J., and Fridman, R. (1994) *Biochem. Biophys. Res. Commun.* 205, 1755–1761
5. Howell, S., Nalbantoglu, J., and Crine, P. (1995) *Peptides (N.Y.)* 16, 647–652
6. Backstrom, J. R., Lim, G. P., Cullen, M. J., and Tokes, Z. A. (1996) *J. Neurosci.* 16, 7910–7919
7. Kaur, D., Yantiri, F., Rajagopalan, S., Kumar, J., Mo, J. Q., Boonplueang, R., Viswanath, V., Jacobs, R., Yang, L., Beal, M. F., DiMonte, D., Volitakis, I., Ellerby, L., Cherny, R. A., Bush, A. I., and Andersen, J. K. (2003) *Neuron* 37, 899–909
8. Ritchie, C. W., Bush, A. I., Mackinnon, A., Macfarlane, S., Mastwyk, M., MacGregor, L., Kiers, L., Cherny, R., Li, Q.-X., Tammer, A., Carrington, D., Mavros, C., Volitakis, I., Xilinas, M., Ames, D., Davis, S., Beyreuther, K., Tanzi, R. E., and Masters, C. L. (2003) *Arch. Neurol.* 60, 1685–1691
9. Ritchie, C. W., Bush, A. I., and Masters, C. L. (2004) *Expert Opin. Investig. Drugs* 13, 1585–1592
10. Cherny, R. A., Atwood, C. S., Xilinas, M. E., Gray, D. N., Jones, W. D., McLean, C. A., Barnham, K. J., Volitakis, I., Fraser, F. W., Kim, Y., Huang, X., Goldstein, L. E., Moir, R. D., Lim, J. T., Beyreuther, K., Zheng, H., Tanzi, R. E., Masters, C. L., and Bush, A. I. (2001) *Neuron* 30, 665–676
11. Treiber, C., Simons, A., Strauss, M., Hafner, M., Cappai, R., Bayer, T. A., and Multhaup, G. (2004) *J. Biol. Chem.* 279, 51958–51964
12. White, A. R., and Cappai, R. (2003) *J. Neurosci. Res.* 71, 889–897
13. Di Vaira, M., Bazzicalupi, C., Orioli, P., Messori, L., Bruni, B., and Zatta, P. (2004) *Inorg. Chem.* 43, 3795–3797
14. Hoke, D. E., Tan, J. L., Ilaya, N. T., Culvenor, J. G., Smith, S. J., White, A. R., Masters, C. L., and Evin, G. M. (2005) *FEBS J.* 272, 5544–5557
15. Chung, K. C., Park, J. H., Kim, C. H., Lee, H. W., Sato, N., Uchiyama, Y., and Ahn, Y. S. (2000) *J. Neurosci. Res.* 59, 117–125
16. Wu, W., Samet, J. M., Silbajoris, R., Dailey, L. A., Sheppard, D., Bromberg, P. A., and Graves, L. M. (2004) *Am. J. Respir. Cell Mol. Biol.* 30, 540–547
17. Liu, S., Yu, S., Hasegawa, Y., Lapushin, R., Xu, H. J., Woodgett, J. R., Mills, G. B., and Fang, X. (2004) *J. Biol. Chem.* 279, 51075–51081
18. Phiel, C. J., Wilson, C. A., Lee, V. M., and Klein, P. S. (2003) *Nature* 423, 435–439
19. Hofmann, U. B., Houben, R., Brocker, E. B., and Becker, J. C. (2005) *Biochimie (Paris)* 87, 307–314
20. Matsuki, Y., Ito, T., Fukuhara, K., Abe, M., Othaki, T., and Nambara, T. (1987) *Arch. Toxicol.* 59, 374–378
21. Frederickson, C. J., Koh, J. Y., and Bush, A. I. (2005) *Nat. Rev. Neurosci.* 6, 449–462
22. Benvenisti-Zarom, L., Chen, J., and Regan, R. F. (2005) *Neuropharmacology* 49, 687–694
23. Ding, W. Q., Liu, B., Vaught, J. L., Yamauchi, H., and Lind, S. E. (2005) *Cancer Res.* 65, 3389–3395
24. Shimoke, K., Yamagishi, S., Yamada, M., Ikeuchi, T., and Hatanaka, H. (1999) *Dev. Brain Res.* 112, 245–253
25. Li, J., Chen, H., Tang, M. S., Shi, X., Amin, S., Desai, D., Costa, M., and Huang, C. (2004) *J. Cell Biol.* 165, 77–86
26. Miyata, Y., Sato, T., Yano, M., and Ito, A. (2004) *Mol. Cancer Ther.* 3, 839–847
27. Zhu, X., Raina, A. K., Rottkamp, C. A., Aliev, G., Perry, G., Boux, H., and Smith, M. A. (2001) *J. Neurochem.* 76, 435–441
28. Pei, J. J., Khatoon, S., An, W. L., Nordlinder, M., Tanaka, T., Braak, H., Tsujio, I., Takeda, M., Alafuzoff, I., Winblad, B., Cowburn, R. F., Grundke-Iqbal, I., and Iqbal, K. (2003) *Acta Neuropathol.* 105, 381–392
29. Ostrakhovitch, E. A., Lordnejad, M. R., Schliess, F., Sies, H., and Klotz, L. O. (2002) *Arch. Biochem. Biophys.* 397, 232–239
30. LaRochelle, O., Gagne, V., Charron, J., Soh, J. W., and Seguin, C. (2001) *J. Biol. Chem.* 276, 41879–41888
31. Wu, W., Graves, L. M., Jaspers, I., Devlin, R. B., Reed, W., and Samet, J. M. (1999) *Am. J. Physiol.* 277, L924–L931
32. Liang, J., and Slingerland, J. M. (2003) *Cell Cycle* 2, 339–345
33. Takada, Y., Fang, X., Jamaluddin, M. S., Boyd, D. D., and Aggarwal, B. B. (2004) *J. Biol. Chem.* 279, 39541–39554
34. Adamson, I. Y., Vincent, R., and Bakowska, J. (2003) *Exp. Lung Res.* 29, 375–388
35. de Souza, A. P., Gerlach, R. F., and Line, S. R. (2000) *Dent. Mater.* 16, 103–108
36. Kubiatowski, T., Jang, T., Lachyankar, M. B., Salmonsen, R., Nabi, R. R., Quesenberry, P. J., Litofsky, N. S., Ross, A. H., and Recht, L. D. (2001) *J. Neurosurg.* 95, 480–488
37. Matsumoto, K., Minamitani, T., Orba, Y., Sato, M., Sawa, H., and Ariga, H. (2004) *Exp. Cell Res.* 297, 404–414
38. Leissring, M. A., Farris, W., Chang, A. Y., Walsh, D. M., Wu, X., Sun, X., Frosch, M. P., and Selkoe, D. J. (2003) *Neuron* 40, 1087–1093
39. Rapala-Kozik, M., Kozik, A., and Travis, J. (1998) *J. Pept. Res.* 52, 315–320
40. Stix, B., Kahne, T., Sletten, K., Raynes, J., Roessner, A., and Rocken, C. (2001) *Am. J. Pathol.* 159, 561–570
41. Deb, S., Zhang, J. W., and Gottschall, P. E. (1999) *J. Neurosci. Res.* 55, 44–53
42. Bayer, T. A., Schafer, S., Simons, A., Kemmling, A., Kamer, T., Tepest, R., Eckert, A., Schussel, K., Eikenberg, O., Sturchler-Pierrat, C., Abramowski, D., Staufenbiel, M., and Multhaup, G. (2003) *Proc. Natl. Acad. Sci. U. S. A.* 100, 14187–14192
43. Phinney, A. L., Drisaldi, B., Schmidt, S. D., Lugowski, S., Coronado, V., Liang, Y., Horne, P., Yang, J., Sekoulidis, J., Coomaraswamy, J., Chishti, M. A., Cox, D. W., Mathews, P. M., Nixon, R. A., Carlson, G. A., St George-Hyslop, P., and Westaway, D. (2003) *Proc. Natl. Acad. Sci. U. S. A.* 100, 14193–14198